

CR-114851

C-1

17618-N97C RG-9C

PROJECT TECHNICAL REPORT

CHARACTERIZATION EVALUATION OF THE ATTITUDE CONTROL PROPULSION SYSTEM

INTERIM REPORT

MSC/TRW TASK 705-1

NAS 9-8166

December, 1970

Prepared for
NATIONAL AERONAUTICS AND SPACE ADMINISTRATION
MARSHAL SPACECRAFT CENTER
HOUSTON, TEXAS

Prepared by
P. F. Thompson
T. J. Walsh
R. S. Hoyle
Propulsion Technology Section
Power Systems Department

Approved by: *P. H. Thompson*
P. H. Thompson Head
Propulsion Technology Section

Approved by: *D. W. Vernon*
D. W. Vernon Manager
Power Systems Department

N 71 - 17566

FACILITY FORM 602

(ACCESSION NUMBER)

135

(THRU)

G3

(PAGES)

CR-114851

(CODE)

28

(NASA CR OR TMX OR AD NUMBER)

(CATEGORY)

CONTENTS	Page No.
1.0 PURPOSE AND CONCLUSIONS -----	1
2.0 INTRODUCTION -----	2
3.0 CHARACTERIZATION EVALUATION -----	5
3.1 Literature/Computer Simulation Search -----	5
3.2 Comparison Review -----	8
3.3 Technique Evaluation -----	21
3.4 Recommended Techniques -----	32
3.4.1 Transient Combustor Model -----	34
3.4.2 Steady-State Combustor -----	46
3.4.3 Supply Lines Transients-----	48
3.4.4 Supply Lines Steady State -----	66
3.4.5 Turbomachinery Transients -----	73
3.4.6 Turbomachinery Steady-State -----	71
3.4.7 Heat Exchanger Transients -----	76
3.4.8 Heat Exchanger Steady-State -----	78
3.4.9 Accumulator & Pressure Vessels Transients -----	80
3.4.10 Accumulator & Pressure Vessels Steady-State --	81
3.4.11 Manifolds and Injectors Transients -----	85
3.4.12 Manifolds and Injectors Steady-State -----	87
3.4.13 Orifices, Pipebends, & Valves Transients -----	88
3.4.14 Orifices, Pipebends, & Valves Steady-state -----	88
3.4.15 Oil Generator Transients -----	94
3.4.16 Oil Generator Steady-State -----	94

TABLES

Page No.

1. COMPUTER PROGRAM CAPABILITY REQUIREMENTS	4
2. TYPICAL ACPS COMPONENTS/SUBASSEMBLIES	7
3. NUMERICAL CODE FOR ACPS FILE	9
4. ACPS RELATED LITERATURE	10
5. ACPS RELATED COMPUTER PROGRAMS	18
6. ACPS (TASK 705-1) CHARACTERIZATION EVALUATION FORMS	22
7. PHASE III TECHNIQUE EVALUATION SYNOPSIS FOR ACPS RELATED LITERATURE	23

ILLUSTRATIONS

1. FLOW DIAGRAM OF ACPS CHARACTERIZATION EVALUATION	6
2. ACPS TURBO PUMP CYCLE	27
3. LOW PRESSURE ACTIVE BIPROPELLANT SYSTEM	28
4. COMBUSTOR CHAMBER MODEL EULER'S INTEGRATION SCHEME	38
5. COMBUSTOR CHAMBER MODEL RUNGE-KUTTA INTEGRATION SCHEME	39
6. COMBUSTOR MODEL SCHEMATIC	40
7a. PRESSURE AT THE VALVE	60
7b. FLOW RATE AT UPSTREAM END	61
8a. PRESSURE AT THE VALVE	62
8b. FLOW RATE AT UPSTREAM END	63
9a. PRESSURE AT THE VALVE	64
9b. FLOW RATE AT UPSTREAM END	65
10a. PRESSURE AT THE VALVE	66
10b. FLOW RATE AT UPSTREAM END	67
11. COMPUTER LIST OF ACPS SUBROUTINES	68
12. COMPUTER LIST OF ACPS SUBROUTINES	69

	Page No.
13. TYPICAL PUMP PERFORMANCE MAP	72
14. TYPICAL PRELIMINARY PUMP PERFORMANCE (HYDROGEN PUMP)	73
15. TYPICAL PUMP PERFORMANCE MAP	74
16. TYPICAL TURBINE PERFORMANCE MAP	75
17. HEAT EXCHANGER BLOCK DIAGRAM	76
18. ACCUMULATOR	80
19. GAS ACCUMULATOR	81
20. GAS/LIQUID PRESSURE VESSEL	81
21. MANIFOLD DIAGRAM	85
22. SIMPLIFIED MANIFOLD/ORIFICE	87

APPENDICES

1. REQUEST FOR LITERATURE SEARCH	99
2. LITERATURE SEARCH ON MATHEMATICAL MODELING FOR STABILITY OF HYDROGEN AND OXYGEN ROCKET PROPULSION ENGINES RESPONSE	101
3. PROGRAMS FOR POTENTIAL USE	109
4. UNAVAILABILITY OF PROGRAM DOCUMENTATION REQUESTED FROM THE ADP PROGRAM SHARING LIBRARY	112
5. APS TRANSIENT COMPUTER PROGRAM LISTING	113

1.0 PURPOSE AND CONCLUSIONS

1.1 Purpose

The purposes of this document are fourfold. They are: (1) to present the results from a literature/computer simulation survey of methods and programs currently used by industry, NASA centers and other government agencies which may be used to simulate the steady-state and dynamic behavior of attitude control propulsion systems (ACPS); (2) to present a comparison of the various simulation techniques which were obtained from the survey; (3) to present an evaluation of the applicable techniques which resulted from the survey; and (4) to recommend to NASA/MSC the techniques which should be used to develop flexible steady-state and dynamic simulations of attitude control propulsion systems. The recommended techniques will result in computer programs which, upon approval of the MSC Task Monitor, will form the basis for the program development effort which will be carried out under Subtask II of this effort.

1.2 Conclusions

The literature search provided extensive information that has been used directly to formulate ACPS component modeling approaches. The applicable documents are referenced specifically throughout section 3.4 of this report. Unfortunately, no computer programs were found that could be directly applied in an efficient and economical manner to the program development objectives of Task 705-1. However, in many cases, techniques used in these programs were adopted. Every attempt was made to choose methods that were proven, that provide a high degree of accuracy and are computationally efficient, reliable, and plausibly efficient.

NOT REPRODUCIBLE

2.0 INTRODUCTION

The design and development of attitude control propulsion systems (ACPS) for future mission applications will require extensive analyses to establish optimum system concepts. These analyses will consist of parametrically generating sufficient component and subsystem data to permit evaluation of ACPS concepts which meet a variety of mission objectives for a wide range of operating conditions. Since emphasis will be placed upon reusability, lightweight, high performance, safety, reliability and low cost for all components of future spacecraft, it is imperative that the analytical tools available for performing these analyses provide the capability to parametrically integrate system components into a variety of ACPS configurations to define optimum subsystem configurations. These analysis programs must also be capable of evaluating point designs of potential systems, determining the effects of component operation on overall system performance, determining system performance under both design and off-design conditions and characterizing final ACPS design configurations. Since the ACPS must be integrated with other vehicle subsystems to achieve optimum overall vehicle performance, the analysis programs must provide the additional capability of determining the effects on ACPS performance of subsystems integration and interaction.

MSC/IRW Task 705-1, "Characterization of Auxiliary Propulsion Systems," was initiated because of these requirements. The objectives of this task are to develop transient and steady-state analysis computer codes in a modular structure with generalized diagnostic capability available for:

- i. Determining ACPS system operation and constraints;
- ii. Predicting system performance characteristics;
- iii. Diagnosing system anomalies.

4. Determining ACPS performance due to vehicle subsystem integration and interaction;

5. Characterizing final design configuration operation.

Under this task all ACPS components will be modeled in sufficient detail to fully characterize the thermodynamic and fluid mechanics performance of each component and its effect on overall system performance. The resulting models will provide the capability for determining fluid pressure and temperature profiles required to operate the ACPS during a mission duty cycle and for determining methods of control and system operation compatible with a given mission duty cycle. In addition, the models will provide the ability to determine ACPS performance while simulating critical system component modes of operation.

The objectives of this Task will be achieved by performing the following three subtasks:

Subtask I Evaluation of various analytical techniques used to characterize the dynamic behavior and performance of propulsion systems and a definition of the recommended approach.

Subtask II Application of the techniques selected in Subtask I to the development of general purpose computer programs to satisfy the requirements listed in Table I.

Subtask III Demonstration and operation of the program by selecting a typical ACPS design and operating the program over a range of conditions on the NSC computer facilities.

This report presents the accomplishments of Subtask I and defines the analytical techniques and recommended characterization approaches for the ACPS modeler. Upon completion, activity to be carried out under Subtask II.

TABLE 1
COMPUTER PROGRAM CAPABILITY REQUIREMENTS

Transient Analysis Program

1. Component Sequencing
2. Subsystem energy requirements
3. Transient total impulse
4. Supply system dynamics
5. Supply system stability feedback:
"line, valve and injector pressure surge, engine and feedline pressure overshoot"
6. Effects of geometry changes on start and shutdown
7. Effect of initial conditions
8. Component malfunction
9. Component performance
10. Varied component design and location
11. Varied engine configuration

Steady-State Program

1. Supply system balance requirements
2. Component performance
3. Varied component design and location
4. Effects of initial conditions
5. Component failures
6. Statistical sampling capability

3.0 CHARACTERIZATION AND EVALUATION

Analytical techniques available for characterizing the dynamic behavior and performance of ACPS components (shown in Table 2) have been evaluated on the basis of: state-of-the-art; efficiency; adaptability to solution by digital computer; previous usage; accuracy; availability of characterization parameters and adaptability to modular computer program construction. Basically, this subtask was divided into four phases, (see Figure 1):

- Phase I Literature/Computer Simulation Search
- Phase II Comparison Review
- Phase III Technique Evaluation
- Phase IV Recommended Techniques

The initial part of this subtask consisted of a survey of methods and programs currently used by industry and other NASA centers and governmental agencies including those at Lewis Research Center (LeRC), Marshall Spaceflight Center (MSFC), Jet Propulsion Laboratory (JPL), Arnold Engineering Development Center (AEDC), and Air Force Rocket Propulsion Laboratory (AFRPL). Contacts were established with companies performing ACPS simulation work on the Shuttle Vehicle, and the computer programs applicable to this task which are being formulated by these companies are being reviewed as they become available.

3.1 LITERATURE/COMPUTER SIMULATION SEARCH (PHASE I)

Several literature search requests covering the entire scope of information deemed pertinent to the modeling of the Shuttle ACPS were submitted to the TRW Technical Information Center. These literature search requests were issued using general descriptions with detailed key word identifiers.

Typical examples of these literature search requests are shown in Appendix C. The return rates on these literature search requests are not yet available in sufficient quantities to indicate

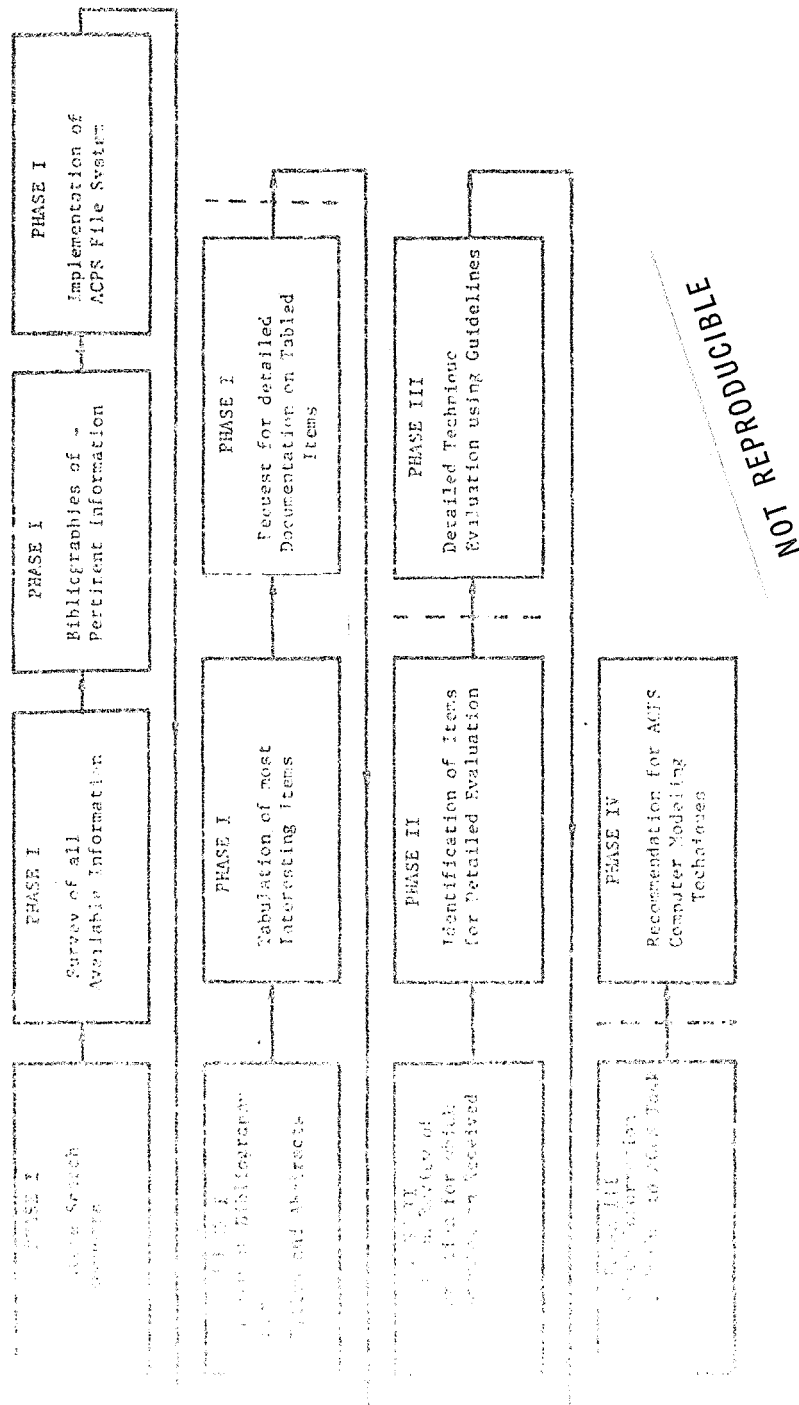


FIGURE 1
FLOW DIAGRAM OF ACPS CHARACTERIZATION EVALUATION

TABLE 2 - TYPICAL ACPS COMPONENTS/SUBASSEMBLIES

◎Combustors

◎Injectors

◎Manifolds

◎Turbopumps

◎Pumps and Compressors

◎Inducers

◎Turbines

◎Electric Motors

◎Heat Exchangers

◎Fluid Supply

◎Accumulators

◎Supply lines

◎Pressure vessels

◎Gas lines

◎Liquid lines

◎Orifices, bends/restrictions

◎Regulators

◎Control Valves

◎Valve Actuators

◎Pneumatic/hydraulic

◎Electrical

◎Mechanical

- 1 - Manually performed survey of all engineering and scientific publications (including advanced degree theses).
- 2 - Manually performed review of indexes containing lists of computer programs shared by all NASA facilities and contractors. Among those indexes which contained the most pertinent information were COSMIC (Computer Software Management and Information Center) and the NASA ADP Resource Sharing System Computer Programs.
- 3 - Computerized search of all information available to NASA facilities and the Defense Documentation Center (DDC)

The bibliography results of Action 1 above are shown in Appendix 2.

Action 2 results are shown in Appendix 3. Action 3 resulted in voluminous computer printouts of titles and abstracts of pertinent ACPS information; these printouts are too massive for inclusion in this report. They are being retained by TRW in the ACPS Literature Search file, and are available upon request.

With the receipt of these bibliographies, the next item accomplished was a review of all titles and abstracts (if available) in order to select information for further examination in the Phase II comparison review. Also at this time, the ACPS Literature Search File was implemented in order to systematically control the receipt and filing of the ACPS information obtained. Table 3 shows the numerical index code used to file and retrieve all ACPS information.

3.2 COMPARISON REVIEW (PHASE II)

After a review of the above mentioned bibliographies, those items indicating strong applicability for the ACPS were chosen for the PHASE II Comparison Review. Table 4 shows, specifically, the selected literature related to the ACPS while Table 5 shows those computer programs pertinent to the task. A preliminary review was made of the literature and computer programs to determine which would be most suitable for comparison, and detailed documentation was obtained. For a detailed review, copies of the computer programs (or detailed descriptions thereof), their documentation, and any other information which may be required, will be furnished to the user upon request.

TABLE 3
NUMERICAL INDEX CODE FOR
ACPS FILE

<u>INDEX</u>	<u>DESCRIPTOR</u>
0.0	ACPS LITERATURE SEARCH RESPONSES
0.1	ACPS LITERATURE SEARCH REQUESTS TO LIBRARY
1.0	TANKS
1.1	LIQUID TANKS
1.2	GAS TANKS
2.0	COMPRESSORS
2.1	LIQUID COMPRESSORS
2.2	GAS COMPRESSORS
3.0	REGULATORS
3.1	LIQUID REGULATORS
3.2	GAS REGULATORS
4.0	VALVES
4.1	LIQUID VALVES
4.2	GAS VALVES
5.0	HEAT EXCHANGERS
6.0	LINES
6.1	LIQUID LINES
6.2	GAS LINES
7.0	ENGINES
7.1	LIQUID ENGINES
7.1.1	LIQUID ENGINES: STEADY STATE
7.1.2	LIQUID ENGINES: TRANSIENTS
7.2	GAS ENGINES
8.0	PROPULSION
8.1	ROTATIONAL PROPULSION
8.2	GAS PROPULSION
9.0	FLUID FLOW AND THERMODYNAMICS
10.0	FLUID THERMODYNAMICS

TABLE 4
ACTS RELATED LITERATURE

REF ID	TITLE	COPY & REF ID		
AD-8525107 AD-8456811 AD-817257	Post Test Analysis of Generart Tank The Combined Laboratory and KC-135 Aircraft zero-g Test Program Tank Mounted Insulation Program	HC MF MF		
AD-8532750 AD-8632611 AP-8441811	Launch System Branch Destratification of Cryo Propellants Thermodynamic Studies of Cryogenic Propellant Management Liquid Hydrogen Pressure Loss Phase	MF MF MF		
AD-843476 AS-6933611	Sundstrand Model 876 APU Part I: (Cryogenic Liquids) Forced Convection Heat Transfer to Supercritical Cryogenic Hydrogen, Part I, lit. Survey	MF MF		
AD-677574 AD-617319 AD-833315 AS-820012	The Prediction of the Wetting of Solids by Liquid Hydrogen and Liquid Oxygen Consistent Vibrations Model of Internal Dynamics of Liquid Hydrogen Zero-g Report Liquid/Liquid Models Feasibility of Using Liquids Other than Hydrogen for Liquid Behavior Tests of zero-g Test Program	RC MF MF MF		
AS-851905 AD-851802 AS-851503 AS-851319 AS-827539 AS-830042	Development of Turbocompressor Performance Rotating Stall Prediction Model Analytical Model for Predicting Turbocompressor Performance with Combined Circumferential and Radial Inlet Distortion Design, Technology, and Performance of High Pressure Turbopumps for Large Thrust LH2 and LOX Rocket Engines. Analytical Model for Use in Design of Pump Inlet Accumulators for Prevention of Liquid Rocket Longitudinal Oscillation An Analysis of Two-Phase Flow in LH2 Pumps for O ₂ /H ₂ Rocket Engines Study Design, and Test of Experimental Liquid Hydrogen Pump for use in Trifast Vehicle System	MF MF MF RC RC MF		
Z-2	* Indicates literature which was referred for Phase III - Technical Evaluation			Z-2
	** HC,MF - Indicates hard copy or microfiche copy received and advised for Phase III - Comparison			

TABLE 4 (Contd.)
ACPS RELATED LITERATURE

TYPE	REF.	STANZ I.D. NO.	TITLE	COPY
CONF.	AD-657008	3,0		
CONF.	AD-657009	3,1		
CONF.	AD-657010	3,2		
CONF.	AD-657011	3,3		
CONF.	AD-657012	3,4		
CONF.	AD-657013	3,5		
CONF.	AD-657014	4,1	AD-6574555 Wide Range Flow Control Program	MF
CONF.	AD-657015	4,2	AD-6572537 Valve, Regulator Relief, Recirculation, System Dev. of Gavitating Venturi Valves for Deep Throttling of Cryogenic Liquids	HC
CONF.	AD-657016	5,0	AD-6570200 Computer Analyzed Hydrogen Refrigerator Cycles for Selection of Optimal Cycle, Rates, and Heat Exchangers	MF
CONF.	AD-657017	5,1	AD-6570231 Analytical Model of Thermal Flow Oscillations in Heat Exchangers for Super Critical Fluids	MF
CONF.	AD-657018	5,2	AD-6570232 On-Line Computer Model for a LOX Manifold System	MF
CONF.	AD-657019	5,3	AD-6570233 Digital Distributed Parameter Model for Computing Dynamic Response of Rocket Propellant Feed Systems to Pressure and Flow Disturbances	HC
CONF.	AD-657020	5,4	AD-6570234 Effect of Propellant Feed System Coupling and Hydraulic Parameters on Analysis of Chugging	HC
CONF.	AD-657021	5,5	AD-6570225 Two CH2 Manifold Assemblies. Two GOX Manifold Assemblies	MF
CONF.	AD-657022	5,6	AD-6570226 Rocket Combustion Chamber Ignition Studied By Mass, Spectroscopy of Chemical Species	MF
CONF.	AD-657023	5,7	AD-6570227 Mathematical Model for Combustion at Zero Gravity At Spacecraft Environments	MF
CONF.	AD-657024	5,8	AD-6570228 Small Rocket Engine Research	MF
CONF.	AD-657025	5,9	AD-6570229 Current Design Technology of Attitude Control Systems for Large Launch Vehicle	MF
CONF.	AD-657026	6,0	AD-6570230 Survey of the Relationship Between Theory and Experiment for Convective Heat Transfer from Rocket Combustion Gases,	MF

TABLE 4 (Contd.)
AIAA RELATED PUBLICATIONS

REF ID	AUTHOR(S)	TITLE	CITATION
ASCE-3724	W. H. Kammann	The Effect of Nozzle View Variations on Engine Performance	NC
ASCE-3725	W. H. Kammann	Effect of Chamber pressure on Performance of Small Reverse Flow Rocket Engine	MF
ASCE-3726	W. H. Kammann, S. S. Sankar, J. S. Speer, Jr., R. L. Strohmeier	Space Propulsion System Specification (MLDA-3 negative)	NC
ASCE-3727	W. H. Kammann, J. S. Speer, Jr.	Compressible Laminar Boundary Layer with Fluid Injection	NC
ASCE-3728	W. H. Kammann, J. S. Speer, Jr.	Transpiration Cooling in Porous Metal Plates	NC
ASCE-3729	W. H. Kammann, J. S. Speer, Jr.	Temperature of a Transpiration Coolant State	NC
ASCE-3730	W. H. Kammann, J. S. Speer, Jr.	Mathematical Model of Cylindrical Electric Gas Dynamic Generator	MF
ASCE-3731	W. H. Kammann, J. S. Speer, Jr.	Performance of High Performance Liquid Fuel Rocket Engine by Opt. of Liq. He2 and He3 on Propulsion	MF
ASCE-3732	W. H. Kammann	Interagency Chemical Rocket Propulsion Survey Method of Testing Measurement Error for Liquid Rocket Engine Performance Parameters Using Uncertainty Tolerance	MF
ASCE-3733	W. H. Kammann	An Analytical Model for Calculating Radiative Heat Transfer from Turbulent Diffusion Flame and Predicting Liquid Fuel Burning Rate	MF
ASCE-3734	W. H. Kammann	Design, Design and Manufacture of a Liquid Hydrogen/Oxygen Thrust Chamber	MF
ASCE-3735	W. H. Kammann	Stabilizing Effects of Several Injector Face Pacific Configurations on Screech At A 20,000 Lbs. Thrust Rocket Thrust Hydrogen/Oxygen Rocket	MF
ASCE-3736	W. H. Kammann	Quantitative Analysis of Liquid Oxygen/Hydrogen Combustion Products	MF
ASCE-3737	W. H. Kammann	The hydrodynamic Calculation of a High-Beta Cylindrical Combustion Chamber of a Liquid Fuel Rocket Engine	MF
ASCE-3738	W. H. Kammann	Small Rocket Engine - Liquid Propellant, Vol. I - Small Engine	MF
ASCE-3739	W. H. Kammann	Design Parameters for Large Liquid-propellant Rocket Engines	MF
ASCE-3740	W. H. Kammann	Quantitative Analysis of Liquid Oxygen - Liquid Hydrogen Combustion Products	MF
ASCE-3741	W. H. Kammann	Study of Cylindrical Reactors For H2/O2 Combustion	MF
ASCE-3742	W. H. Kammann	General Equations for Constructing Mathematical Model on Steady State Liquid Propellant Rocket Engine Performance, and Determining its Solution	MF
ASCE-3743	W. H. Kammann	Development and State-of-Art in Analytical, Steady-State Liquid Propellant Rocket Combustion Models	MF
ASCE-3744	W. H. Kammann	Combustion and Thermodynamics in High Temperature Cases	MF

TABLE 4 (CONT'D)
ACPS RELATED LITERATURE

REF ID	STAR I.D. NO.	TYPE	COPY
TRW-2014	AT&T 107	Experimental Investigation of High Frequency Longitudinal Combustion Instability in Gaseous Propellant Rocket Motors	HCA
TRW-2015	AT&T 107	Rocket Thrust Termination Transients	HCA
TRW-2016	AT&T 107	TRW proposal Report, "Generalized Monopropellant Propulsion System Transient Computer Simulation," 12 June 1960.	HCA
TRW-2017	AT&T 107	Matrix of JDS Physics (cont'd) 1969	HCA
TRW-2018	AT&T 107	Theory of Transport Coefficients for Moderately Dense Cases	HCA
TRW-2019	AT&T 107	Variational Calculation of Transport Coefficients in a Binary Mixture	HCA
TRW-2020	AT&T 107	Transport Phenomena in Reacting Gas Mixtures	HCA
TRW-2021	AT&T 107	Combustion Process Influence on Stability	HCA
TRW-2022	AT&T 107	WSR-23-1312 The Effect of Turbulence on the Flame Velocity in Gas Mixtures	HCA
TRW-2023	AT&T 107	Jet Prop., #26 Low Frequency Comb. Instability	HCA
TRW-2024	AT&T 107	Jet Propulsion Structure and Propagation Mechanism of Turbulent Flames in High Speed Flow	HCA
TRW-2025	AT&T 107	J. Spacecraft. Mixing in Turbulent Axially Symm. Free Jets	HCA
TRW-2026	AT&T 107	AT&T Jour., #2 A Shock Wave Model of Unstable Rocket Combustors	HCA
TRW-2027	AT&T 107	Rocket Comb. Instability	HCA

TABLE 6 (Cont'd)
ACPS RELATED LITERATURE

REF ID	TYPE	AUTHOR	TITLE	COPY
1A-37008	CONF	J. G. SP. I.D.	Mathematical Model for Solving 3-dimensional Combustion Instability in Liquid Propellant Rocket Engines	HC, MF
1A-27572	CONF		Nonlinear Model for Calculating Combustion Stability in Liquid Propellant Rocket Engines	MF
956-19130	CONF		Mathematical Model to Determine Longitudinal Instabilities In Liquid Propellants Rocket Vehicle	MF
1A70-2861	CONF		Boundary Value Problems and Cauchy Problems Considered for Mathematical Model of Turbulent Motion in Liquid or Gas	AC
1A76-30-156	CONF		Theory for Ignition and Deflagration of Fuel Drops	MF
1C3-20743	CONF		Rocket Combustion Instability Studied Experimentally Using Theoretical Model Characterizing Combustion by Time Lag and Interaction Index	MF
1A62-18700	CONF		Nonsteady Combustion Models for Gases, Liquid Fuels, and Solid Propellants, Considering Errors in Physical and Mathematical	AC
1A70-17007	CONF		Nonlinear Combustion Instabilities in Liquid Propellant Rockers, Considering Various Combustion Models and Experimental Techniques	MF
1A76-12011	CONF		Three Dimensional Linear Combustion Instability in Liquid Propellant Rocket Motors Netes Concentrated Combustion Nede, Presenting Mathematical Analysis as Boundary Value Problem	AC
1D-3742-959	CONF		Analytical Model Development to Study Liquid Rocket Engine Combustion Instability at High Chamber Pressures	MF
1A7-37005	CONF		Analytical Model for Describing Combustion Chamber Disturbances During Start Transient and Steady-State Operations of Hypergolic Liquid	MF
1A76-25372	CONF		Double Road-Time Model for Combustion Stability Analysis in Liquid Bipropellant Rocket Engines	MF
1A76-46923	CONF		Linearized Mathematical Models of Feed System Coupled Combustion Instability of Liquid Propellant Rocket Engines	AC
1A76-37007	CONF		Theoretical Propellant Combustion Model for Rapid Depressurization Effects	MF
1A7-26342	CONF		Mathematical Development of Sensitive Time Lag Theory of Liquid Rocket Engine Characteristics Instability	MF
1A76-37009	CONF		Mathematical Model of Ignition Transient for Hypersonic Rocket Propellants	AC
1A76-37011	CONF		Combustion Stability Model of Advanced Injector for Use on High Pressure Hydrogen Oxygen Engines	AC

TABLE 6. (CONT'D)
ACPS RELATED LITERATURE

REF.	AUTHOR	TITLE	COPY
197	Y. S. Tsoi, J. C. Hwang, and C. Y. Lin	Effect of Reactor Design Errors in non-Steady Comb. Theory in the past Decade	WC
198	J. C. Hwang	Research on Combustion Instability in Liquid propellant Rockets	HC
199	J. C. Hwang	Stability of Mi-Frequency Press. Oscill. in Rocket Comb. Chambers	HC
200	J. C. Hwang	Theory of acoustic Instability in Solid propellant Rockets	WS
201	J. C. Hwang	Transverse Wave & Entropy Wave Combustion Instability in Liqu. Prop. Rockets	WT
202	J. C. Hwang	Instability Time Lags Theory and Its Application to Liqu. Rocket Comb. Instab.	HC
203	J. C. Hwang	Comb. Instab. Analysis at High Chamber Pressure	HC
204	J. C. Hwang	5th ICRCG Combustion Conference	HC
205	J. C. Hwang	Spark Ignition of Flowing Gases	HC

TABLE 4 (Cont'd)
AGS RELATED LITERATURE

REF ID	REF ID CROSS REF	PAGE	STK#	TITLE	CITY
AD-615798	7.4	167-27227	7.4.1	Test Firings and Analytical Model Used to Evaluate Chugging Instability In Subscale Experiments with LOX/Gaseous Hydrogen Combustors	NY, NC
AD-615875		N-17-22360		Spacecraft Attitude Control Gas Systems Analysis Final Report	NY, NC
		7.043		Effect of Combustor Parameters on the Stability of Gaseous Hydrogen-Liquid Oxygen Engine	
AD-615798				Steady State Rocket Combustion of Gaseous Hydrogen and Liquid Oxygen	NY
AD-615875				Heat Transfer and Performance Studies on Propellant Combination Gaseous Hydrogen / Gaseous Oxygen, Part 3	
AD-617981				Thrust Variation of a Gaseous Propellant Rocket Engine	NYA
AD-622737				An Investigation of the Performance of Various Mixtures of Hydrogen and Methane	NYC
See Table 7				TRW Briefing Report on O2/H2 Thruster (Prop)	NYC
See Table 7				TRW R.B. Proposal for High Pressure ACPS to MSFC	NYC
See Table 7				TRW R.E. Proposal for Low Pressure ACPS to MSFC	NYC
See Table 7				TAB Capabilities in O2/H2 Igniter and Injector Flow Characterization	NYC
See Table 7				TRW Capabilities Relative to Development of a Generalized Shuttle Thruster Model	NYC
See Table 7				An Experimental Investigation of Longitudinal Combustion Instability in a Rocket Motor Using Premixed Gaseous Propellants	NYC
See Table 7				NASA Memo on O2/H2 Perf. Curve Plot, Feb. 1976.	NYC
See Table 7				TAB Memo "Space Shuttle APS Dynamic Analysis"	NYC
DCS-22403				Summary of Experimental Investigation of Combustion Pressure Oscillations in Gaseous Propellant Rocket Motors	NY
See Table 7				Analysis of High Freq. Comb. Instab. in a Gas Filled Rocket Motor	NY
See Table 7				Digital Computer Programs, Mathematical Models and Propulsive System Disruptive Functions for Integrating Engine and Inlet Dynamic Concepts in Turbine Engine Design	NY

TABLE 4 (Cont'd)
ACPS RELATED LITERATURE

PART	PUB. I.D.	TITLE	COPY
10.2	Y60-10620	Computer Models for Inducer System of Hydraulic Turbine Drive for Liquid Hydrogen	NF HC
10.2	AP-832654	An Investigation of the Effects of Secondary Stream Turbulation on the Throat Augmentation of an Ejector-Afterburner	NF
10.2	AP-832655	Convective Heat Transfer to Gas Turbine Blade Surfaces	NF HC
10.2	AP-832656	Propellant Zerf. Handbook, Vol. V, Part B, Oxygen/Hydrogen	NF
10.2	AP-832657	Table of Thermal Prop. of Normal H ₂ From Low Temp. to 540°K and from 10 ⁻⁶ to 10 ⁶ psia. PBS Tech. Note	NF HC
11.2	See Table 7	Space Shuttle Low Pressure Auxiliary Propulsion Subsystem Definition - Macroc	NF
11.2	See Table 7	Space Shuttle High Pressure Auxiliary Propulsion Subsystem Definition - Micro	NF
11.2	A - Conceptual Design Study Review - TRW		NF

Table 5
ACPS COMPUTER PROGRAMS

PROG. NO.	PROG. NAME	TYPE	CGC
1.1 NSC 9820	Tank Pressurization Program		
1.2 NSC 3093	Analysis of Propellant Tank Pressurization		
1.3 NSC 37676	Automatic Propellant Heating		
1.4 NSC 6125	Ultimate Pressure Variation with Temperature		
1.5 NSC 47426	Low-G Liquid-Vapor Interface		
2.1 NSC 8731	Oxygen Cryogenic Program		
2.2 NSC 33453	Heat Transfer to a Spherical Container		
2.3 NSC 54541	Heat Transfer Sphere		
2.4 NSC 7246	Nuclear Shuttle Hydrogen Program		
2.5 T-100 55230	STV Pump Cooling		
2.6 J-NSC 1671	Fan, Blower, and Pump Design	HC	
2.7 NSC 1297	Optimization/Evaluation of Fans, Compressors, and Pumps	HC	
2.8 NSC 1675	Orifice Sizing for Fluid Systems		
2.9 NSC 1933	Actuation Timing of a Linear Actuated Valve		
2.10 NSC 41649	Computer Programs for the Design & Performance Analysis of Compact Multi-Fluid Heat Exchanger	HC *	
2.11 NSC 2422	Heat Exchanger Program	HC	
2.12 NSC 19169	Transient and/or Steady State Thermal Analysis with Coupled Fluid Flow and Heat Conduction	HC	
2.13 NSC 738	Generalized Explicit Two-Phase Flow Finite Difference Generalized Heat Exchanger	HC	
	PG - Indicates program documentation received and reviewed for Phase II - Comparison Review.		
	* Indicates program which was reviewed for Phase III - Technique Evaluation		

1.000

Table 5 (Contd)
ACCS RELATED COMPUTER PROGRAMS

ACCS No.	FILE NAME	TYPE OF REPORT	TITLE	COPY
5.1.1.1	ACC 10C JC57	Design and Performance Analysis of Compact Heat Exchangers	NA	NA
5.1.1.2	ACC 134076	Vest Exchange	NA	NA
5.1.1.3	ACC 2994	Propellant Feedline Heat Exchanger	HC *	HC *
5.1.1.4	ACC F-942	Spacecraft ECS Heat Exchanger Program	NA	NA
5.1.1.5	ACC M230	Three-Fluid Cross Flow Heat Exchanger Program	HC	NA
5.1.1.6	ACC 253461	Transient Start-Up	NA	NA
5.1.1.7	ACC 30.6-26540	PUTMAN II Computer Program for Aerothermodynamic Behavior of Compact Heat Exchanger Component Models for Nuclear Ramjet and Rocket Engines Based on Real Gas Properties	HF	HF
5.1.1.8	ACC 37420	Zero-G Fluid Dynamics	HC	NA
5.1.1.9	ACC ARI37	SPS Feed Lines	NA	NA
5.1.1.10	ACC 524	Computer Program for the Prediction of Flow Distribution in a Ring Injector	HC	HC *
5.1.1.11	ACC 463	Solution of Compressible Flows in Piping Systems	NA	NA
5.1.1.12	ACC 21620	Heat Transfer and Thermal Problems	NA	NA
5.1.1.13	ACC 35320	Duct Flow T/D, Q, DA	NA	NA
5.1.1.14	ACC 37010	Anisotropic Two-Phase Perfect Gas Program	NA	NA
5.1.1.15	ACC M120	Lunar Module Reaction Control System Engine Injector	HC	HC
5.1.1.16	ACC 37045	RCS Steady State Analysis	NA	NA
5.1.1.17	ACC 35347	Gas Generator Combustion Program	NA	NA
5.1.1.18	ACC 37048	Computer Simulation of Rocket Engine Ignition Transients	HC	HC

TABLE 5 (CONT'D) LISTED PROGRAMS

REF.	ACM NUMBER OR SPAN NO.	TITLE	COPY
11.1	4699 No. 152-17537	TRAN Computer Program for Predicting Aerodynamic and Heat Transfer Characteristics of Annular and Rectangular Gas Turbine Combustors	NF
	1536-16241	Radial Turbine Synthetic (sic) Mapping Program	
11.2	1539 No. 152-16230	Formulation and Digital Coding of Approximate Hydrogen Properties for Application to Heat Transfer and Fluid Flow Computation	
11.3	NSC 8086	Fifth-Order Runge-Kutta Integration Subroutine	HC
11.4	NSC 8120	Newton Real Root Approximation Subroutine	HC
11.5	NSC 8132	Non-Linear Simultaneous Equations Solver	RC
11.6	NSC Rep. 152-16230	General Propellant Pressurization Program	HC
11.7	NSC Rep. 152-16230	Low Pressure APS Computer Model - Grumman	HC *

had been received (HC-hard copy or MF-microfiche). Comparisons were made to determine similarities and differences between the analytical approaches as well as to ascertain their detailed applicability to the ACPS task. Unique solution techniques were evaluated to the extent necessary to assess the validity and accuracy of approach.

3.3 TECHNIQUE EVALUATION (PHASE III)

The candidates defined in Section 3.2 were further reviewed to determine the final, pertinent information of the ACPS characterization evaluation. This was accomplished by using the Table 6 form guidelines for each finally selected item of Section 3.2. Information which was selected in Phase III is considered the most useful to the ACPS task and is indicated in Tables 4 and 5 by asterisks. Table 4 information denoted by asterisks is more oriented toward descriptive analytical techniques and background information necessary for the ACPS computer modeling. Table 5 items denoted by asterisks are actual computer programs which may be utilized in the ACPS computer simulation. A synopsis of the PHASE III information items is presented in Table 7.

A cursory review was also performed of the Space Shuttle High and Low Pressure Auxiliary Control Propulsion Subsystem Definition studies (References 1, 2, 3, and 4). These studies are being performed by McDonnell-Douglas Corporation and TRW Systems Group, Redondo Beach. A typical high pressure turbopump cycle was obtained from Reference 3 and is shown in Figure 2. A typical low pressure system was obtained from Reference 4 and is shown in Figure 3. These figures represent configurations which are currently considered for the SHAC in ACPS. Therefore, the following will

TABLE 6
ACPS CHARACTERIZATION EVALUATION FORM

TITLE & CLASSIFICATION:

STATE OF THE ART:

PREVIOUS USAGE:

ACCURACY RESULTS:

AVAILABILITY OF CHARACTERIZATION PARAMETERS:

ADAPTABLE OF MODULAR COMPUTER PROGRAM CONSTRUCTION:

ANALYTICAL TECHNIQUES:

APPLICABLE TO ACPS MODELING:

TRANSIENT

STEADY STATE

TABLE 2
PHASE III - IN-STORE EVALUATION SYNOPSIS FOR AGPS RELATED LITERATURE

INDEX	REMARKS	STAR I.D. NO.
1.1	ATA Paper. Advanced state-of-the-art. Highly detailed modeling of turbomachinery designed to miniaturize size and thus reduce tank pressurization (and weight) plus childhood time. NASA study contract. Design data on blade configuration.	A 69-32759
2.1	Executive report of piston-pump configuration, etc. Report deals with detailed design aspects of two-phase pumping such as materials requirements, bearing lubrication, probable too detailed for initial AGPS modeling, however, could be used for later analysis of two phase pumps if weight savings become of paramount importance.	AD-A32042
6.1	Precise state-of-the-art. Models pump, tank, line and couples to liquid engine. Contains plan method of characteristics. Can be utilized for transient analysis if modified for gas-gas system. Gives listing of computer programs.	X65-32330
6.1	Very similar to above document. Used to analyze chattering instability in liquid oxygen. Must be modified for gas-gas system if used in AGPS. Provides good background for feed system coupled stability analysis.	X67-23795
7.1	Precise state-of-the-art; description of steady-state analysis of combustion chamber, liquid tanks, liquid tanks, etc. Very oriented towards J-2 engine. Related to computer program TENSOR.	X67-14913

NOT REPRODUCIBLE

TABLE 7 (CONT'D.)

TOPIC	REMARKS	STAR I.D. NO.
7.3.2 Periodic thermodynamic analysis of hydrodynamic combustion chamber and injector Frontline background for transient analysis but probably too detailed for direct ACPS application.		Frontl. Ppt. Contract WAS7-467
7.3.2 ARIS Journal Paper: Background information for liquid hyperolic engine transient analysis.	ARIS Journal Time 6/9	ARIS Journal Time 6/9
7.3.2 Background information for hyperolic engine transient analysis. Refined peak capabilities in transient analysis.	Described TRB Report No. ARIS 721-6-9-1937	In Response to Report No. ARIS 721-6-9-1937
7.3.2 Part 3 is heat transfer by radiation - other parts (1 and 2) would have more interest. Technical Information Center is trying to locate these.		STAR No. A345587
7.3.2 Testers' Guide concerning testing of a H ₂ /H ₂ engine at different conditions. No analytical models presented; however, provides test data which may be of interest.		STAR No. A345588
7.3.2 ARIS Journal Paper: Hyperolic engine transient analysis. Frontline background information related to hardware.	ARIS Journal Time 6/9	No. Report No. Date probably June 1979 Report No. A345263
7.3.2 Background information.		Report No. 1977-590
7.3.2 Background information.		NOT REPRODUCIBLE

TABLE I (CONT'D)

ITEM	NUMBER	DESCRIPTION	NOTES	STAN. U.S. NO.
7.1	7.1	Background Information		TWA LOC 73-4712-4-93 MAY, 1970
7.2	7.2	Packet and information on transient simulation capabilities with analog computer.	RECS OF steady state performance characteristics such as C, CA, Tsp for 0-2R2 generated from NASA Lewis Thermochanical program.	TRW INC 70-4712-2-23 Feb. 29/70
7.3	7.3	Background information on transient simulation capabilities with digital computer.	More rigor verification. Could be used in steady state analysis of ACPS where the endothermic properties of propellants are necessary.	NASA MEMO from Dugan Hyatt to Traylor and SIE No. 40105-011
7.4	7.4	Indicated data useful for steady state analysis of ACPS.		NASA-TRN 12C
7.5	7.5	Background information.		Contract No. NAS 9-11012
7.6	7.6	Background information.		Contract No. NAS 9-11013
7.7	7.7	Background information.	Initial 1. Order counter flow, crown flow, literature configuration. No. of transistors and No. of logic functions.	REF. NO. 70-4712-4-93 SIE 40105-011

TABLE 7 (CONT'D)

ITEM	REF.	REMARKS	I. D. NO.
1.1.1.1	1.1.1.1	Applicable to Apollo fluid cells with two-phase flow. Parallel flow, finite difference solution technique for steady-state or transient analysis. Radiation heat transfer excluded. Good analysis of two-phase flow considerations.	ADP No. F MSC 420
1.1.1.2	1.1.1.2	Hand-drawn heat exchanger for fixed helical coil configuration. No change of pipe capabilities - could be modified to include this. Applicable to potential AGC heat exchanger configuration.	ADP No. H MSC 1274
1.1.1.3	1.1.1.3	Steady-state, compressible gas flow with or without heat transfer: multiple pipe heat exchanger systems. Ideal for AGC steady-state flow.	ADP No. MSC 461
1.1.1.4	1.1.1.4	Transient steady-state modeling of components with some transient simulations. Currently being revised by Grusman.	GAC Rep. 3 31-43 "49 June 1979 .. ."

NOT REPRODUCIBLE

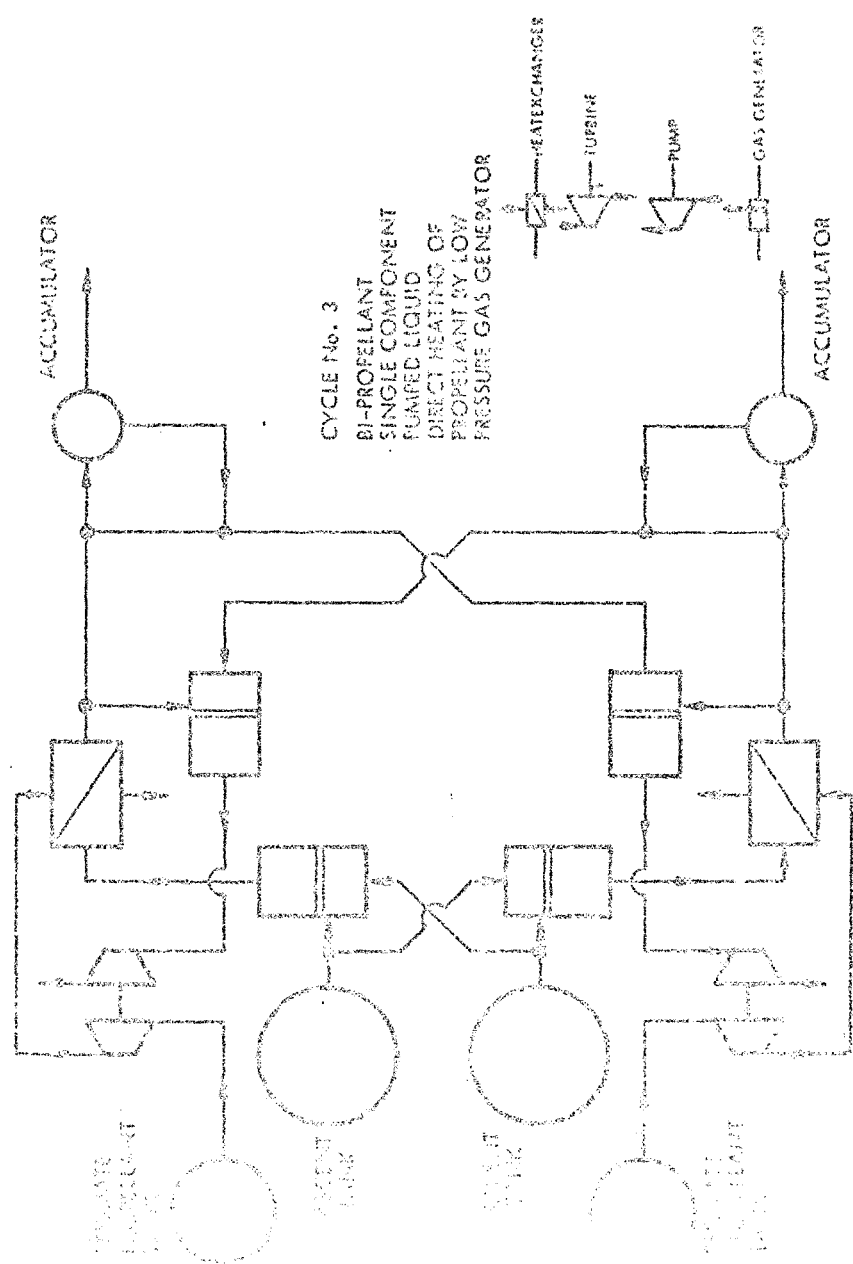


FIGURE 2
ACPS HIGH PRESSURE TURBOPUMP CYCLE

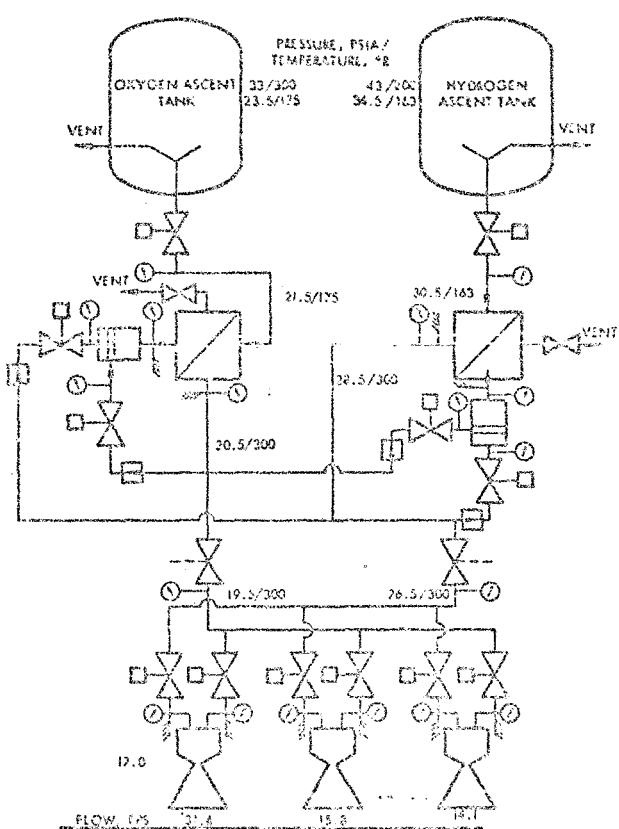


FIGURE 3
ASCENT GAS SYSTEM

The technique evaluation was performed extensively on the supply line model, combustor model and general program organization. Running time, integration techniques, model adequacy (accuracy) and digital computer adaptability (Univac 1108) were evaluated.

The general program organization was evaluated by initially reviewing the Pipetran Computer Program, Reference 5, the Matrix Oriented Production Assembly System (MOPAS), Reference 6, the Propulsion Analysis Program (PAP), Reference 7, and a generalized method of characteristic water hammer program (DVP) by Dr. F. Young supplied to IRW from MSC Auxiliary Propulsion and Pyrotechnics Branch. The ideas and forms associated with the configuration selection, executive operation and modularized form of these programs were useful in setting up the general ACPS programs. The namelist data input was selected for program input due to ease of handling for the engineer. The executive program operation was fashioned after that of the Pipetran program with the configuration selection as input data and the executive driver handling the coupling of components and the solutions of simultaneous equations.

The line model was established as the main program link due to the coupling of line segments with the other ACPS modularized components. The liquid flow or low Mach number gas-line model was, therefore, extensively evaluated. Four programs were established as possible candidates. The method of characteristics solution for the equations governing the unsteady flow of liquids in closed systems (GSL), Reference 8, DVP Program as mentioned above, Pipetran, and a preliminary dynamic line model of the space Nuclear Vehicle from the MPPAC and its Preliminary Design and Analysis, 9, was used. The Pipetran Computer Program was chosen and modified slightly for

the partial differential equations. The dynamics line model from TRW/Redondo Beach was eliminated because it is simplified and not generalized enough for this application. This left two programs which were closely related, the ORI and DYP programs. The DYP program is a generalized model and the ORI program is not. Both programs use the method of characteristics solution as presented in Reference 9 to solve the transient fluid flow equations (including friction terms). The method of characteristics solution technique transforms the partial differential transient fluid flow equations into ordinary differential equations which are then solved by the first order finite difference method. The other method of solution considered was to solve the partial differential equations directly using the finite difference solution. But since this solution may present stability problems, it was decided not to use this approach. Therefore, since both the DYP and ORI programs used the method of characteristics for their solution technique, it was decided to incorporate this technique in the ACPS dynamic line model (Reference Section 3.4.3). The ORI program has substantial documentation with several checkout cases, but the DYP program has been used by the Auxiliary Propulsion and Pyrotechnics Branch at MSC to evaluate Apollo transient data and Skylab propulsion test transient data. It has, therefore, demonstrated its adequacy utilizing actual test data. Therefore, the ACPS supply line model developed for this task will be verified by comparison with the DYP model. Since the solution technique was well understood and neither the ORI nor the DYP programs had the necessary flexibility to fit transient data, the DYP-like ACPS program will be used. The DYP-like ACPS program will be able to handle the transient data and will be able to predict the transient behavior of the system.

approximation. In the ORI model, the Roberts extrapolation procedure (Reference 10) was used to increase the accuracy of the computations and the need for this approach will be evaluated, but at present it does not appear necessary. After evaluating the four programs, it was decided to:

1. Use the method of characteristics.
2. Construct the generalized model using the Streeter (Reference 11) technique as a baseline.
3. Check finite-difference integration for adequacy after model buildup and if necessary, incorporate a more elaborate integration scheme (Roberts, Runge-Kutta, Predictor Corrector, etc.)

The preliminary line model developed on this basis is described in Section 3.4.3.

In selecting a combustion chamber transient model, two TRW models were reviewed. The first was developed for solution on an analog computer and is the one adapted for use in this program. A Runge-Kutta integration scheme was incorporated to adapt it for use on a digital computer. This model is described in Section 3.4.1, as is the evaluation that led to the adoption of the integration scheme. The second model used the rather interesting approach of linearizing the equations over each time step and obtaining a semi-analytical solution. This approach has some merit, but in this particular formulation the treatment of sonic flow into the chamber and of the valve forcing function did not appear to be satisfactory. The claimed advantage of this second approach is that the computational time step sizes could be double that which can be used with the Runge-Kutta scheme. However, realization of this advantage would require that the two models be put into incompatible codes, which may not differ in more than just their interface. The first model is much easier to code than the second. After all,

3.4 RECOMMENDED TECHNIQUES

The fourth phase of the characterization evaluation was to recommend to the NASA Task Monitor those techniques identified in PHASE III of this subtask as applicable to the characterization of ACPS components. The recommended techniques provide a high degree of accuracy and are amenable to computer solutions. The results of this subtask upon approval by the NASA Task Monitor will form the basis for the program development under Subtask II.

This section recommends transients and steady-state modeling techniques for the following components:

Combustors and gas generators

Manifolds and Injectors

Turbomachinery

Heat Exchangers

Accumulators and Pressure Vessels

Supply Lines

Orifices, Pipebends and Valves

The steady-state program will consist of a main-driver program and subroutines representing the components. After initialization, the steady-state program will essentially consist of a set of non-linear simultaneous algebraic equations written in implicit form. The choice of which variables are known and which ones are to be solved for will be determined by input selected by the user. For example, in the combustor chamber, the chamber pressure and area (for interface) may be known and the throat area and chamber pressure unknown.

13 pages

program. The nature of the equations in the transient program will require that hardware dimensions and hardware characteristics, such as resistances, be input, and flow conditions, e.g., velocity, pressure, etc., will be calculated by the program as a function of time.

3.4.1 TRANSIENT COMBUSTOR MODEL

A preliminary dynamic model of an ACPS combustor has been developed on the time share terminal and implemented on the MSC 1108 computer. This basic model will be used as the combustor component of the total ACPS transient program. A study was performed utilizing this preliminary combustor model to determine its numerical stability and running time, and to investigate the advantages of various numerical integration techniques. This model will eventually be expanded to include curve fits of combustor performance data for a typical engine thruster.

Based on the study results, the following conclusions were made:

- 1 - Representation of the ACPS combustors with this type model appears satisfactory and a more detailed model will be constructed with this characterization as the foundation.
- 2 - Numerical integration of the model equations utilizing Euler's integration scheme is relatively unstable. After thrust build-up and during the period that the engine simulation is in steady-state, the simulated chamber pressure oscillates ± 0.3 psia with a 0.01 millisecond (ms) computation interval and ± 2 psia with a 0.25 ms computation interval. The solution never stabilizes.
- 3 - The Runge-Kutta integration scheme operates very well with the model equations. No oscillations were observed during any of the computation intervals. The solution stabilizes after 2.4 ms of calculations and only becomes unstable if a computation interval is 0.5 ms or greater.

model has been set up initially as a "stand alone" model which operates with a constant pressure boundary upstream of the chamber, thereby eliminating the effects of any feedline perturbations for this study only. This was done to simplify the stability, time step, and integration study.

During the checkout phase of the program development, the combustor model was exercised as a "stand alone" program for simulating a typical engine. For this checkout phase, a test case was employed with the combustor model to utilize gaseous oxygen and gaseous hydrogen as propellants with the following input data: characteristic exhaust velocity = 7500 ft/sec, nozzle throat area = 5.1 in^2 , combustor gas temperature = 6000°R , and the specific heat ratio was fixed at 1.4. The propellant feedlines to the combustor were maintained as a constant pressure boundary of 360 psia and a temperature of 530°R . The propellant flow control valves were opened instantaneously and transient profiles of the propellant flow into the combustor and the chamber pressure were calculated.

The model was exercised at various integration step sizes using both the Euler and the Runge-Kutta numerical integration schemes. Arbitrary variations were used for the integration step sizes to evaluate the maximum integration interval which can be effectively utilized, the accuracy of the results and the model's stability. The integration step sizes examined were 0.01, 0.10, 0.25 and 0.4 ms. As noted on Figure 4 the simple Euler integration scheme has a transient response which is somewhat erratic except for the 0.01 ms step size. With a step size of 0.5 ms the Euler scheme exhibits a rather slow and steady transient.

At a step size of 0.25 ms, the oscillations are ± 2 psia while for a step size of 0.1 ms, the oscillations are approximately ± 5 psia.

In an attempt to decrease the running time and increase the accuracy achieved with the Euler technique, the Runge-Kutta integration scheme was evaluated at calculation intervals of 0.01, 0.1, 0.25, and 0.4 ms.

Stable solutions were obtained as noted in Figure 5. As the integration interval was increased to 0.5 ms, the transient pressure rise becomes less accurate during the period from 0.8 ms to 4.0 ms of elapsed time as noted from the slow pressure buildup shown in Figure 5. By 4 ms, all solutions reached a steady-state simulation of 310 psia chamber pressure. The integration step size was increased to 0.5 ms and the solution diverged extensively from the true physical system and went unstable because too much propellant was allowed into the chamber, thus driving the model into a reverse flow situation.

From this study it was concluded that a Runge-Kutta integration scheme will be satisfactory. A computational step size of approximately 0.25 ms, which is one-fourth the step size being utilized with the dynamic feedline model, appears to be ideal.

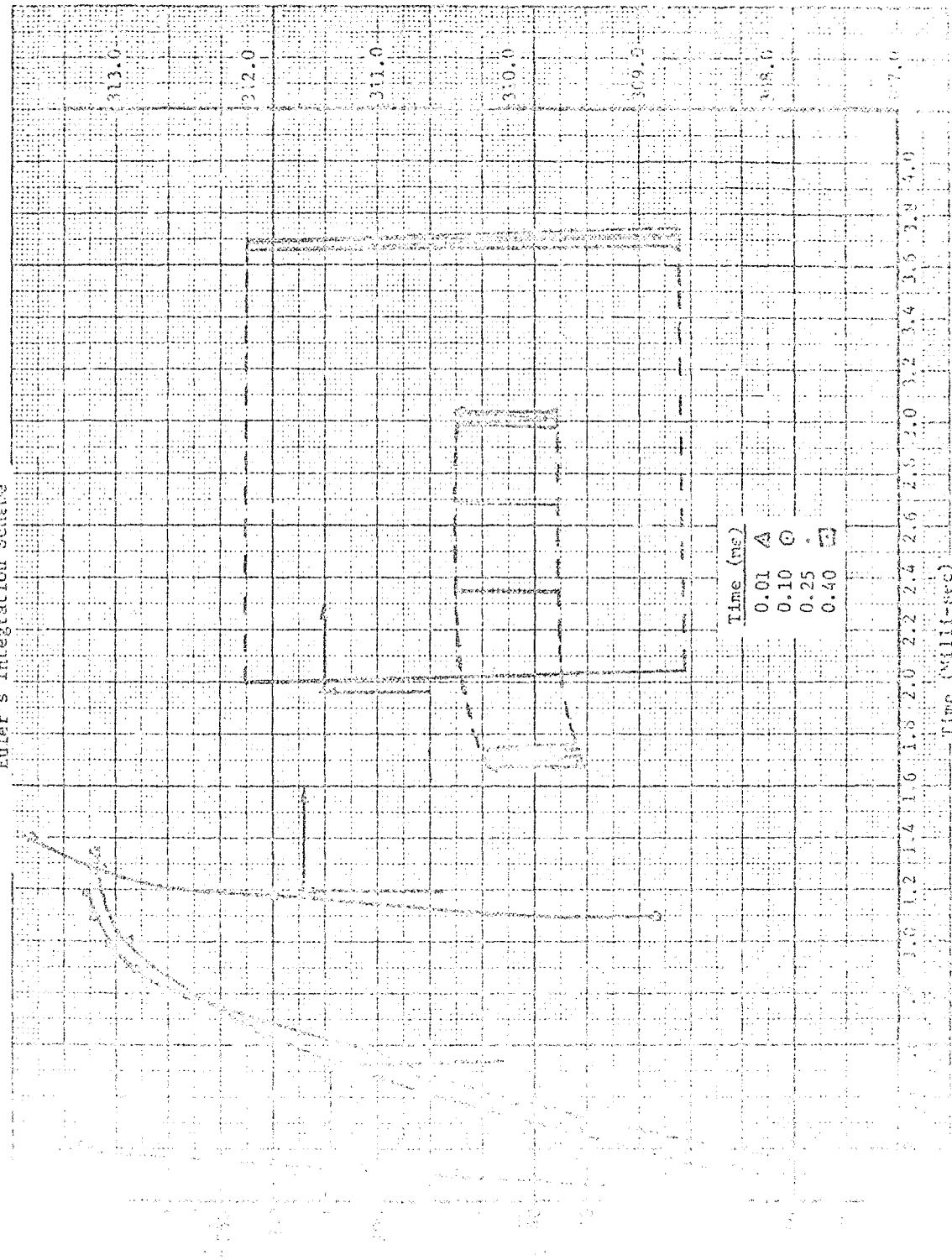
Implementation of more extensive combustor performance data, a manifold accumulation model, and a flow control valve characterization are still required for the combustor model. Performance for a typical thruster will be generated using the data from the ICRPC computer programs (References 12-16). This will consist of specific impulse as a function of mixture ratio, combustor inlet preselected temperatures, thrust, expansion ratio and possibly, chamber pressure. For various thrust levels, it will be desired to determine the total mass delivered per second using the CFC code developed at the Department of

calculated from chamber pressure, vacuum thrust coefficient and combustor throat area. The combustion temperature will be calculated as a function of mixture ratio and possibly of chamber pressure. Implementation of the preceding will complete the dynamic combustor model development.

NO. 2104M SIEGMUND GRAPH PAPER
MILLIMETERS

EUGENE OTTERSON CO.
MADE IN U. S. A.

Figure 4 Combustor Chamber Model
Euler's Integration Scheme

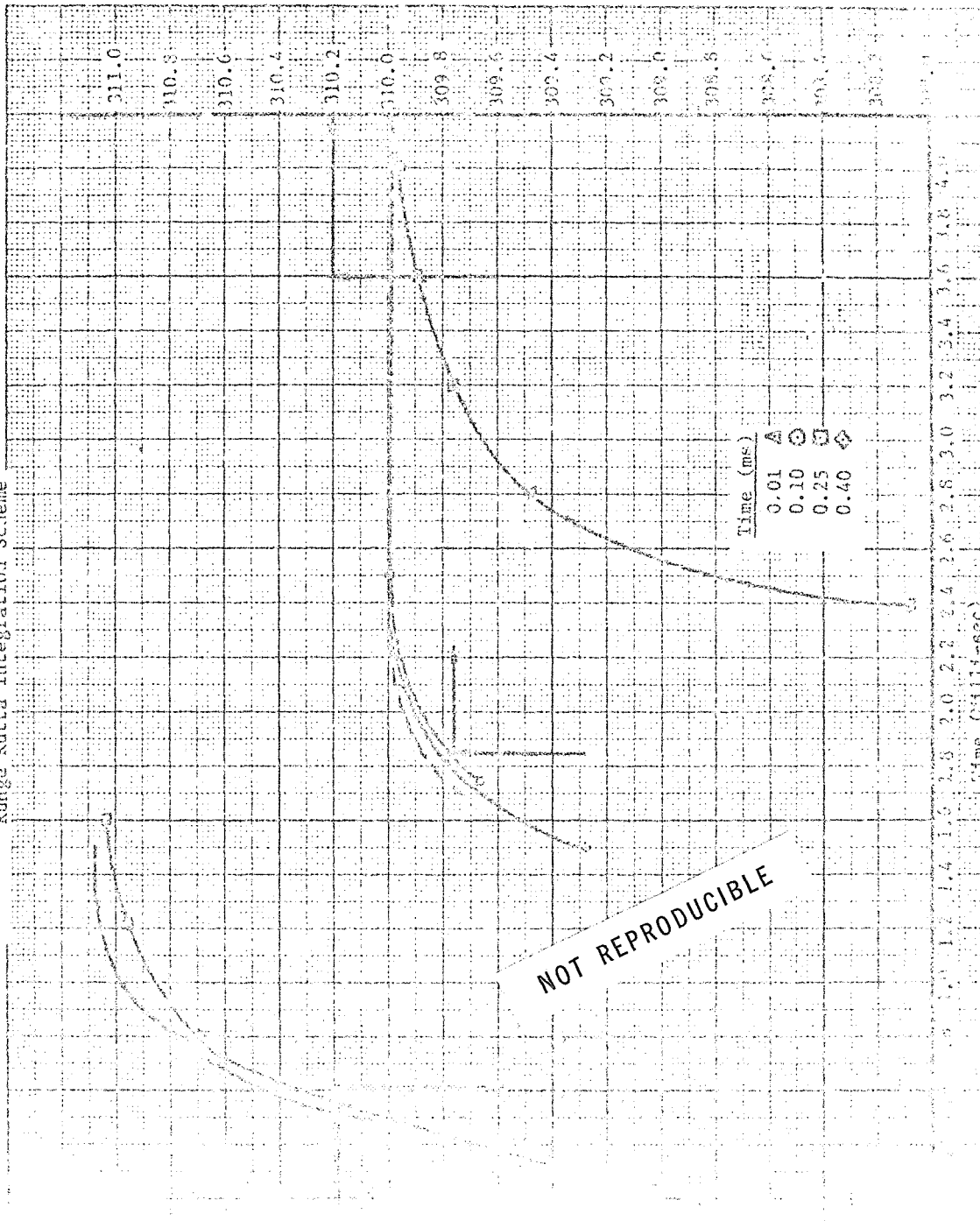


NO. 2000-4 CUTTING BRANCH SAPPER
MATERIAL

EUGENE DITZGEN CO.
MADE IN U. S. A.

100

Figure 5 Combustor Chamber Model Runge Kutta Integration Scheme



COMBUSTOR DYNAMIC ACPS MODEL EQUATIONS

The combustor model is schematically shown in Figure 6. The combustor model to be utilized in the ACPS transient program interfaces with the feed line model and will utilize input from that model to solve a set of simulations equations for a variable number of thrusters and feed lines. The model will use a Newton-Raphson technique to solve the equations and will operate with the use of the Runge-Kutta integration scheme. The program nomenclature and units are described at the end of this discussion.

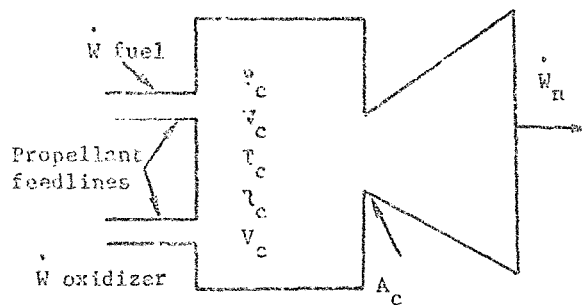


FIGURE 6 - Combustor Model Schematic

The initial entry into the combustor model establishes the following:

- 1) The number of combustors
 - 2) The number lines connected to combustor I.
 - 3) The number of the feedline hooked to combustor I and Line II.
 - 4) The specific heat ratio of combustor gases
 - 5) The volume of 1th combustor.
 - 6) The gas content of combustor I.

Then, the following section will introduce the proposed model and its implementation. The last section will conclude the paper.

The combustor model utilizes the data from the last two nodal points to the inlet feedlines to calculate the (n+1) point of the junctions between the combustor and feedlines.

The parameters (v_R , z_R , p_R) at point R, are calculated in the same fashion as in the line model (Section 3.4.3). See Section 3.4.3 for nomenclature for v_R , z_R , and p_R .

$$w_R = \frac{v_{i,j}^n - \phi_i a_i (v_{i,j}^n - v_{i,j-1}^n)}{1 + \phi_i (v_{i,j}^n - v_{i,j-1}^n) / (\rho_i A_i)}$$

$$z_R = z_{i,j} - \phi_i \left(\frac{v_R}{\rho_i A_i} + a_i \right) (z_{i,j} - z_{i,j-1})$$

$$p_R = p_{i,j}^n + \frac{g \rho_i z_{i,j}}{g_c 144} - \phi_i \left(\frac{v_R}{A_i \rho_i} + a_i \right)$$

$$\left(p_{i,j}^n + \frac{g \rho_i z_{i,j}}{g_c 144} - p_{i,j-1}^n - \frac{g \rho_i z_{i,j-1}}{g_c 144} \right) - \frac{g \rho_i z_R}{g_c 144}$$

The weight of gas in the combustor is calculated based on the flowrate in the feedlines since the nozzle flow:

$$V_{\text{combustor}} \approx \int_{j=1}^{j=n} (A_{j,\text{feed}} - A_{j,\text{nozzle}}) \cdot Q_j$$

This equation is calculated using Runge-Kutta integration.

The chamber pressure is calculated based on the perfect gas equation of state,

$$P_c = \frac{W_c R_c T_c}{V_c}$$

The nozzle flowrate is calculated from the characteristic exhaust velocity equation.

$$\dot{W}_n = \frac{P_c A_n \epsilon_c}{C^*}$$

If sonic flow exists in the injector orifices, the flowrate into the chamber for each line is

$$\dot{W}_c = A_i P_1 C_v \sqrt{\frac{\epsilon_c}{RT}} \left(\frac{2}{\gamma+1} \right)^{(\gamma+1)/(\gamma-1)} \quad (1)$$

, and the pressure at the junction of the lines less the manifold pressure loss is equivalent to the pressure in the injector orifices; therefore,

$$P_{\text{into combustor}} = \Delta P_{\text{manifold}} + P_{\text{lines}} \quad (2)$$

The flow from the line model (Section 3.4.3) into the chamber is as follows:

$$\dot{W} = C3 - P_1 \text{ (final node)} \quad (3)$$

where:

$$C3 = -w_R + \frac{A_i}{s_i} (g s_i z_{I,j} - 166 s_i P_R - \delta s_i x_R) + \frac{A_i}{s_i} w_R (\sin \alpha_i) \Delta z + \frac{C_v w_i |_{x_i}}{2(G_i^2 / I_i^2) s_i z_i}$$

(See Section 3.4.3 for nomenclature)

$$C3 = \frac{(P_{\text{manifold}} - P_{\text{lines}})^2}{G_i^2 / I_i^2}$$

ignoring the nozzle flow losses for 1 so that flow is assumed to enter the chamber at 1. The 2 above gives the following:

$$w_i = \sqrt{\frac{P_{\text{manifold}}^2 - P_{\text{lines}}^2}{G_i^2 / I_i^2}}$$

NOT REPRODUCIBLE

Solving for the pressure in the manifold orifice one gets

$$P_1 = \frac{C_3}{C_1 + A C_v \sqrt{\frac{R}{RT}} \left(\frac{2}{\gamma+1} \right)^{(\gamma+1)/(\gamma-1)}}$$

If the flow through the injector is subsonic it is defined by the compressible gas flow relationship

$$\dot{m}_c = P_1 A C_v \sqrt{\frac{R_c}{RT}} \left[\left(\frac{P_c}{P_1} \right)^{2/\gamma} - \left(\frac{P_c}{P_1} \right)^{(\gamma+1)/\gamma} \right] = P_1 A C_v \phi \quad (4)$$

Equating Equation 4 to Equation 3 and setting that equal to zero a function C_7 is defined

$$C_7 = 0 = C_3 - P_1 C_1 - P_1 C_v \phi \quad (5)$$

Calculating the derivative of Equation 5, one gets:

$$\frac{dC_7}{dP} = -C_1 - C_v A \phi + \frac{P_1}{2\beta} \left[\frac{2}{\gamma} \left(\frac{P_c}{P} \right)^{\frac{2-\gamma/\gamma}{\gamma}} \left(-\frac{P_c}{(P)^2} \right) - \frac{\gamma+1}{\gamma} \left(\frac{P_c}{P} \right)^{1/2} \left(-\frac{P_c}{(P)^2} \right) \right]$$

Using Newton-Raphson method of solution;

$$P_1 = P_1 - \frac{C_7}{dC_7/dP}$$

and iterate until the following convergence criteria is obtained

$$\frac{|dC_7|}{dP} < 0.001$$

NOMENCLATURE FOR COMBUSTOR MODEL COMPUTER SUBROUTINE CHAM (7)

<u>NAME</u>		<u>UNITS</u>
γ	Specific heat ratio	
NLC	Number lines connected to the I^{th} combustor	
ICHAM	The I^{th} combustor connected to the N^{th} line	
C	Constant portion of SP equation	
C1	Constant portion of WP equation	
\dot{w}_n	Nozzle flow of I^{th} combustor	lbm/sec
w_c	Weight of gas in the I^{th} combustor	lbm
p_c	Chamber pressure in I^{th} combustor	psia
R_c	Gas constant on combustor	ft/lb $^{\circ}$ R
T_c	Temperature of gas in combustor	$^{\circ}$ R
V_c	Volume of I^{th} Combustor	in 3
A_i	Area injector	in
A_n	Nozzle throat area I^{th} combustor	in 2
C6,8,9,10	Constants in derivative of pressure equation	
$\frac{dC7}{dp}$	Derivative of pressure equation variable	
C7	Pressure equation expression for subsonic flow	
\dot{w}	Temporary injector flow rate	lbm/sec
r_{cr}	Critical pressure ratio I^{th} line J^{th} node	
C_v	Flux coefficient	
\dot{w}_c	Weight flow rate into chamber	lbm/sec
F_1	Injector orifice specific resistance	psi 2 /sec

Further, it is proposed to add the following conditions to
the present contract, as follows:

S Value interpolated in the X-direction lying on a right running characteristic that passes through the grid point at which the flow variables are to be determined.

3.4.2 Steady-State Combustor

The steady-state model of an ACPS combustor will use curve fits of chamber performance data, calculated using the ICREG programs, to describe the steady-state operation of combustion chamber parameters. Curves are presently available, but may require modifications to account for effects of chamber pressure variations. Evaluation of the curve fits are being performed by comparing them with data from TRW Redondo Beach's high and low pressure ACPS studies.

The model calculations will be performed as follows:

The specific impulse is given by:

$$ISP_v = f(MR, T_{O_2}, T_{H_2}, F, \epsilon, P_c)$$

The thrust coefficient is given by:

$$C_f = \text{Constant}$$

The characteristic exhaust velocity if given by:

$$C^* = \frac{g_c ISP}{C_f}$$

The nozzle flowrate is given by:

$$\dot{m}_n = \frac{P_c A_t g_c}{C^*}$$

The combustion gas temperature is given by:

$$T_c = f(MR \text{ and possibly } P_c)$$

NOMENCLATURE

T_{O_2}	Inlet Temperature	$^{\circ}\text{R}$
T_{H_2}	Inlet Temperature	$^{\circ}\text{R}$
A_t	Area Combustor Throat	
F	Thrust	lbf
ϵ	Expansion Ratio	
P_c	Chamber Pressure	psia
ISP_v	Vacuum Specific Impulse	sec
T_c	Chamber Temperature	$^{\circ}\text{R}$
C^*	Characteristic Exhaust Velocity	ft/sec
W_{O_2}	Oxidizer flowrate	lbm/sec
W_{H_2}	Fuel flowrate	lbm/sec
W_n	Nozzle flowrate	lbm/sec
MR	Mixture ratio	
g_c	Conversion constant	$32.2 \frac{\text{lbm-ft}}{\text{sec}^2 \cdot \text{lbf}}$

3.4.3 Supply Line Transients

In order to model the ACPS transients, analytical representations of the fluid lines must be available. A generalized line network model has been programmed on the Univac 1108 computer. The model is suitable for both gases at low Mach numbers and liquids. The program, which is in the preliminary stages of development and checkout, will be able to handle networks of considerable complexity. Presently, it can treat networks consisting of distributed lines, junctions, valves, pressure boundaries, and flow boundaries. Pressure boundaries are pipe ends at which the pressure as a function of time is specified. Flow boundaries are similar except that the flow rate as a function of time is specified. In the case of valves, the resistance versus time must be given. As components which are necessary for the computation of an ACPS transient are developed, they will be incorporated into the program. For instance, the combustor model described in Section 3.4.1 will be added shortly. In the paragraphs that follow, the equations used are described and some results are given.

The partial differential equations representing the one-dimensional flow of a liquid in a pipe are given in Reference 11 as

$$R \frac{\partial H}{\partial t} + d^2 \frac{\partial V}{\partial X} + \rho V \frac{\partial H}{\partial X} + gV \sin \alpha = 0 \quad (1)$$

$$d \frac{\partial H}{\partial X} + V \frac{\partial V}{\partial X} + \frac{\partial V}{\partial t} + \frac{fV|V|}{2g} = 0 \quad (2)$$

H is the head, α is the angle of incline, g is the local acceleration, V is the velocity of the fluid, L is the distance along the pipe, R is the pipe radius, f is the pipe friction factor, t is time, and ρ is the density of the fluid. The value of the friction factor for pipes of diameter 1 in. and 10 ft is 0.020.

or nearly zero, the above two equations are not satisfactory. This is because the product of g times H as g approaches zero becomes the indeterminate form of $0/0$. The equations can be readily put into a form suitable for use at both zero and non-zero g^2 by making the substitution:

$$H = 144 \frac{g_c}{g} \frac{P}{\rho} + Z \quad (3)$$

P is the static pressure, ρ is the fluid density, Z is the elevation, and g_c is a conversion factor.

Equations 1 and 2 which are hyperbolic in form can be solved by substituting directly a finite-difference approximation for each term or by converting them into four equivalent ordinary differential equations by the method of characteristics and then substituting finite-difference approximations into them (see References 17, 18, and 19). The former approach has some advantages (see References 18 and 19), but there appear to be no cases reported in the literature of equations having exactly the form of Equations 1 and 2 being solved in this manner, although there are examples for somewhat similar sets (References 17 and 20). In Reference 11, the method of characteristics was used and in this reference are presented several comparisons of the computational results with experimental data. The agreement was excellent. Thus, for the sake of expediting the task, the method of characteristics was chosen to solve (3) and (2). It would be interesting, however, to make a comparison between the two approaches and this will be done if time allows. The equations used in the transient fluid flow program are presented at the end of this section. They may easily be derived from the equations given in Reference 13, substituting Equation 3 where required.

Equations 1 and 2 are "frozen" in the computer code of Reference 13.

It is felt that the appropriate way to obtain the desired approximation is to use a different numerical scheme and to

the density is constant, Equations 1 and 2 become, respectively,

$$\frac{144 g_c}{\rho} \frac{\partial P}{\partial t} + a^2 \frac{\partial V}{\partial X} + 144 g_c \frac{V}{\rho} \frac{\partial P}{\partial X} = 0 \quad (5)$$

$$\frac{144 g_c}{\rho} \frac{\partial P}{\partial X} + V \frac{\partial V}{\partial X} + \frac{\partial V}{\partial t} + \frac{fV|V|}{2D} = 0 \quad (6)$$

The continuity equation and equation of motion suitable for the one-dimensional flow of a gas are from Reference 21, p. 972,

$$\frac{\partial P}{\partial t} + \rho \frac{\partial V}{\partial X} + V \frac{\partial \rho}{\partial X} = 0 \quad (7)$$

$$\frac{144 g_c}{\rho} \frac{\partial P}{\partial X} + V \frac{\partial V}{\partial X} + \frac{\partial V}{\partial t} + \frac{fV|V|}{2D} = 0 \quad (8)$$

Equation 8 is identical to Equation 6.

Multiplying both sides of Equation 7 by $\frac{\partial P}{\partial \rho}$ and a conversion factor gives

$$144 \frac{\partial P}{\partial \rho} \frac{\partial \rho}{\partial t} + 144 \rho \frac{\partial P}{\partial \rho} \frac{\partial V}{\partial X} + 144 V \frac{\partial P}{\partial \rho} \frac{\partial \rho}{\partial X} = 0 \quad (9)$$

Using the fact that for an isentropic process

$$\frac{144 \frac{\partial P}{\partial \rho}}{\partial \rho} = \frac{a^2}{E_c} \quad (10)$$

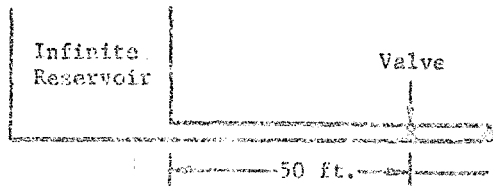
Equation 9 becomes identical to Equation 5.

The equations in Appendix A are based on the speed of sound remaining constant in the pipe and the density being independent of the velocity. In a gas, these assumptions hold fairly well for Mach numbers less than about 0.2. For higher Mach numbers, the energy equation and the equation of state must be solved along with Equations 7 and 8.

To check the transient model, the flow rates and pressures at points in a 50-foot horizontal, frictionless steel pipe were calculated after the sudden closure of a valve (see the following illustration). Before the valve closed, the fluid which occupied most of the pipe was flowing steadily. The calculations

for a 50-foot pipe maintained the conditions given. Starting with the initial conditions given above, the flow rate and pressure at point 1 were calculated.

in References 19 and 22. The plot of pressure at the valve as a function of time should be nearly a perfect square wave. Since this analytical model takes into account the fact that the wave velocity with respect to the pipe travels at the speed of sound plus or minus the velocity of the fluid, the wave shape will differ from a square wave. However, at the fluid velocity used in this example, about 1.64 ft/sec, the difference should be imperceptible. At very high fluid velocities the wave shape will differ considerably from a square wave.



Fluid velocity, 1.64 ft/sec
 Speed of sound in pipe, 4067 ft/sec
 Friction factor, 0
 Pressure in pipe before valve closure, 100 psia

TEST CASE

Four different computer "runs" were made. The first was for a computational time increment of 1.0 ms and a value of S of 0.001. S is a value which determines the size of the length increment, ΔX , once the time increment, Δt has been selected. It is shown in References 19 and 22 that S must equal or exceed the ratio of the maximum velocity in the pipe to the speed of sound in the pipe. The pressure at the valve is shown in Figure 1a and the flow rate at the entrance to the pipe is shown in Figure 1b. The results agree quite satisfactorily with those anticipated. The pressure amplitude agrees exactly with the predicted sinusoidal variation. The flow rate

but S was set to 0.2. Increasing S has the effect of introducing an artificial dampening which again is the result of the numerical approximations. Reducing the time increment, however, will eliminate the effect. This is shown in Figures 9a and 9b where S is equal to 0.2, but the time increment is 0.15 ms. The effect of violating the stability criterion is depicted in Figures 10a and 10b. In these, S is -0.2 and the time increment is 1.0 ms. In this case, the solution diverges wildly. The results given in Figures 7-10 indicate that for maximum accuracy for a given time increment, S should be as small as possible without violating the stability criterion.

EQUATIONS FOR TRANSIENT FLUID FLOW PROGRAM

Initial Calculations

$$a_i = \sqrt{\frac{144 B_i g_c}{\rho_i (1 + \frac{B_i D_i}{E} e_i) c}} \quad \text{-- for liquid line} \quad (1a)$$

$$a_i = \sqrt{\gamma_i \epsilon_c R_i T_i} \quad \text{-- for gas line} \quad (1b)$$

$$\text{Minimum } \Delta X_i = (1. + S) (\Delta t) a_i \quad (2)$$

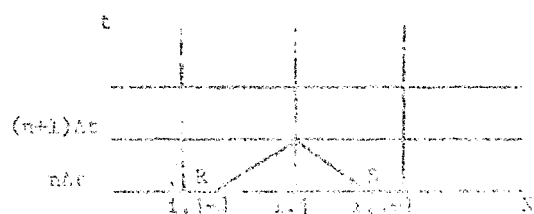
$$N_i = \frac{L_i}{\text{Minimum } \Delta X_i} + i \quad (N_i \text{ is an integer } \leq \text{ to the R.H.S.}) \quad (3)$$

$$\Delta X_i = \frac{L_i}{N_i - 1} \quad (4)$$

$$A_i = \frac{\pi D_i^2}{4(144)} \quad (5)$$

$$\epsilon_i = \Delta t / \Delta X_i \quad (6)$$

Interior Pipeline Points



Computing grid

$$\begin{aligned} \frac{dV}{dt} &= \frac{dV}{dx} \frac{dx}{dt} = V_{i,j+1} - V_{i,j-1} \\ \frac{dV}{dt} &= \frac{dV}{dx} \frac{dx}{dt} = V_{i,j+1} - V_{i,j-1} \end{aligned}$$

NOT REPRODUCIBLE

$$z_R = z_{i,j} - \theta_1 \left(\frac{v_R}{\rho_i A_i} + a_i \right) (z_{i,j} - z_{i,j+1}) \quad (9)$$

$$z_S = z_{i,j} + \theta_1 \left(\frac{v_S}{\rho_i A_i} - a_i \right) (z_{i,j} - z_{i,j+1}) \quad (10)$$

$$\begin{aligned} p_R &= p_{i,j}^n + \frac{\rho_i z_{j,j+1}}{\rho_c 144} - \theta_1 \left(\frac{v_R}{\rho_i A_i} + a_i \right) \left(p_{i,j}^n + \frac{\rho_i z_{i,j}}{\rho_c 144} - \frac{p_{i,j+1}^n - \rho_i z_{i,j+1}}{\rho_c 144} \right) \\ &\quad - \frac{\rho_i z_R}{\rho_c 144} \end{aligned} \quad (11)$$

$$\begin{aligned} p_S &= p_{i,j}^n + \frac{\rho_i z_{i,j}}{\rho_c 144} + \theta_1 \left(\frac{v_S}{\rho_i A_i} - a_i \right) \left(p_{i,j}^n + \frac{\rho_i z_{i,j}}{\rho_c 144} - \frac{p_{i,j+1}^n - \rho_i z_{i,j+1}}{\rho_c 144} \right) \\ &\quad - \frac{\rho_i z_S}{\rho_c 144} \end{aligned} \quad (12)$$

$$\begin{aligned} v_{i,j}^{n+1} &= 0.5 \left[v_R + v_S + \frac{A_i}{A_j} \left(144 \rho_c p_R + \rho_i \rho_S - 144 \rho_c p_S - \rho_i \rho_R \right) \right. \\ &\quad \left. - \frac{A_i}{A_j} \rho_S \sin(\phi_i) (v_R - v_S) - \frac{f_i \Delta x (\rho_i \sin(\phi_i) v_R - v_S)}{2 \rho_i A_i (D_i / 12)} \right] \quad (13) \end{aligned}$$

$$\begin{aligned} v_{i,j}^{n+1} &= 0.5 \left[v_R + \frac{\rho_i \rho_S}{144 \rho_c} + \frac{v_R + \rho_i \rho_S - v_S}{144 \rho_c} + \frac{v_R + \rho_i \rho_S - v_S}{144 \rho_c} - \frac{\rho_i \rho_S - v_R}{144 \rho_c} \right. \\ &\quad \left. - \frac{f_i \Delta x (\rho_i \sin(\phi_i) v_R - v_S)}{2 \rho_i A_i (D_i / 12)} \right] \end{aligned}$$

NOT REPRODUCIBLE

PRESSURE BOUNDARY

$P_b = f(t)$ is given.

a) Boundary is at upstream end of pipe. $j = 1$

Compute w_S , z_S , and P_S using Equations 8, 10 and 12, respectively.

$$\begin{aligned} w_{i,j}^{n+1} &= w_S + \frac{A_i}{a_i} (144 g_c P_b + g c_j z_{i,j} - 144 g_c P_S - g c_i z_S) + g \frac{v_S}{a_i} (\sin \alpha_i) \Delta t \\ &\quad - \frac{c_i v_S |w_S| \Delta t}{2 A_i^2 (O_i/12)} \end{aligned} \quad (15)$$

b) Boundary is at downstream end of pipe. $j = N_j$

Compute w_R , z_R , P_R using Equations 7, 9, and 11, respectively.

$$\begin{aligned} w_{i,j}^{n+1} &= w_R + \frac{A_i}{a_i} (144 g_c P_b + g c_j z_{i,j} - 144 g_c P_R - g c_i z_R) - g \frac{v_R}{a_i} (\sin \alpha_i) \Delta t \\ &\quad - \frac{c_i v_R |w_R| \Delta t}{2 A_i^2 (O_i/12)} \end{aligned} \quad (16)$$

VALVE

Set i to its value for the downstream pipe. $j = 1$

Compute w_S , z_S , and P_S using Equations 8, 10 and 12, respectively.

$$C1 \approx -w_S + \frac{c_i}{a_i} (g c_1 z_{j,1} - 144 g_c P_S - g c_i z_S) + g \frac{v_S (\sin \alpha_i) \Delta t}{a_i} - \frac{c_i v_S |w_S| \Delta t}{2 (O_i/12)} \quad (17)$$

$$CP \approx -w_S + \frac{c_i}{a_i} (144 g_c P_S + g c_1 z_{j,1} - 144 g_c P_S - g c_i z_S) + g \frac{v_S (\sin \alpha_i) \Delta t}{a_i} - \frac{c_i v_S |w_S| \Delta t}{2 (O_i/12)}$$

and 1 for computation of w_S for the upstream pipe.

$$\begin{aligned} w_{i,j}^{n+1} &= w_S + \frac{A_i}{a_i} (144 g_c P_S + g c_1 z_{j,1} - 144 g_c P_S - g c_i z_S) \\ &\quad + g \frac{v_S}{a_i} (\sin \alpha_i) \Delta t \end{aligned}$$

$$C_4 = \frac{A_i}{a_i} g_c 144 \quad (20)$$

$$C_5 = 2k^2 g_c p(144) \left(\frac{1}{C_4} - \frac{1}{C_2} \right) \quad (21)$$

$$C_6 = 2k^2 g_c p(144) \left(\frac{C_3}{C_4} - \frac{C_1}{C_2} \right) \quad (22)$$

$$\text{If } C_6 < 0, v = \frac{C_5}{2} - \sqrt{\frac{C_5^2 + 4C_6}{2}} \quad (23)$$

$$\text{If } C_6 \geq 0, v = -\frac{C_5}{2} + \sqrt{\frac{C_5^2 + 4C_6}{2}} \quad (24)$$

$$w_{i,j}^{n+1} = v \quad (25)$$

$$p_{i,j}^{n+1} = -\frac{v_{i,j}^{n+1}}{C_2} - \frac{C_3}{C_4} \quad (26)$$

Set i again to its value for the downstream pipe. $j=1$

$$w_{i,j}^{n+1} = w \quad (27)$$

$$p_{i,j}^{n+1} = -\frac{w_{i,j}^{n+1}}{C_2} - \frac{C_3}{C_2} \quad (28)$$

FLOW RATE BOUNDARY

$w_b = f(t)$ is given

a) Boundary is at upstream end of pipe. $j=1$

Compute w_s, f_s, p_s

Compute C_1 and C_2 using Equations 17 and 18, respectively.

$$w_{i,j}^{n+1} = w_b \quad (29)$$

NOT REPRODUCIBLE

$$\frac{C_1}{C_2} = \frac{w_s^{n+1}}{w_b}$$

b) Boundary is at upstream end of pipe. $j = N_i$

Compute w_R , z_R , p_R

Compute $C3$ and $C4$ using Equations 19 and 20, respectively.

$$w_{i,j}^{n+1} = w_b \quad (31)$$

$$p_{i,j}^{n+1} = -\frac{C3}{C4} + \frac{w_{i,j}^{n+1}}{C4} \quad (32)$$

N-PIPE JUNCTION

For each pipe downstream of the junction. $j = 1$

Compute w_S , z_S , p_S

Compute $C1_j$ using Equation 17 and $C2_j$ using Equation 18.

For each pipe upstream of the junction. $j = N_i$

Compute w_R , z_R , p_R

Compute $C1_j$ using Equation 19 and $C2_j$ using Equation 20.

$$p = -\frac{\sum C1_j}{\sum C2_j} \quad (33)$$

If pipe is upstream $j = N_i$, if downstream $j = 1$.

$$p_{i,j}^{n+1} = p \quad (34)$$

$$z_{i,j}^{n+1} = z_{i,N_i} + C1_j \quad (35)$$

NOMENCLATURE

A	Cross-sectional area of pipe	ft^2
a	Speed of sound	ft/sec
c	Correction for the effect of Poisson's ratio	
E	Young's modulus of pipe	psi
D	Pipe diameter	in
e	Pipe thickness	in
f	Friction factor	
g	Acceleration	ft/sec^2
g_c	32.174	$\text{lbf-ft}/(\text{sec}^2 \cdot \text{lbf})$
B	Bulk modulus of elasticity of liquid	psi
L	Pipe Length	ft
N	Number of nodes in pipe	
P	Pressure	psi
Q	Flow rate	lbm/sec
z	Elevation	ft
t	Time	sec
X	Distance along pipe	ft
Δt	Time increment	sec
ΔX	Length increment	ft
α	Angle pipe makes with horizontal	deg.
ρ	Density	lbf/ft^3
ν	Viscosity coefficient	ft^2/sec
μ	Correlation length	$\text{ft}, \text{m}, \text{miles}$
ϵ_{ref}	Reference error	%
ϵ_{rel}	Relative error	%

NOMENCLATURE (Continued)

Subscripts

- i Indicates ith pipe
- j Indicates jth node in pipe
- R Value interpolated in the X-direction lying on a left running characteristic that passes through the grid point at which the flow variables are to be determined.
- S Value interpolated in the X-direction lying on a right running characteristic that passes through the grid point at which the flow variables are to be determined.
- b Value specified at end of pipe

Superscripts

- n Indicates nth time interval

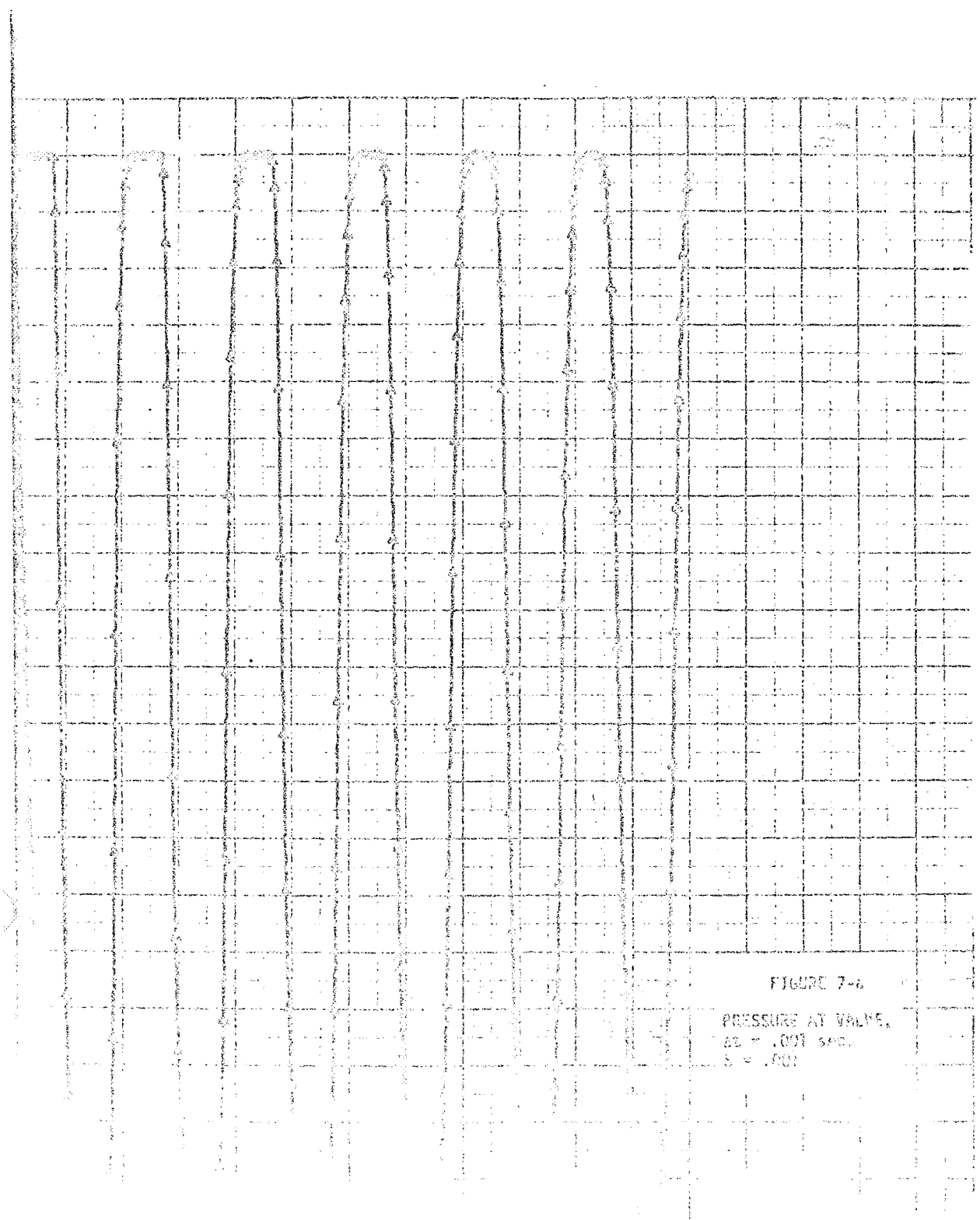
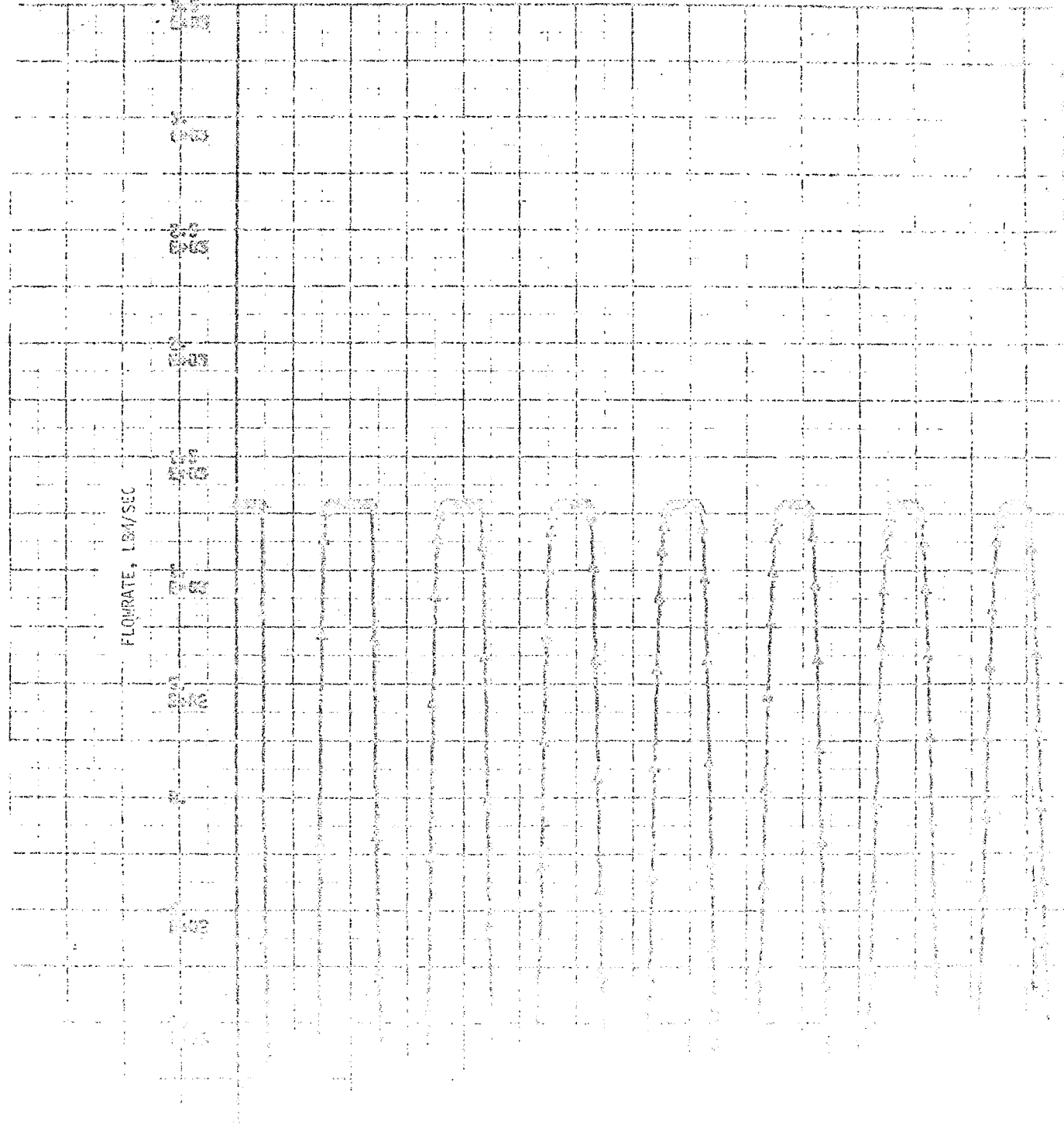
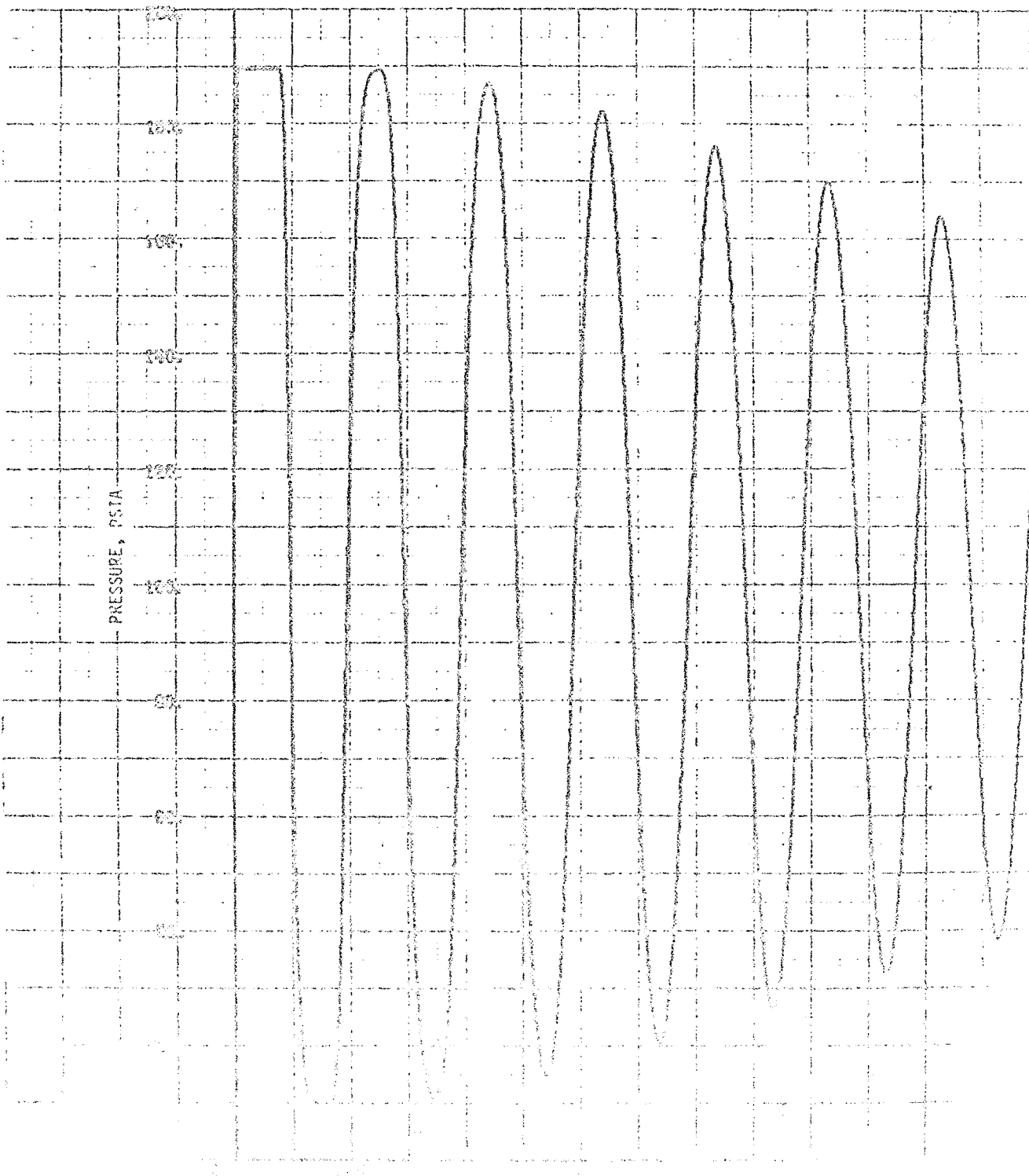


FIGURE 7-6

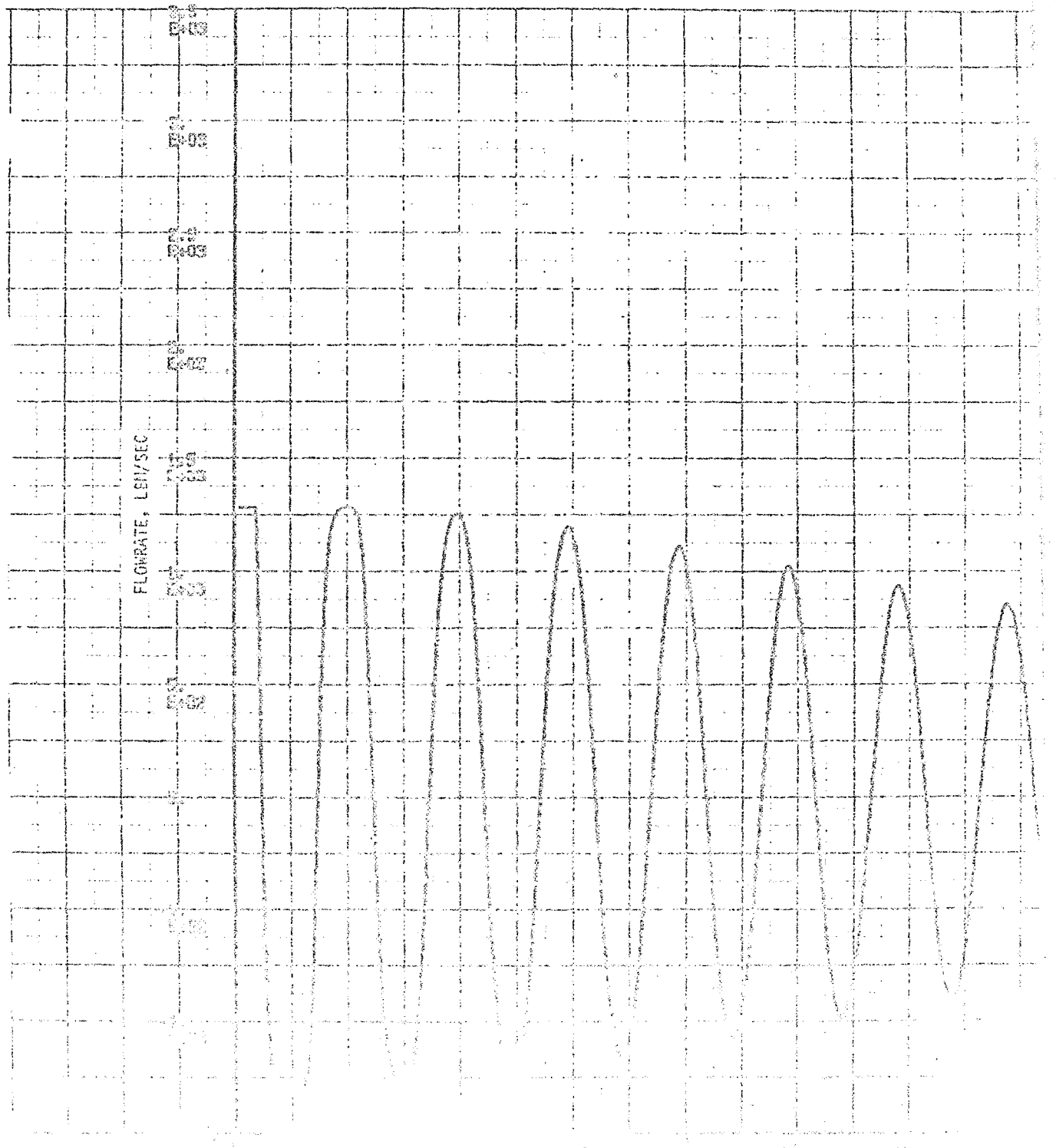
PRESSURE AT VALVE,
 $\Delta P = .001 \text{ atm}$,
 $\delta = .001$



ESTIMATE OF SYSTEMIC RISKS	
1.	Systemic Risk
2.	Systemic Risk
3.	Systemic Risk
4.	Systemic Risk
5.	Systemic Risk
6.	Systemic Risk
7.	Systemic Risk
8.	Systemic Risk
9.	Systemic Risk
10.	Systemic Risk
11.	Systemic Risk
12.	Systemic Risk
13.	Systemic Risk
14.	Systemic Risk
15.	Systemic Risk
16.	Systemic Risk
17.	Systemic Risk
18.	Systemic Risk
19.	Systemic Risk
20.	Systemic Risk
21.	Systemic Risk
22.	Systemic Risk
23.	Systemic Risk
24.	Systemic Risk
25.	Systemic Risk
26.	Systemic Risk
27.	Systemic Risk
28.	Systemic Risk
29.	Systemic Risk
30.	Systemic Risk
31.	Systemic Risk
32.	Systemic Risk
33.	Systemic Risk
34.	Systemic Risk
35.	Systemic Risk
36.	Systemic Risk
37.	Systemic Risk
38.	Systemic Risk
39.	Systemic Risk
40.	Systemic Risk
41.	Systemic Risk
42.	Systemic Risk
43.	Systemic Risk
44.	Systemic Risk
45.	Systemic Risk
46.	Systemic Risk
47.	Systemic Risk
48.	Systemic Risk
49.	Systemic Risk
50.	Systemic Risk
51.	Systemic Risk
52.	Systemic Risk
53.	Systemic Risk
54.	Systemic Risk
55.	Systemic Risk
56.	Systemic Risk
57.	Systemic Risk
58.	Systemic Risk
59.	Systemic Risk
60.	Systemic Risk
61.	Systemic Risk
62.	Systemic Risk
63.	Systemic Risk
64.	Systemic Risk
65.	Systemic Risk
66.	Systemic Risk
67.	Systemic Risk
68.	Systemic Risk
69.	Systemic Risk
70.	Systemic Risk
71.	Systemic Risk
72.	Systemic Risk
73.	Systemic Risk
74.	Systemic Risk
75.	Systemic Risk
76.	Systemic Risk
77.	Systemic Risk
78.	Systemic Risk
79.	Systemic Risk
80.	Systemic Risk
81.	Systemic Risk
82.	Systemic Risk
83.	Systemic Risk
84.	Systemic Risk
85.	Systemic Risk
86.	Systemic Risk
87.	Systemic Risk
88.	Systemic Risk
89.	Systemic Risk
90.	Systemic Risk
91.	Systemic Risk
92.	Systemic Risk
93.	Systemic Risk
94.	Systemic Risk
95.	Systemic Risk
96.	Systemic Risk
97.	Systemic Risk
98.	Systemic Risk
99.	Systemic Risk
100.	Systemic Risk







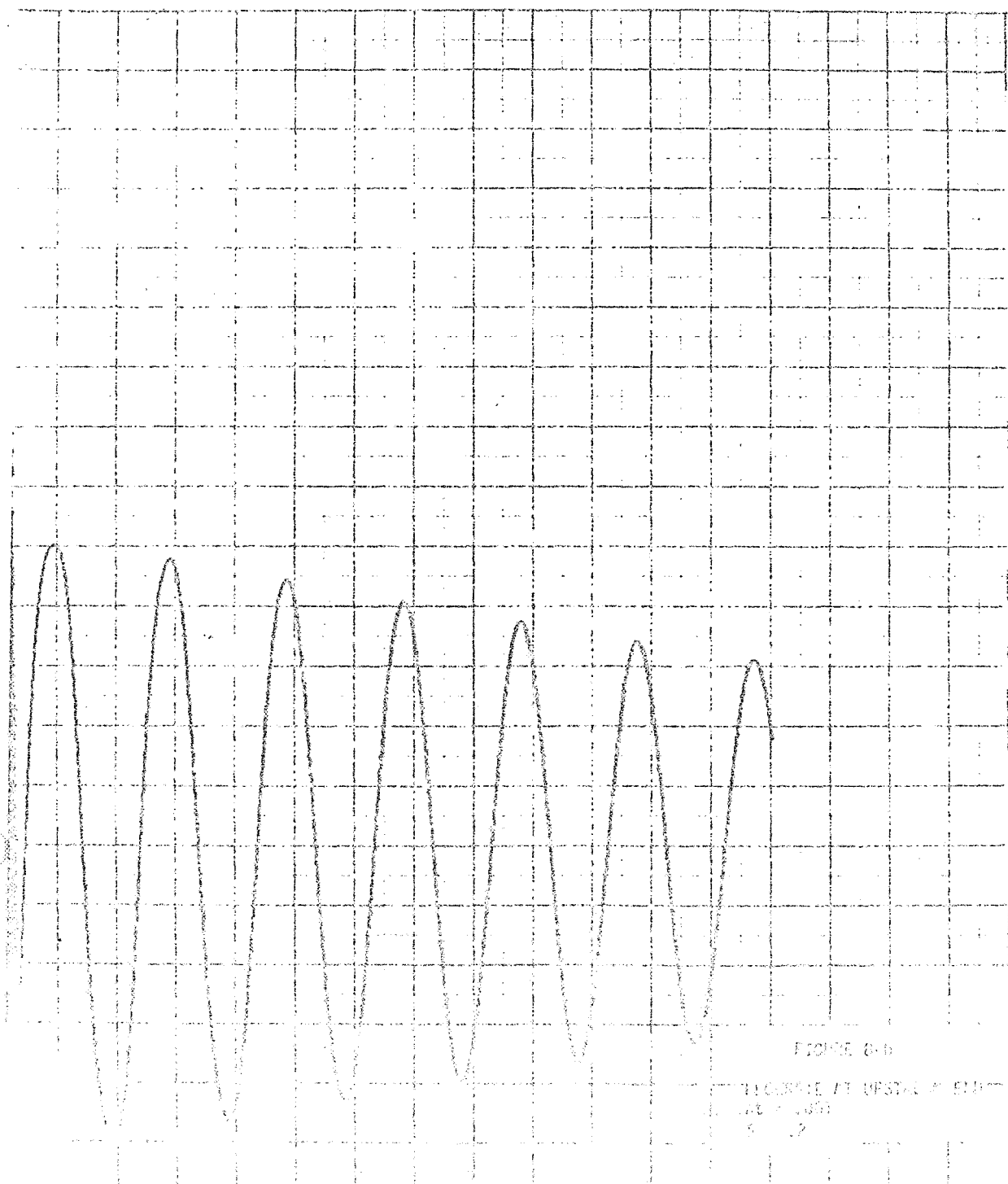
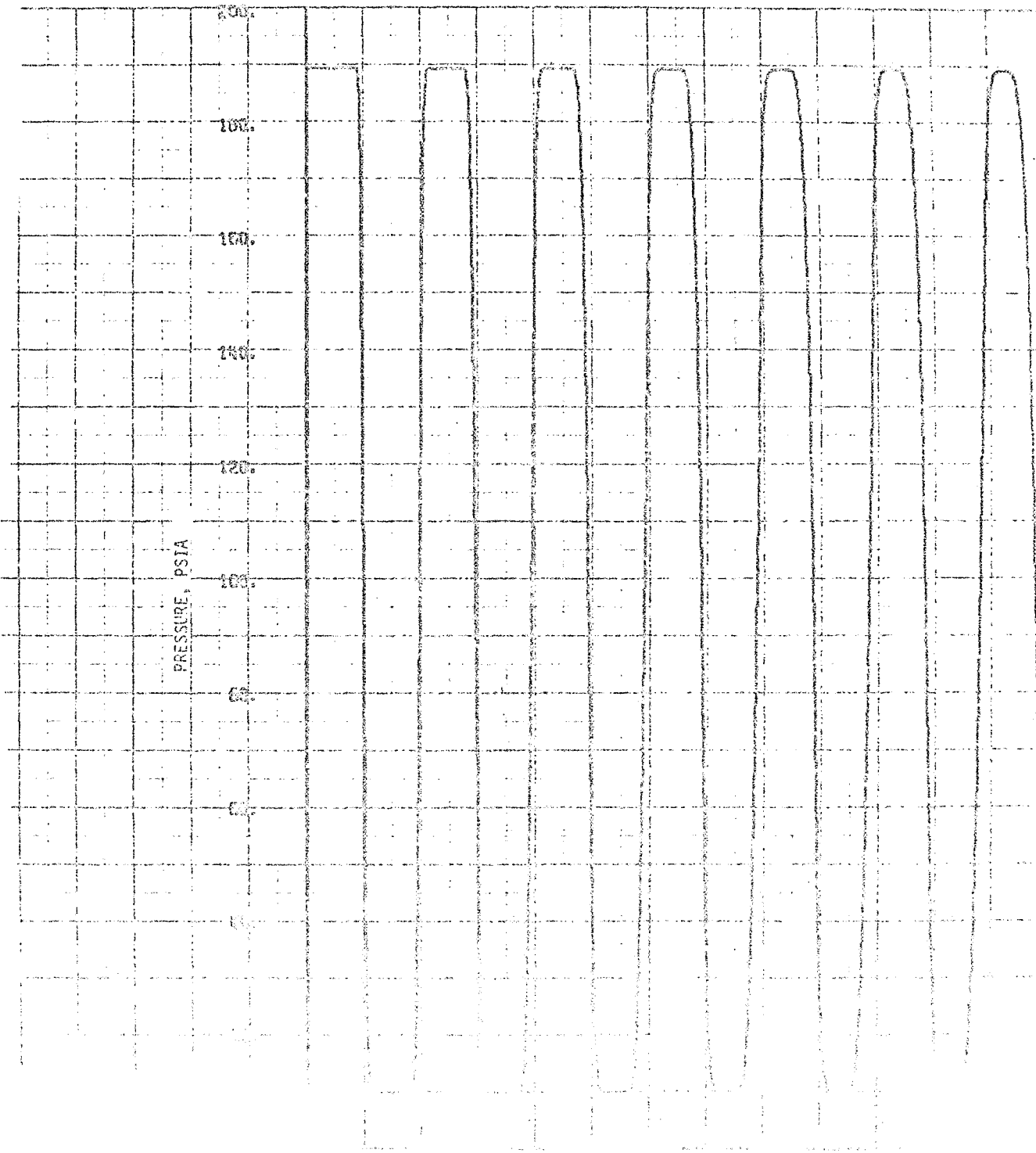


FIGURE 6-6

WAVELET RESPONSE



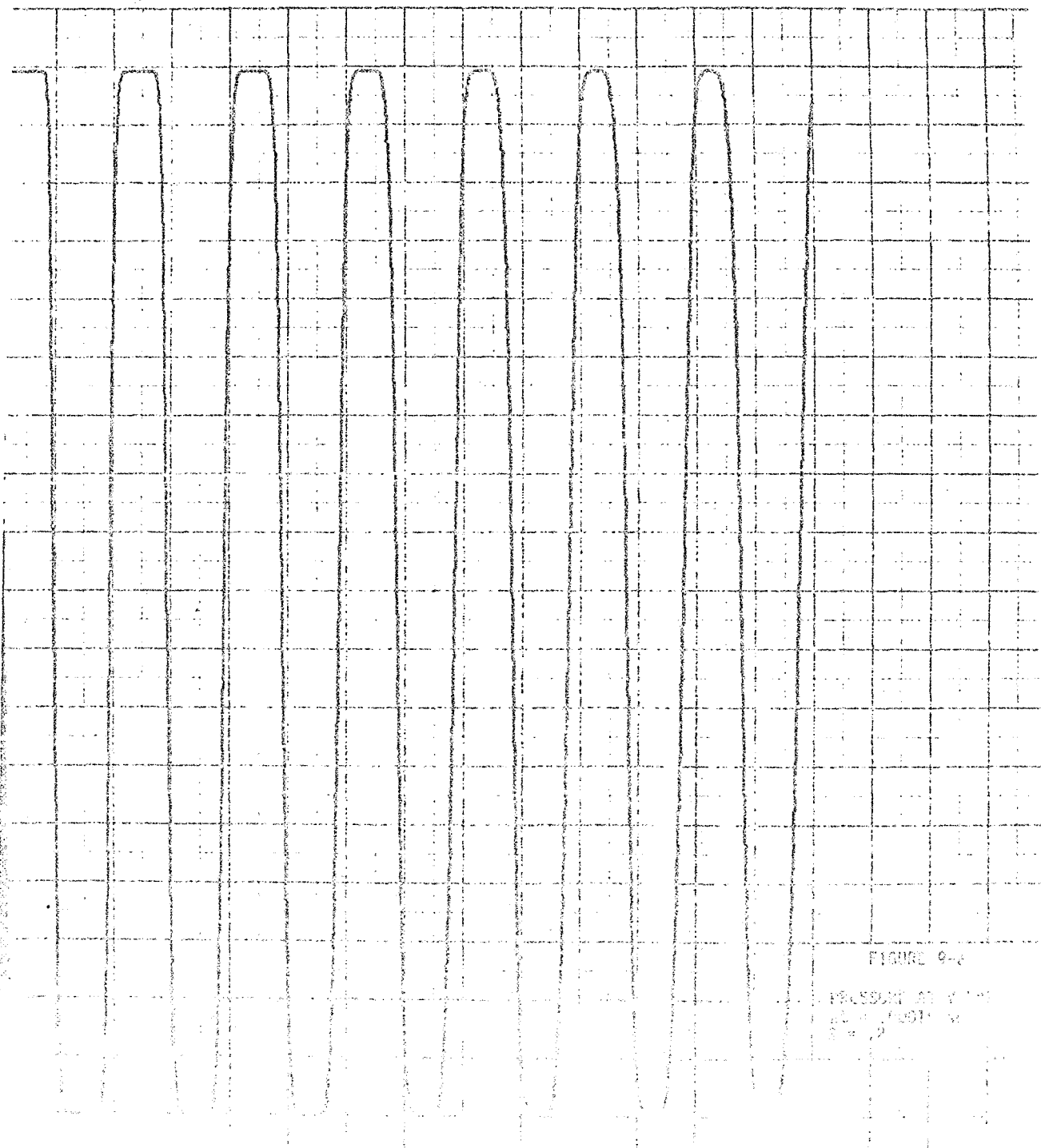
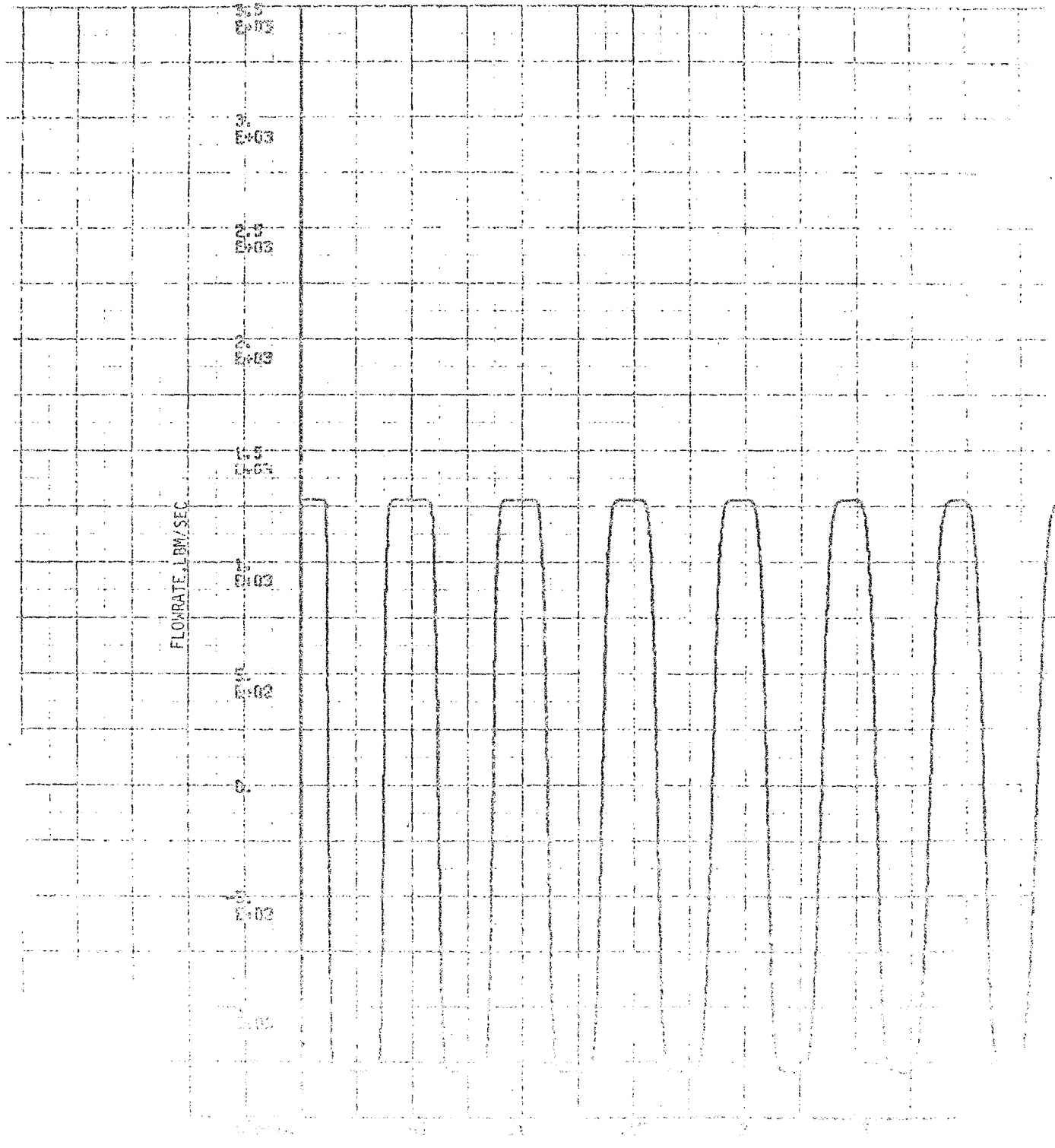
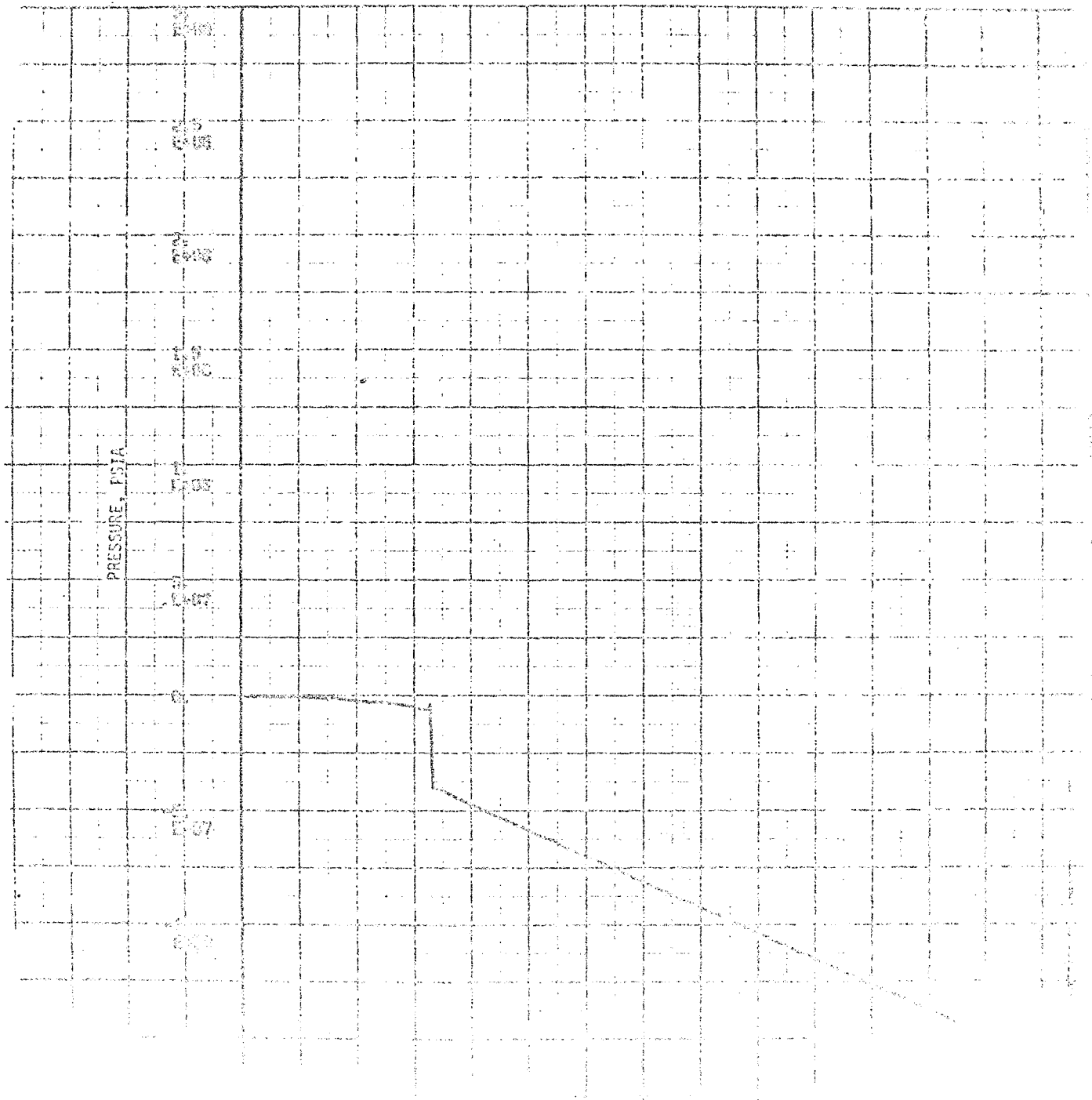


FIGURE 6-2

PRESSURE AT 1000
feet







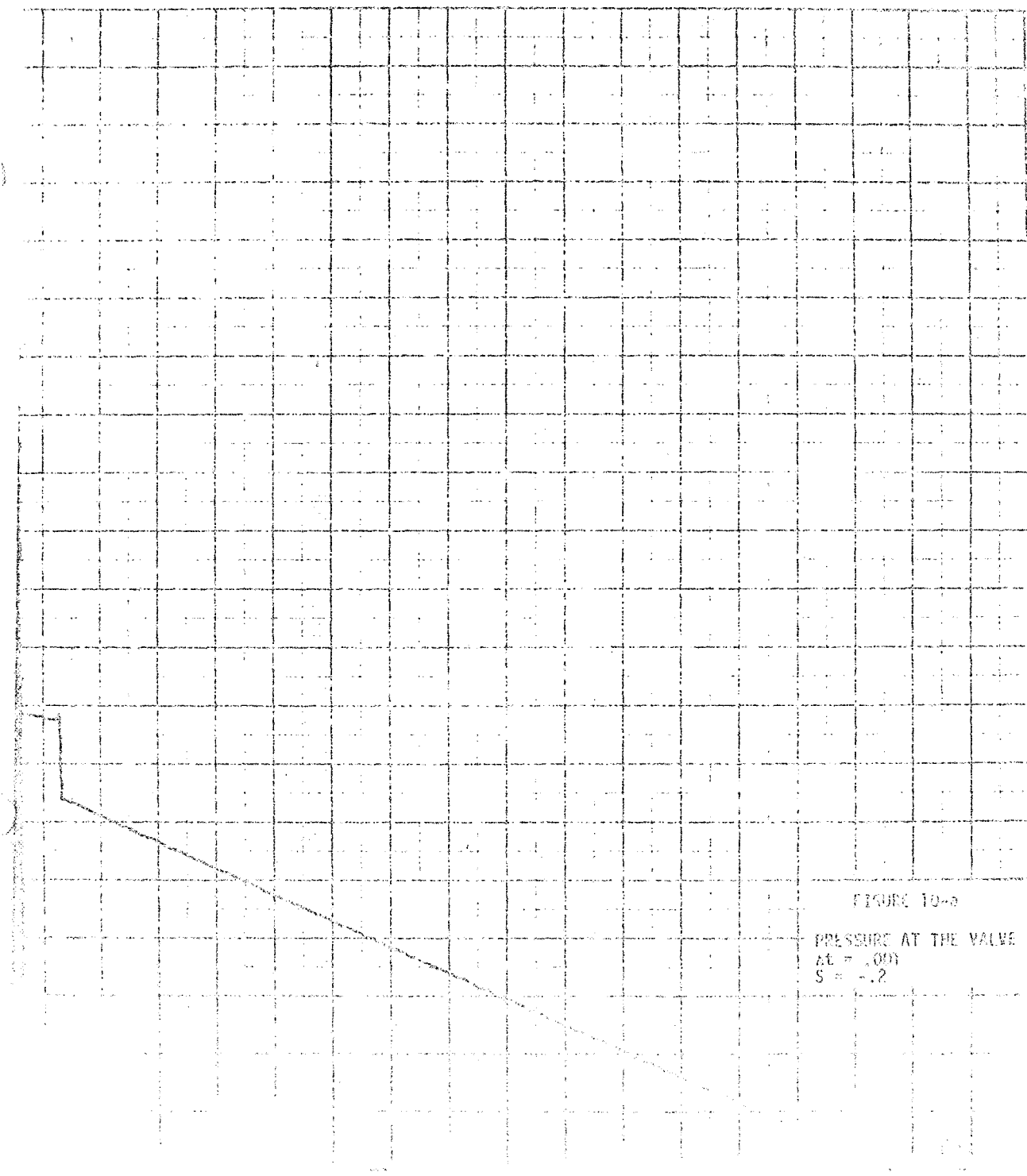
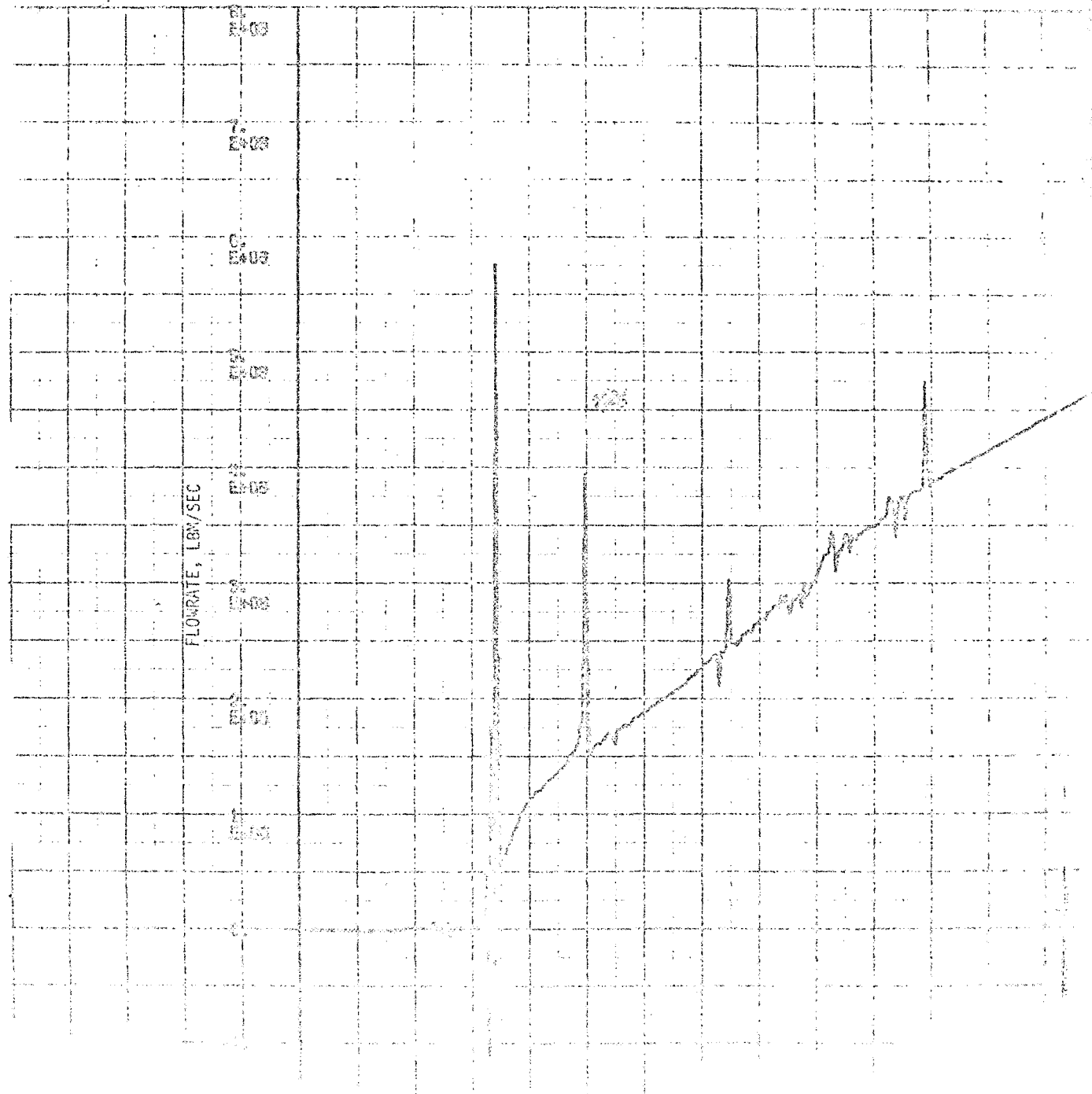


FIGURE 10-9

PRESSURE AT THE VALVE
 $\Delta t = .001$
 $S = .2$



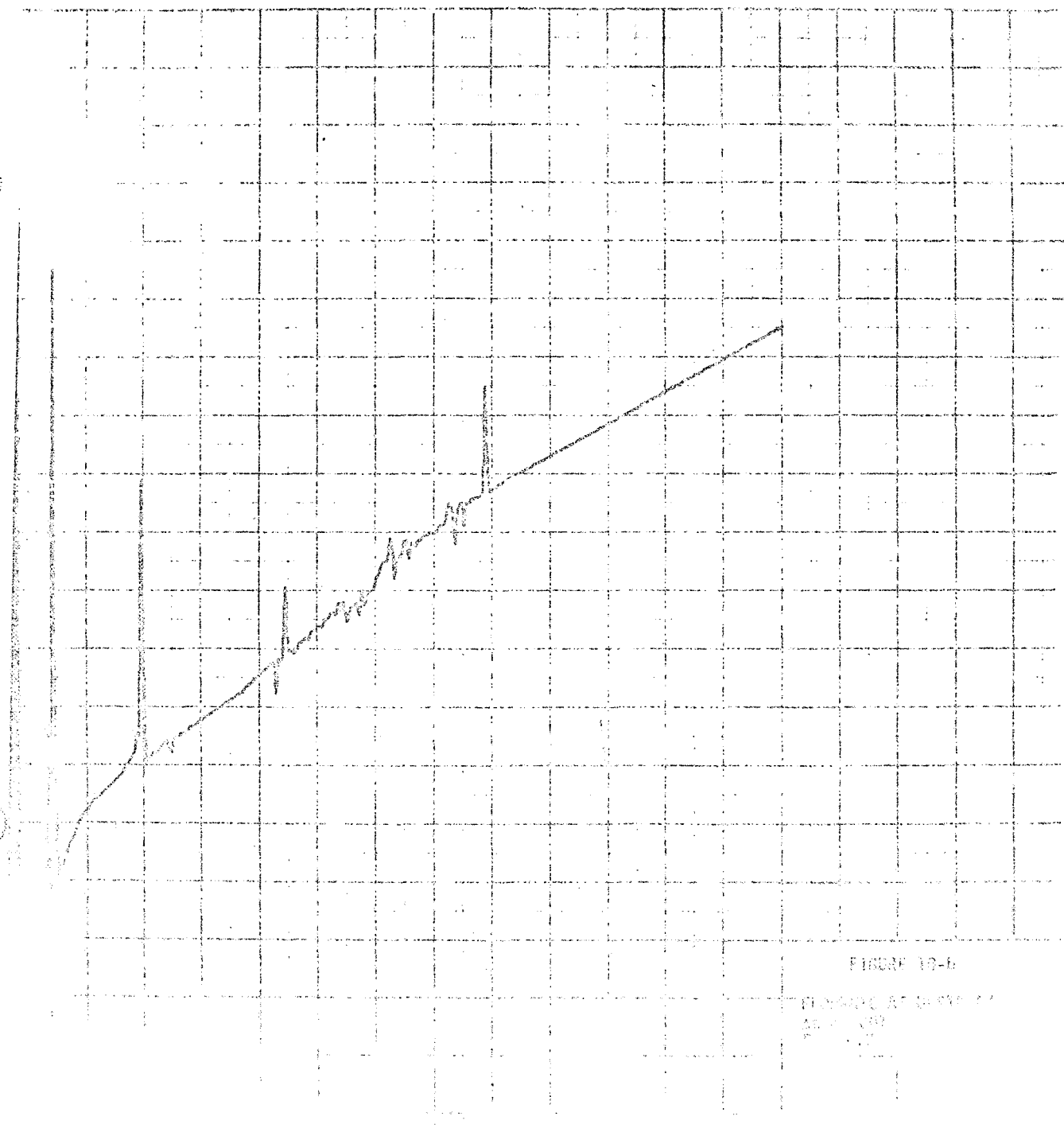


FIGURE 10-6

PIECEWISE LINEAR
FUNCTION

3.4.4 Supply Lines Steady-State

The supply lines for the steady-state model will be simulated assuming a constant heat flux into the lines (Figure 11). Therefore, the heat transfer coefficient, h , is a constant. Heat transfer into the fluid flowing in long gas lines will be treated by numerical integration with respect to distance. The supply line model will handle the case of combined friction and heat transfer. The nomenclature is included at the end of this section.

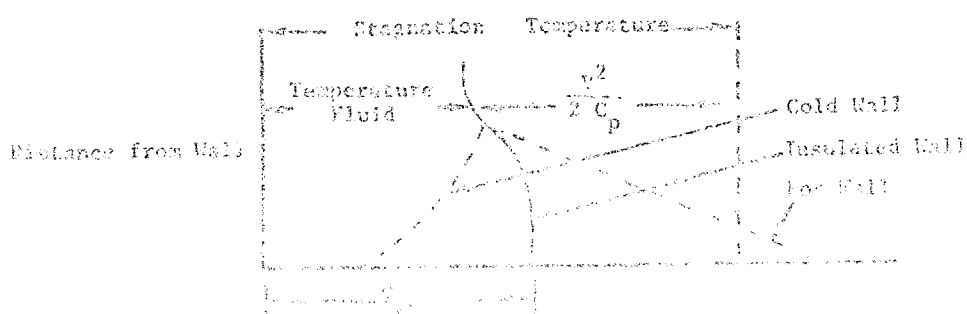
The general approach will utilize the energy equation expressed as a function of the heat transfer coefficient (page 243 of Reference 20).

$$\dot{W} dQ = \frac{\pi}{4} D^2 \rho V (C_p dT_o) = h \pi D dx (T_w - T_{aw}) \quad (1)$$

where T_{aw} = Adiabatic wall temperature (Figure 12).



FIGURE 11 - CONSTANT HEAT FLUX INTO LINE ELEMENT



For subsonic flow the adiabatic wall temperature, T_{aw} , does not differ much from the stagnation temperature T_o . Therefore, $T_{aw} \approx T_o$ and Equation 1 becomes

$$\frac{dT_c}{T_w - T_o} = \frac{4 h dx}{\rho V C D} \quad (2)$$

using Reynolds Analogy between friction and heat transfer;

$$\frac{dT_o}{T_w - T_c} = \frac{2 f dx}{D}$$

and integrating yields

$$\frac{\frac{T_o}{T_w} - \frac{T_o}{T_1}}{\frac{T_w}{T_1} - \frac{T_w}{T_2}} = 2f \left(\frac{x_2 - x_1}{D} \right)$$

Therefore, T_o can be calculated for any value of line length, x .

Now the Mach number can be obtained by the finite difference iterative integration

$$dM^2 = \left(\frac{T_o}{T_w} + 1 - \frac{2T_o}{T_w - T_o} \right) R_f - \frac{dx}{T_o}$$

where the influence coefficients are as follows:

$$R_{T_w} = \frac{M^2(1+M^2)(1+\frac{1-M^2}{M^2}M^2)}{1-M^2}$$

$$R_f = \frac{M^4(1+\frac{1-M^2}{M^2}M^2)}{1-M^2}$$

Evaluating, the finite difference equation is written

$$\left[\frac{T_o^2 - T_1^2}{T_w^2 - T_1^2} \right]^{x_1} = \left[\frac{\left(\frac{T_o}{T_w} + 1 - \frac{2T_o}{T_w - T_o} \right) R_f}{1 - M^2} \right]^{x_1} \left[\frac{T_o^2 - T_2^2}{T_w^2 - T_2^2} \right]^{x_2} = \left[\frac{\left(\frac{T_o}{T_w} + 1 - \frac{2T_o}{T_w - T_o} \right) R_f}{1 - M^2} \right]^{x_2}$$

If additional accuracy is required, the simplifications in this model can be eliminated. That is, the adiabatic wall temperature would not be assumed equal to the stagnation temperature and the Reynolds Analogy between friction and heat transfer would not be used. This would complicate the model extensively and at present, the minimal accuracy the improvement gains does not warrant this additional complication.

NOMENCLATURE

T_f , T_0	Temperature Fluid or Temperature Stagnation Fluid	"R
V	Velocity fluid initial	ft/sec
P	Pressure	psia
W	Flowrate	lbm/sec
D	Diameter line	in.
dx	Pipe segment	ft.
Q	Constant heat flux into pipe	BTU/sec
ρ	Density fluid	lbm/sec ³
μ	Viscosity fluid	Centipoise
f	Friction factor	
C_p	Specific heat constant pressure	BTU/"R
M	Mach number down pipe	
T_w	Temperature wall	"R
T_n	Temperature fluid down pipe	"R
h	heat transfer coe. fluid	$\frac{\text{BTU}}{\text{hr ft}^2 \text{ "F}}$

Symbols have meaning

3.4.5 Turbomachinery Transients

Fluid flow through the turbomachinery may be adequately described by utilizing steady-state plots of turbomachinery characteristics. Typical examples of pump characteristics curves are shown in Figures 13 and 15, and examples of turbine characteristic curves are shown in Figure 16. The relationships represented by these curves along with the equality between the pump speed and turbine speed and the equality between turbine power output and pump power required are solved with the line flow equations to give the turbine and pump operating points at each instant of time. The hydrogen pump performance curve, Figure 14, was obtained from AiResearch through TRW/Redondo Beach Product Design and Analysis Department. This performance curve was based on the ACPS studies being performed for the shuttle conceptual design activities. Justification for using steady-state flow relations is that the fluid capacitance of the turbomachinery is usually far less than that of other components of the system. The acceleration of the turbomachinery rotors may be taken into account by a relationship of the form:

$$T = T \frac{dN}{dt}$$

where:

T is the net torque supplied to the rotor, I is the moment of inertia of the rotor and the entrapped fluids and N is the rotor speed.

3.4.6 Turbomachinery Steady-State

Relationships of the type shown in Figures 13 through 16 are sufficient to represent the turbopump and turbine in a steady-state problem when the turbine power and pump power quantity constraints are satisfied simultaneously with the propellant compatibility constraint as described in Section 3.4.3. The steady-state relations for the pump and turbine are given below. The first two relations are the pump and turbine head-flow relations. The third relation is the pump and turbine power relation.

REFERENCE: Aerojet General Corporation
Proposal No. U8-501-D
Fuel Turbopump Modification Program
Revision A, dated 22 February 1968

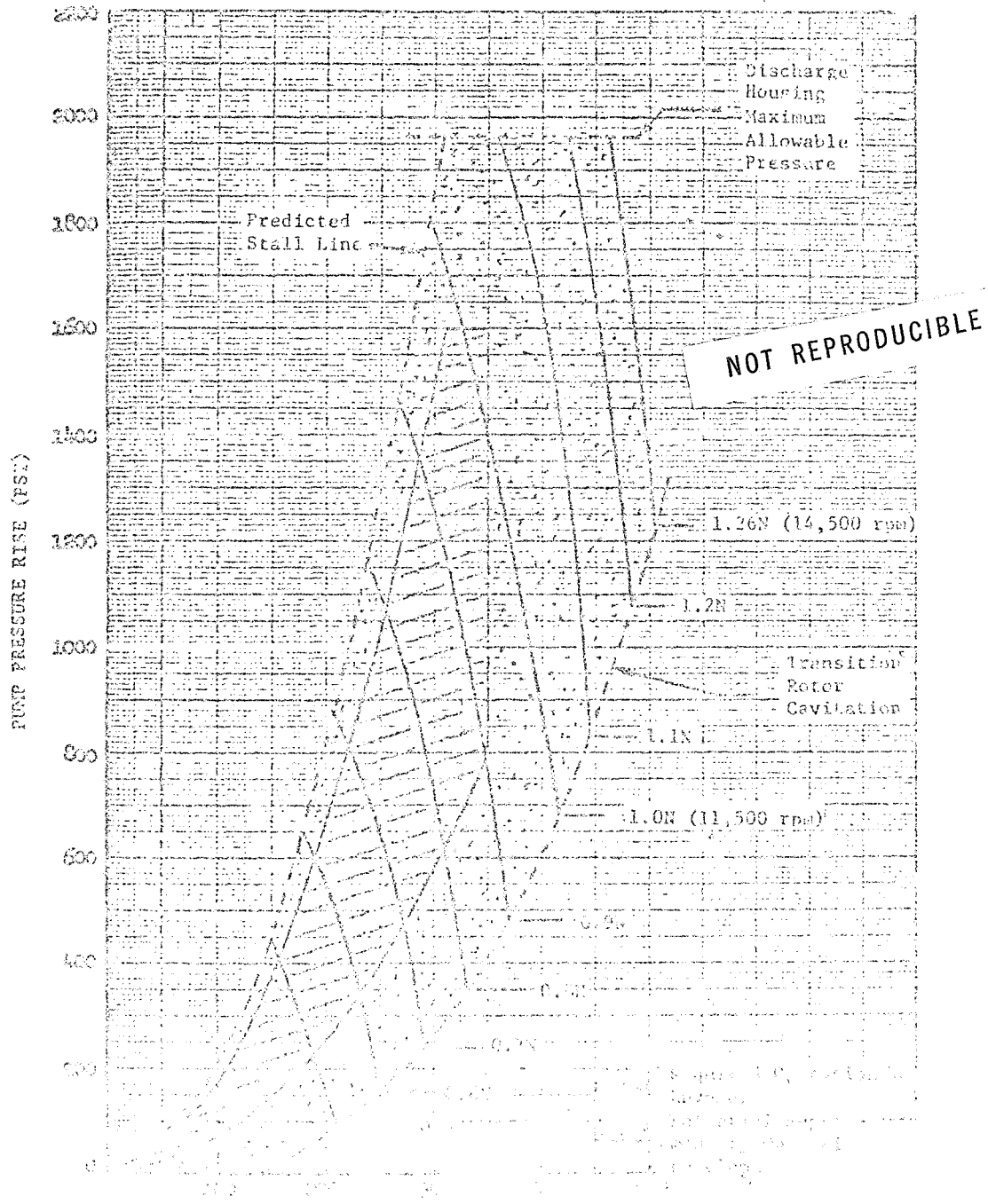
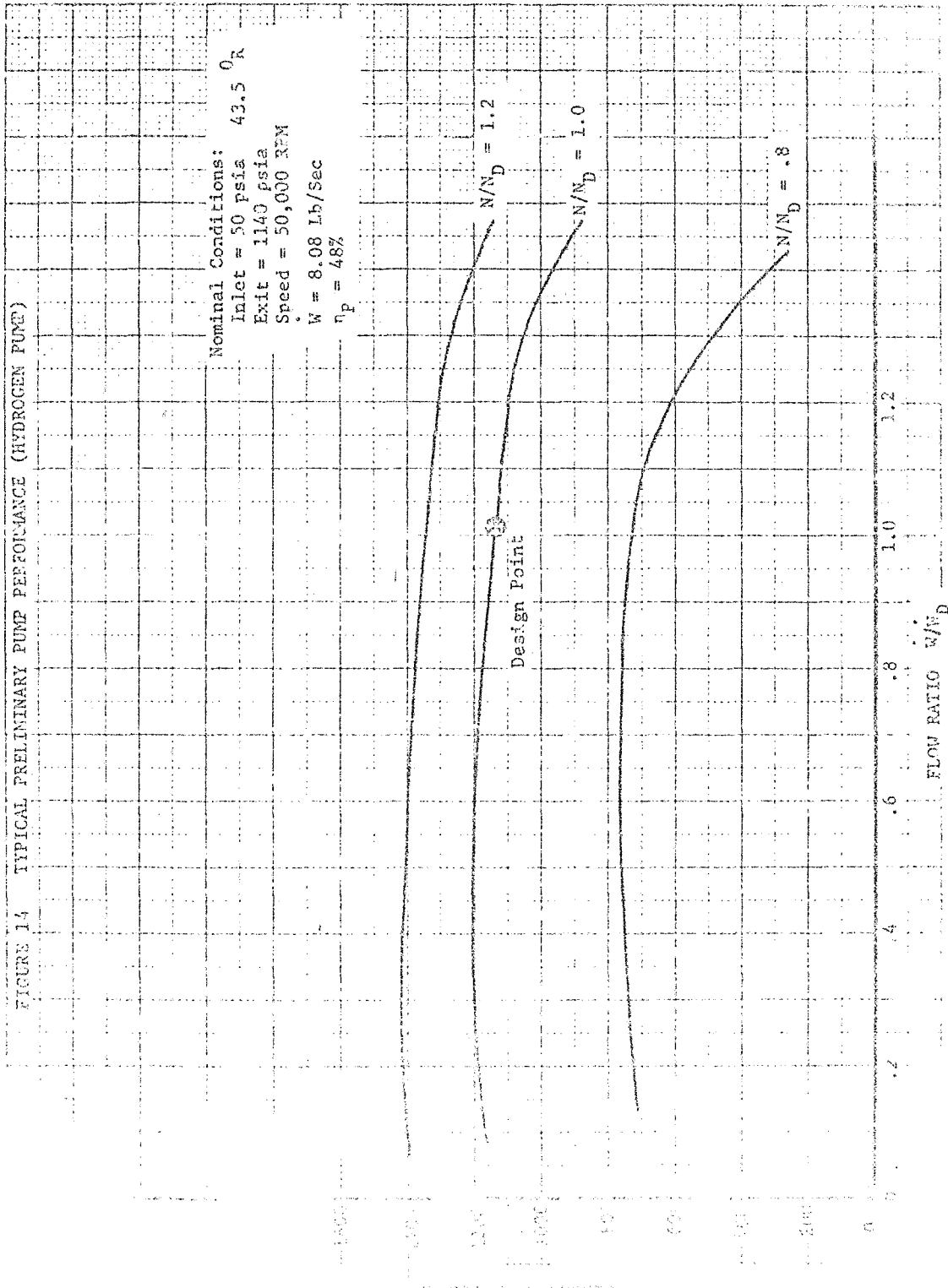
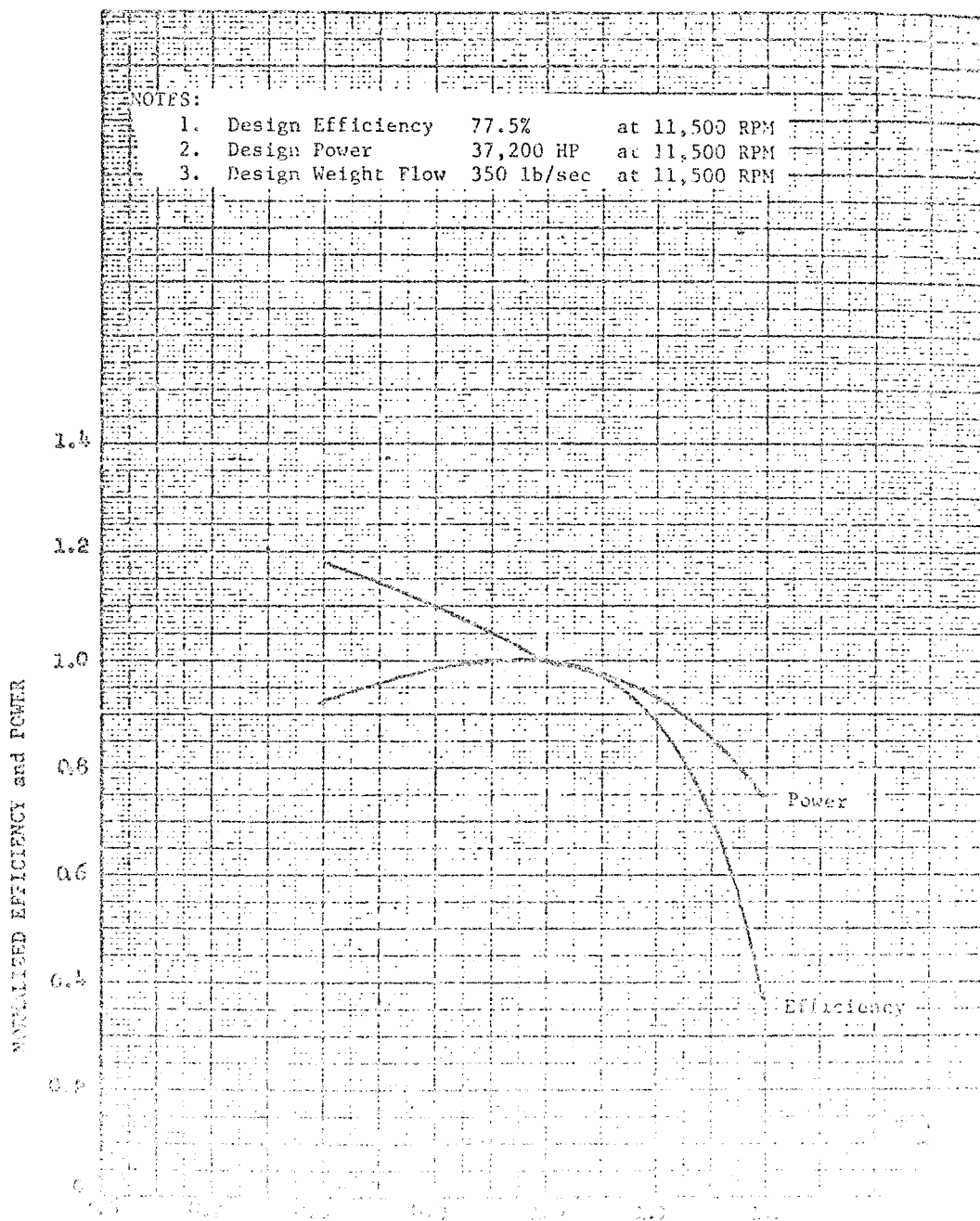
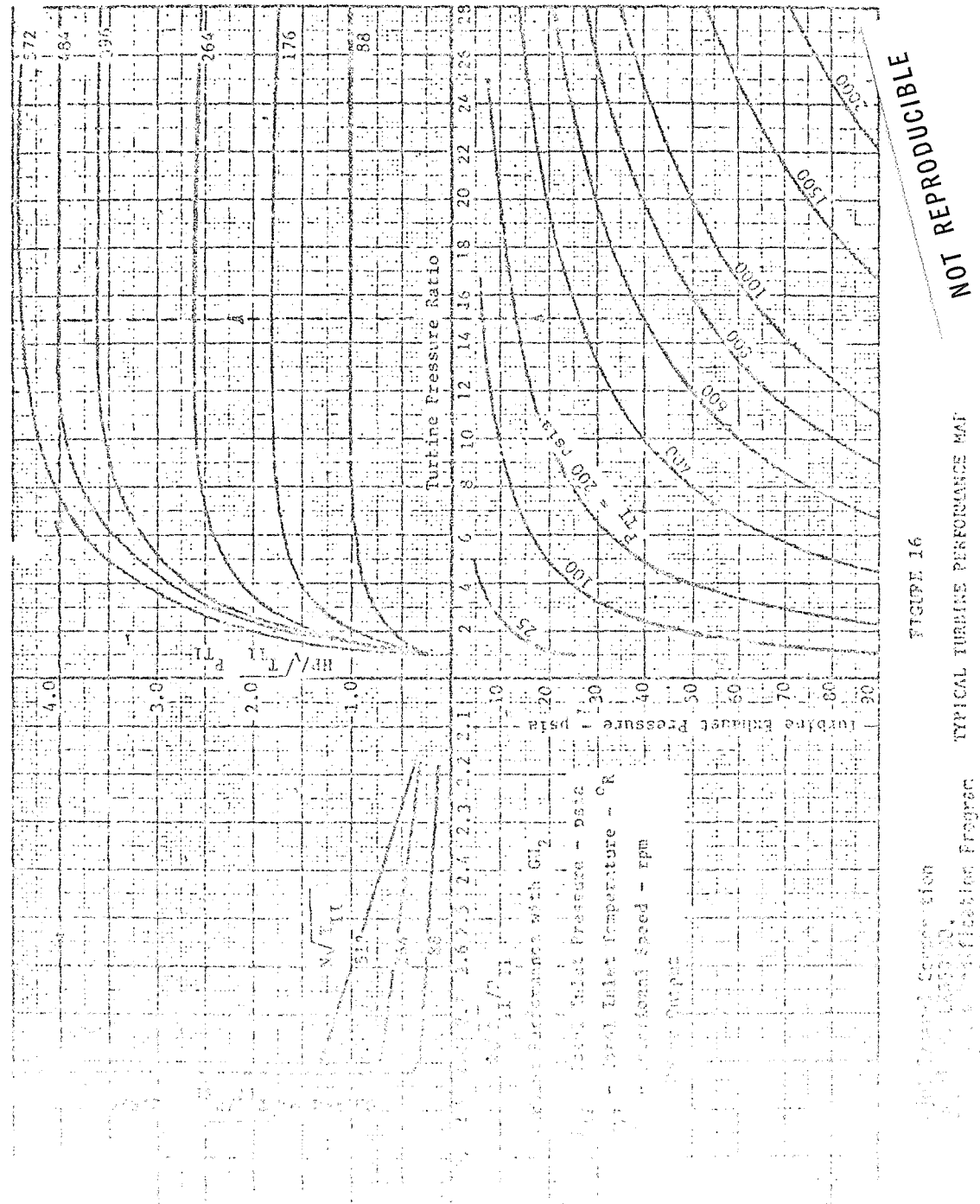


FIGURE 14 TYPICAL PRELIMINARY PUMP PERFORMANCE (HYDROGEN PUMP)



REFERENCE: Aerojet General Corporation
Proposal No. LR650100,
Fuel Turbopump Modification Program
Revision A, dated 22 February 1965





3.4.7 Heat Exchanger Transient Model

At the present time it is anticipated that the heat exchanger model will consist of three parts: preheater, boiler, and superheater. When all three subroutines are used consecutively, they will simulate the conditioning of a liquid to a superheated gaseous state. However, each subroutine may be used separately as the simulation of heat exchangers which may start with a fluid at a cool liquid, boiling liquid, or gaseous condition and, for the appropriate initial fluid state, will condition the fluid to either a boiling liquid, cool gas, or superheated gaseous state. This is shown schematically in Figure 17.

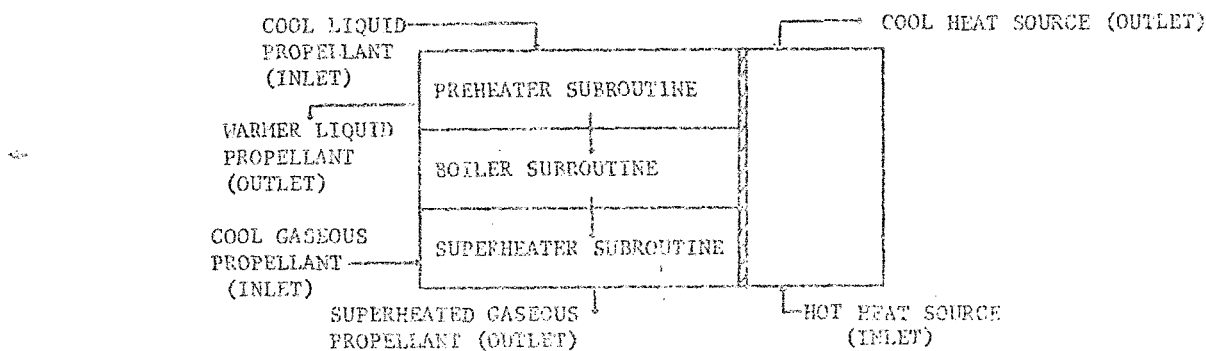


FIGURE 17 - HEAT EXCHANGER BLOCK DIAGRAM

The preheater has the function of elevating the liquid state to a boiling condition. The boiler section accounts for the heat transfer required to vaporize the liquid. The superheater increases the gas to a higher temperature.

An important piece of our model must allow (1) the incorporation of real empirical data, (2) variation in density, specific heat, and thermal conductivity, and (3) varying fluid properties such as viscosity, diffusion coefficient, and thermal diffusivity.

Figure 17 shows how the counter-flow heat exchanger model will be set up. A slight increase in complexity will result when options are provided in the model for parallel and cross-flow heat exchange. A computer program for the design and performance analysis of Compact Multi-Fluid Heat Exchangers was located in the literature search (Reference Appendix 3, Program N70-10069). This program includes parallel, counter, multi-fluid cross-flow and plates/fins configurations. This program is presently being obtained from MSC and extensive use may be made of it if evaluations indicate it will be useful.

The heat transfer balance equations with counter flow are (see Reference 22);

$$\frac{1}{\rho_1 A_1 C_{p1} \frac{\partial}{\partial t} T_1(x,t) + W_1 C_{p1} \frac{\partial T_1}{\partial X}(x,t) - h_1 C_1 [T_1(x,t) - \bar{T}_2(t)]}{\rho_2 A_2 C_{p2} \frac{\partial}{\partial t} T_2(x,t) = -W_2 C_{p2} \frac{\partial T_2}{\partial X}(x,t) + h_2 C_2 [T_2(x,t) - \bar{T}_1(t)]}$$

where ρ = density 1 = conditioned fluid

A = flow area 2 = heat source

C_p = specific heat X = length

W = flow rate t = time

h = film coefficient

C = circumference

T = Temperature

$$\bar{T} = \frac{1}{L} \int_0^L T dx \quad L = \text{Total length}$$

These equations apply to all cases except boiling and will largely form the basis for the model.

For the case of the bottom condition, the conditioned fluid is a known quantity and the heat source is a constant. The top condition is also a known quantity and the heat source is a constant.

$$\frac{W_L H}{L} = -V_1 C_1 [T_1 - \bar{T}_2(i)] \quad H = \text{latent heat of vaporization}$$

3.4.8 Heat Exchanger Steady-State Model

The steady-state equations for heat exchangers are well developed and will be utilized for this application. The principal mechanism for the transfer of heat in the heat exchangers planned for the ACPS is that of convection. The heat transferred by convection is determined from the relation:

$$Q = hA(\Delta T) \quad (1)$$

where Q is the heat transfer rate, h is the film coefficient, and ΔT is the appropriate temperature difference. The film coefficient depends upon the shapes of the exchanger parts and upon whether the convection is natural or forced. Reference 23 gives the following empirically determined relation for natural convection from a cylinder, to a surrounding medium.

$$\frac{hD}{k} = 0.53 \left| \left(G_R P_R \right)^{.25} \right|$$

where

$$G_R = \frac{B_S \Delta T \rho^2 D^3}{\mu^2}, \text{ is the Grashof number.} \quad (2)$$

$$P_R = \frac{C_p u}{k}, \text{ is the Prandtl number.}$$

D is the cylinder diameter, k is the fluid thermal conductivity, B is the fluid bulk modulus of thermal expansion, ρ is the fluid density, μ is the fluid viscosity, C_p is the fluid specific heat, and g is the local acceleration.

The value of the film coefficient for forced convection to a cylindrical tube is a function of the fluid properties and the Reynolds number.

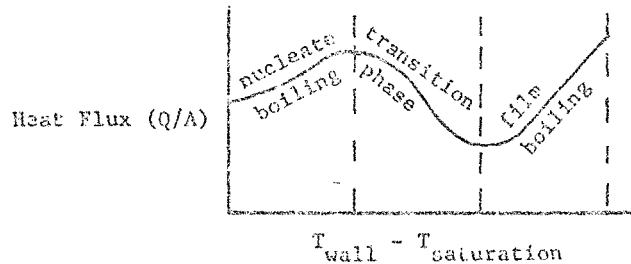
For laminar flow, $h = 0.023 \cdot \frac{Re^{.5}}{Pr^{.33}} \cdot \frac{C_p}{\rho g} \cdot \frac{k}{D}$

for $Re < 2300$

NOT REPRODUCIBLE

if the heat flow is from the cylinder wall to the fluid, the Franklin number exponent is 0.4 rather than 0.3. These relationships, or a similar approach, will likely serve as the basis of development of the model.

The previous heat transfer Equations (2 & 3) are valid strictly for single phase flow. In order to handle the region of two phase flow, in both liquid and gas, three regions of heat exchange must be considered, nucleate boiling, transition phase, and film boiling. The oxygen and hydrogen boiling curves, for example,



will be used to determine the heat transfer coefficient averaging method which will be utilized to model this heat transfer region. The heat transfer entrance and exit effects will be further investigated for possible inclusion in this model.

3.4.2 Accumulators and Pressure Vessel transients

If an accumulator is long enough so that it would require at least two calculation nodes, and if treated as a distributed parameter line, then the line subroutines described in Section 3.4.3 can be used to simulate it. If the accumulator is so short that the selection of a time interval to give it two nodes results in an impractically small interval, then a lumped parameter representation will be used. (Figure 18)



Figure 38 Accumulator

$$W_{ij} = f_{ij}(P_{ij}, P_{ji}) \quad (1)$$

$$W_0 = f_2(P_a, P_0) \quad (2)$$

$$\frac{dP_a}{dt} = \frac{RT}{V_a} (\dot{Q}_a - \dot{V}_a) \quad (3)$$

W_a is the flow rate into the accumulator, W_o is the flow rate out of the accumulator, P_{in} is the pressure upstream of the accumulator, P_o is the pressure in the accumulator, P_{down} is the pressure downstream of the accumulator, γ is the ratio of specific heats, R is the gas constant, T is the temperature, and V_g is the gas volume. Equations 1 and 2 are steady-flow relations between inlet and outlet existing flow, and initial pressure drop and boundary 3 is the flow rate from the accumulator exit valve.

3.4.10 Accumulators and Pressure Vessels Steady-State

The modeling of the steady-state accumulators and pressure vessels will account for heat transfer through the walls and liquid surface, venting reverse flow and mass/volume changes (Figures 19 and 20, Reference 25). The following approach will be used and the nomenclature is included at the end of this section.

The initial pressure (P) will be obtained from the initial ullage volume (v), gas mass (W) and initial average gas temperature (T) based on the equation of state for a perfect gas.

$$Pv = W R T$$

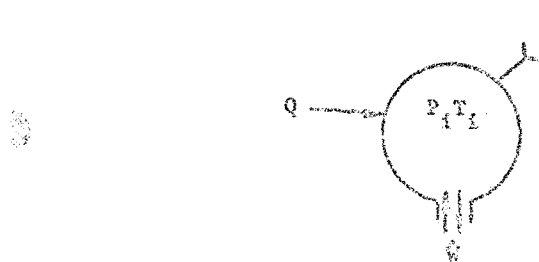


Figure 19 Gas Accumulator

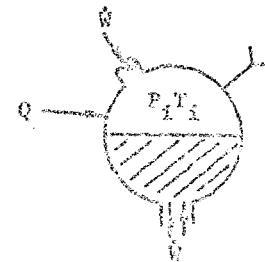


Figure 20 Gas/Liquid Pressure Vessel

$$\text{if } P_g > P_s$$

the entering pipe rate, (lbm/sec) is

$$F_g = \frac{A}{\rho} \left(\frac{P_g - P_s}{R(T_i) + \frac{P_g}{\rho}} \right)^{\frac{1}{2}}$$

$$F_g = F_{g1} + F_{g2}$$

$$F_{g1} = F_{g2}$$

The volume change, (ft^3) is

$$V_2 = V_1 - \frac{12 W}{\rho A} \Delta t; \quad dV = V_2 - V_1 \quad (3)$$

The ullage or accumulator volume change, (ft^3) is

$$dV = W_e dt \quad (4)$$

The ullage mass (lbm) is

$$W_g = W_{g-1} + W_g dt \quad (5)$$

If the pressure in the tank is greater than the vent pressure, calculate venting flowrates.

$$W = \text{seepage flow} \quad (6)$$

Calculate heat transfer across gas-liquid interface (BTU), if necessary

$$Q_{gl} = h A_l (T_i - T_1) \quad (7)$$

where $h = f(\text{Prandtl, Grashof, or Reynolds numbers})$

$A_l = \text{liquid surface area}$

The energy of incoming mass (BTU) is:

$$E_{in} = C_p W_{in} dt \quad (8)$$

where $in = \text{entering}$

The energy venting mass (BTU) is

$$E_{vent} = W_{VR} T_u C_p dt \quad (9)$$

The expansion work (BTU) is

$$E_g = p_g (V_t - V_{t-1}) \quad (10)$$

The internal energy is

$$U = C_v T \quad (11)$$

Volume transfer through the vent valve is

$$\frac{dV}{dt} = \frac{dV}{dt} + \frac{dV}{dt} = \dot{V}_{in} + \dot{V}_{out}$$

The energy balance then yields the ullage temperature ($^{\circ}\text{R}$)

$$T_u = \frac{U - E_{\text{in}} - Q_{g1} - E_V - E_s - Q_W}{C_V}$$

Final ullage pressure (psia) is

$$P_f = \frac{W R T_i}{V_i}$$

When the fluids are stored under supercritical conditions, they cannot be treated using thermodynamic relationships based on the ideal gas law. For quasi-steady flow, it is common to use the thermodynamic functions θ and ϕ which are defined as

$$\phi(P, \rho) = \frac{1}{\rho} \left(\frac{\partial P}{\partial U} \right)_\rho$$

$$\theta(P, \rho) = -\rho \left(\frac{\partial H}{\partial P} \right)_P$$

The pressure change in the tank as a function of flowrate out and heat added is then

$$\frac{dP}{dt} = \frac{A}{V} \left(\frac{dQ}{dt} + \dot{m} \dot{H}_e \right)$$

The ϕ and θ functions are readily available for oxygen and hydrogen as the result of work on other programs.

NOTATION

P	Pressure	psia
V	Volume	ft^3
W	Weight of gas in bottle	lbm
R	Gas constant	$\text{ft}^3 \cdot \text{lbf}/\text{lbm}^{\circ}\text{R}$
\dot{m}	Mass flow rate, lbm/s	
\dot{V}	Volume flow rate	

NOMENCLATURE (Continued)

ρ	Density	lbm/ft ³
A_w	Surface area tank walls	ft ²
A	Flow area	ft ²
A_l	Liquid/gas surface area	ft ²
c_p	Specific heat constant pressure	BTU/°R
c_v	Specific heat constant volume	BTU/°R
U	Internal Energy	BTU
E_{in}	Energy of incoming mass	BTU
Q_{g1}	Heat transfer thru gas interface	BTU
E_v	Energy Venting mass	BTU
E_s	Expansion work on surroundings	BTU
Q_w	Heat transfer thru tank walls	BTU
Q	Total heat added to tank	
H	Enthalpy	BTU
ϵ_c	Conversion constant	32.2 $\frac{\text{lbm-ft}}{\text{sec}^2 \text{lbf}}$
	Subscripts	

e Exit

i Internal

t Time

p Present

v Ullage

l Liquid

3.4.11 Manifold and Injector Transients

A rigorous treatment of the flow downstream of the thrust chamber valve would be a very difficult matter. Even making the assumptions that the flow is one-dimensional, inviscid, and adiabatic would involve solving the continuity and momentum equations, which are partial differential equations, and the algebraic equations of state and the isentropic relationships. In addition, discontinuities in the solution (shocks and interfaces) would have to be followed. A search of the literature has so far revealed no simplified models which are substantiated by experimental data. The proposed simplified model (Figure 21) is typical of the treatment of transient flow through the manifold and injectors.

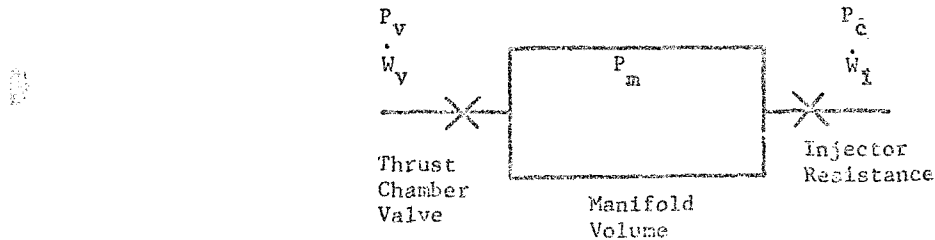


FIGURE 21 - MANIFOLD DIAGRAM

The flow into the manifold is given by

$$\dot{W}_v = f_v A_v C_v \sqrt{\frac{P_c}{RT} \left(\frac{2\gamma}{\gamma-1} \right) \left(\frac{P_m^2}{P_v^2} \right)^{\frac{\gamma+1}{\gamma-1}} \left(\frac{P_m}{P_v} \right)^{\frac{2\gamma}{\gamma-1}}} \quad (1a)$$

for unchoked flow, or, if the flow is choked by

$$\dot{W}_v = P_v A_v C_v \sqrt{\frac{P_c}{RT} \left(\frac{2}{\gamma+2} \right)^{\frac{\gamma+1}{\gamma-1}}} \quad (1b)$$

\dot{W}_v is the flow through the valve, A_v is the effective area of the valve, C_v is the valve coefficient, P_c is the chamber pressure, P_m is the manifold pressure, P_v is the valve pressure, R is the universal gas constant, T is the total temperature, γ is the specific heat ratio, and f_v is the friction factor.

cific heats, P_m is the manifold pressure, and T is the total temperature of the gas. Similarly, for flow from the manifold into the chamber

$$\dot{W}_i = P_m A_i C_i \sqrt{\frac{g_c}{RT} \left(\frac{2}{\gamma-1} \right)} \left[\left(\frac{P_c}{P_m} \right)^{\frac{2}{\gamma}} - \left(\frac{P_c}{P_m} \right)^{\frac{\gamma+1}{\gamma}} \right] \quad (2a)$$

for unchoked flow, or

$$\dot{W}_i = P_m A_i C_i \sqrt{\frac{g_c \gamma}{RT} \left(\frac{2}{\gamma+1} \right)^{\frac{\gamma+1}{\gamma-1}}} \quad (2b)$$

for choked flow. \dot{W}_i is the flow through the injector, and A_i is the injector area.

The pressure in the manifold volume will be found from the differential equation

$$\frac{dp_m}{dt} = \frac{\gamma RT}{V_m} (\dot{W}_v - \dot{W}_m) \quad (3)$$

V_m is the volume of the injector. For the valve flow to be unchoked

$$\frac{P_m}{P_v} > \left(\frac{2}{\gamma+1} \right)^{\frac{\gamma}{\gamma-1}} \quad (4)$$

and for the injector flow to be unchoked

$$\frac{P_c}{P_m} > \left(\frac{2}{\gamma+1} \right)^{\frac{\gamma}{\gamma-1}} \quad (5)$$

Equations 1 and 2 are the steady flow relations for flow through a constriction, and Equation 3 is the continuity equation (see Section 3.4.3, Equation 1) put into finite difference form in the longitudinal dimension and the convective terms dropped. For the numerical analysis program, Equations 3-5 will be solved in the ordinary manner.

3.4.12 Manifolds and Injector Steady-State

The manifolds and injectors will be treated as lines and orifices (Figure 22).

The flowrate calculation will be performed as follows

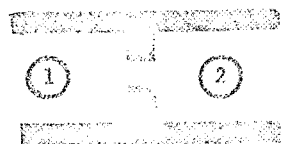


FIGURE 22 - SIMPLIFIED MANIFOLD ORIFICE

$$\dot{W} = Q \cdot K \cdot (D^2) \cdot \sqrt{\frac{(P_1 - P_2) \cdot P_1 \cdot (MW)}{T}}$$

where: $K = C \cdot Y$; $C = \frac{Cd}{\sqrt{1 + \left(\frac{d_o}{d_1}\right)^2}}$; $Y = f(Y, \frac{dt}{P}, \frac{d_o}{d_1})$;

$$Q = \frac{\pi}{4} \sqrt{\frac{2(32.174)}{1545.4}} = \text{conversion factor}$$

NOMENCLATURE

MW	Molecular weight	moles
D	Diameter line	in.
T	Temperature line	°R
W	Flowrate (assumed)	lbm/sec
P	Pressure	psic
C	Flow coefficient	--
Y	Expansion factor	--
K	Iteration of flow depending on what is connected to the manifold line	lbm/sec

Source: 1968

Upd 1/84

3.4.13 Orifices, Pipebends and Valves Transients

During transients, orifices, pipebends and valves will be represented by quasi-steady flow relations similar to those used in Section 3.4.12. Flows of gases across lumped resistances may be treated as Joule-Thompson expansions. Valve resistances as a function of both position and time will be considered in the simulation. The resistances of orifices, pipebends, and valves will be required as input. The resistances of bends and orifices may be obtained from standard references works. (See Reference 26). Valve resistances are usually provided by the manufacturer and will be put into the program in tabular form.

3.4.14 Orifices, Pipebends and Valves Steady-State

The only difference between the transient and steady-state models will be that the valve positions and thus resistances will not be functions of time.

3.4.15 Gas Generator Transients

The gas generator transient model will be characterized by the fluid flow equations used in the combustor model, Section 3.4.1, and the compressible gas flow relationships.

The initial flow out of the gas generator, when it is operated in a vacuum, will be choked. As the back pressure in the duct leading to the turbine increases, the velocity of the flow will change to subsonic. The following equations will be used:

The velocity at the gas generator for choked flow is:

$$V_t = a^* = \left(g_c \gamma R T_t \right)^{1/2} = \left[g_c R T_t \left(\frac{\gamma}{\gamma+1} \right) \right]^{1/2} \quad (5)$$

The pressure at the throat is

$$P_t = P_c \left(\frac{2}{\gamma+1} \right)^{\gamma/(\gamma-1)} \quad (6)$$

The temperature at the throat is

$$T_t = T_c \left(\frac{2}{\gamma+1} \right)^{1/(\gamma-1)} \quad (7)$$

The equations to determine the thermodynamic state at a position downstream in the ducts are:

$$\frac{V_x}{V_t} = \left[\left(\frac{\gamma+1}{\gamma-1} \right) \left[1 + \frac{2}{\gamma-1} \left(\frac{P_x}{P_t} \right)^{\frac{\gamma-1}{\gamma}} \right] \right]^{1/2}; \quad (8)$$

$$\frac{A_x}{A_t} = \left(\frac{P_t}{P_x} \right)^{1/2} \left(\frac{A_t}{A_x} \right); \quad (9)$$

$$\frac{P_x}{P_t} = \left(\frac{A_t}{A_x} \right)^2 \left(\frac{A_x}{A_t} \right)^{1/2} \left(\frac{P_t}{P_x} \right)^{1/2}; \quad (10)$$

Substituting Equation 10 into Equation 8, the velocity ratio, and V_t , may be solved for

$$\frac{V_x}{V_t} = \left(\frac{\gamma+1}{\gamma-1} \left[1 - \frac{2}{\gamma+1} \left(\frac{A_t V_t}{A_x V_x} \right)^{\frac{\gamma-1}{\gamma+1}} \right] \right)^{1/2} \quad (11)$$

The duct pressure is

$$P_x = P_t \left(\frac{A_t V_t}{A_x V_x} \right)^\gamma \quad (12)$$

The duct temperature is

$$T_x = T_t \left(\frac{P_x}{P_t} \right)^{\frac{\gamma-1}{\gamma}} \quad (13)$$

For subsonic flow:

The duct pressure is

$$P_x = P_{GG} - \frac{K_w^2}{P_{GG}} T_{GG} + R \quad (14)$$

The duct temperature is

$$T_x = T_{GG} \quad (15)$$

NOMENCLATURE

V	Velocity	ft/sec
γ	Specific heat ratio	
T	Temperature	°R
R	Gas constant	ft-lbf/lbm°R
a^*	Sonic velocity	ft/sec
G	Gravitational constant	ft/sec ²
m	Molecular weight	
C_V	Specific heat at constant pressure	BTU/lbm
V	Volume	ft ³ /sec
		psi
		°F, °C

NOMENCLATURE (Continued)

Subscripts

x	duct
c	Critical
t	Throat
CG	Gas generator

3.4.16 Steady-State Modeling - Gas Generator (high & low Pressure)

The gas generator will be a combustor model operating at a different mixture ratio. The model will use the same basic fluid flow equations as the combustor model with some additional calculations to determine the thermodynamic conditions at the gas generator exits (duct entrance). (Reference Section 3.4.2, Steady-State Combustor for Modeling and Basic Input/Output). The combustion equations will be based on curve fits of data calculated with the ICCEG program (Reference 12-16). The gas generator exhaust gas may be ducted to a turbine or to a heat exchanger (in series or separately) and there will likely be a duct connecting the gas generator to the next component. The duct length may vary from negligibly short to rather long; therefore, this simulation requires a duct model to determine the change in thermodynamic state of the fluid between the gas generator exit and the entrance to the next component. Likewise, this same duct simulation may be used between succeeding components (turbine exit to heat exchanger entrance, heat exchanger exit to space vacuum, etc.).

The basic approach to be used is described by the following equations; the nomenclature is found at the end of this section. The combustion temperature, specific heat ratio, specific heat, and molecular weight will be calculated from the following curve fits:

$$T_d = f(\chi_2) \quad (1)$$

$$\gamma = g(T_d) \quad (2)$$

$$C_p = h'(T_d) \quad (3)$$

121

The duct temperature

$$T_x = T_{GG} \quad (6)$$

NOMENCLATURE

T	Temperature	°R
MR	Mixture ratio	
Y	Specific heat ratio	
C _p	Specific heat constant pressure	BTU/°R
MW	Molecular weight	
P	Pressure	psia
K	Duct pressure loss coefficient	$\frac{\text{psi} \cdot \text{sec}^2}{\text{lbm} \cdot \text{ft}^3}$

Subscripts

x	Duct
GG	Gas generator
c	Combustion

3.4.17 Solution of a System of Implicit Equations

In the steady-state analysis program, it is necessary to have a subroutine or set of subroutines that computes a solution to the system of equations $F(X) = 0$. These routines must be accurate, reliable, and easy to use. They must take a minimum of care and execution as they will be used extensively. During the literature search, a set of subroutines were discovered which meet these specifications.

BEGS is a subroutine that, given N functions $F = (f_1, \dots, f_N)$ in M variables $X = (x_1, \dots, x_M)$, computes X such that $\|F(X)\|^2 = \sum_{i=1}^N f_i^2(X)$ is a minimum. If $M = N$, it seeks the solution of the system of equations $F(X) = 0$ using the Newton Method. BEGS requires two auxiliary subroutines. One routine must be provided to compute $F(X)$ for a given value of X . The other is subroutine LEGS. LEGS is used to solve an over-determined linear system of equations $AX = B$ in the least squares sense, i.e., to solve the normal equations $A^T A X = A^T B$.

These routines have proven to be accurate and reliable. They are in use in several programs at TRW/Houston and TRW/Redondo Beach.

3.4.18 Integration Subroutine

Both the steady-state and transient analysis programs have a need for an integration subroutine for the conductor model. Through the use of the TRW/VCS terminal stations, a library integration subroutine was located.

The subroutine is capable of solving a set of 4 simultaneous, first order, ordinary differential equations of the form:

$$y_1' = f_1(t, y_1, y_2, y_3, y_4), \quad y_2' = f_2(t, y_1, y_2, y_3, y_4),$$

etc. It is implemented using double precision. It can integrate

integration scheme will be evaluated after the ACPS models have been formulated.

This Runge-Kutta method was tested against the Euler method in the combustor transient model for accuracy, stability, and convergence. The Runge-Kutta method proved superior to the Euler method as discussed in Section 3.4.1.

REFERENCES

1. "High Pressure Auxiliary Propulsion Subsystem Definition Study," Contract No. NAS 8-26248, McDonnell-Douglas Corporation, 6 October 1970.
 2. "Low Pressure APS Study," Contract No. NAS 9-11012, "Conceptual Sub-System Definition Review," McDonnell-Douglas Corporation, 7 October 1970.
 3. "Space Shuttle High Pressure Auxiliary Propulsion Subsystem Definition," Contract NAS 9-11013, TRW Systems Group, 8 October 1970.
 4. "Space Shuttle Low Pressure Auxiliary Propulsion Subsystem Definition," Contract NAS 8-26249, TRW Systems Group, 5 October 1970.
 5. Halbert, P. W., and Lotito, L. A., The Simulation of Gas Flow Dynamics in Pipeline Networks, March, 1970.
 6. Matrix Oriented Program Assembly System (MOPAS) User's Manual, Chrysler Space Division, April, 1968.
 7. Powers, C. S. and Smith, L. H., "Oracle-Mafia Program (Propulsion Analysis Program, PAP)," Report 05952-6178-T000, 27 September 1967.
 8. Krane, R. J. and Reiff, A., "A Method of Characteristics Solution for the Equations Governing the Unsteady Flow of Liquids in Closed Systems," Technical Report No. 388, Operations Research Inc., 30 August 1966.
 9. Streeter, Victor L., and Lai, Chintu, "Water-Hammer Analysis Including Fluid Friction," Journal of the Hydraulics Division Proceedings of the American Society of Civil Engineers, May, 1962.
 10. Roberts, L., "On the Numerical Solution of the Equations for Spherical Waves of Finite Amplitude," Journal of Math and Physics, Vol. XXXVI, No. 4., January 1958.
 11. Streeter, V. L., and Wylie, E. B., Hydraulic Transients, McGraw-Hill Book Company, 1967.
 12. One-Dimensional Equilibrium Nozzle Analysis Computer Program Developed by NASA-Lewis Research Center.
 13. Turbulent Boundary Layer Models analysis Computer Program, Developed by Pratt & Whitney Aircraft.
 14. Two-dimensional Equilibrium Nozzle Analysis Computer Program, Developed by Pratt & Whitney Aircraft.
- (continued on next page)

REFERENCES (Continued)

16. ICRPG One-Dimensional Kinetic Nozzle Analysis Computer Program, July 1968, Interagency Chemical Rocket Propulsion Group, Army-Navy-Air Force-ARPA-NASA Performance Standardization Working Group.
17. Ralston, A. and Wilf, H. S., Mathematical Methods for Digital Computers, John Wiley & Sons, Inc., 1960.
18. Forsythe, G. E. and Wasow, W. R., Finite-Difference Methods for Partial Differential Equations, John Wiley & Sons, Inc., 1960.
19. Fox, L., Numerical Solution of Ordinary and Partial Differential Equations, Addison-Wesley Publishing, Inc., 1962.
20. Shapiro, A. H., The Dynamics and Thermodynamics of Compressible Fluid Flow, Ronald Press Co., 1953, Vol. 1 and 2.
21. Richtmyer, R. D., Difference Methods for Initial-Value Problems, Interscience Publishers, Inc., 1957.
22. London, A. L., Biancardi, F. R., and Mitchell, J. W., The Transient Response of Gas Turbine Plant Heat Exchangers Regenerators, Trans. ASME, Vol. 81, p. 433, 1959.
23. McAdams, W. H., Heat Transmission, McGraw-Hill Book Company, 1954.
24. Knudsen, J. C., and Katz, D. L., Fluid Dynamics and Heat Transfer, McGraw Hill Book Company, 1958.
25. Janak, P. H., "General Propellant Pressurization Program", Brown Engineering Company, Inc., Technical Report No. BSVD-P-67-SR-006, August 4, 1967.
26. Crane Industrial Products Group Technical Paper No. 410, "Flow Fluids Through Valves, Fittings, and Pipes," Engineering Division, 1957.

BIBLIOGRAPHY

1. Saito, T., "Self-Excited Vibrations of Hydraulic Control Valve Pipelines," Bulletin of JSME, Vol. 5, No. 19, 1962.
2. Ezekiel, F. D., "The Effect of Conduit Dynamics on Control-Valve Stability," Transactions of the ASME, May, 1958.
3. Jaeger, C., "The Theory of Resonance in Hydropower Systems. Discussions of Incidents and Accidents Occurring in Pressure Systems," Journal of Basic Engineering, December 1962/631.
4. Jaeger, C., "A Review of Surge Tank Stability Criteria," Journal of Basic Engineering, December 1960/765.
5. Ruderger, George, Wave Diagrams for Nonsteady Flow in Ducts, D. VanNostrand Company, Inc., 1955.
6. Parneckian, John, Waterhammer Analysis, Prentice-Hall Civil Engineering and Engineering Mechanics Series, 1955.
7. Rich, George R., Hydraulic Transients, Dover Publications, Inc., 1963.
8. Carnahan, Price, H. A. Luther, and James O. Wilkes, Applied Numerical Methods, John Wiley & Sons, 1969.
9. Zucrow, J. J., Aircraft and Missile Propulsion, Volume I and II, John Wiley & Sons, Inc., 1958.

APPENDIX I

REQUEST FOR LITERATURE SEARCH

I. Please conduct a literature search on the following subject:

Rocket propulsion systems using propellant stored as liquid hydrogen and liquid oxygen (cryogenics); and which have these liquid propellants to a gas (gas/gas system) for combustion in the rocket engine.

The following information is furnished to satisfy TIC requirements:

A. Specific terms which may be of use in locating items:

Gaseous Hydrogen/Gaseous Oxygen Rocket Engines.	
" " " "	Injectors,
" " " "	Valves
" " " "	Plumbing
" " " "	Accumulators
Liquid Hydrogen and Liquid Oxygen Heat Exchangers	
" " " "	Propellant Vaporizers
" " " "	Propellant Pumps
" " " "	Propellant Tanks

B. Terms or subjects to be excluded:

Thermodynamic properties of liquid hydrogen, liquid oxygen, gaseous hydrogen, and gaseous oxygen.

C. Additional information of possible assistance: None

D. Cost Code: 4354 Job Number: 1275-20

Note: For information purposes only. No charges levied for literature search or bibliographies.

E. Date results Needed:

F. Coverage (years): 1960-1970

G. Number of entries desired:

H. Level of classified material desired: Unclassified

I. Computer search on: Defense Documentation Service and DIAIS (Allow a minimum of 10 working days for a computerized search)

In accordance with literature search on the following subjects:

(1) Propellant storage tanks and propellant lines
(2) Propellant vaporization and propellant vaporizers
(3) Propellant pumps

The following information is furnished to satisfy TIC requirements.

A. Specific terms which may be of use in locating items:

Digital computer simulations; transient rocket engine analysis; steady-state rocket engine analysis; gaseous hydrogen and gaseous oxygen rocket engines; transient flow analysis for gas in pipes and tubes.

B. Terms or subjects to be excluded:

Thermodynamic properties of liquid hydrogen, liquid oxygen, gaseous hydrogen and gaseous oxygen.

C. Additional information of possible assistance: None

D. Cost Code: 4354 Job Number: 1275-26

Note: For information purposes only. No charges levied for literature search or bibliographies.

E. Date results needed:

F. Coverage (years): 1960-1970.

G. Number of entries desired:

H. Level of classified material desired: Unclassified.

I. Computer search by: None

III. It is requested that a literature search be conducted for any dynamic analysis or dynamic math modeling pertaining to the following items:

- A. Rocket Engines
- B. Propulsion Systems - Auxiliary and Primary
- C. Propellant Feed Systems
- D. Propellant Tanks and Accumulators
- E. Propellant Lines - Liquid and Gas
- F. Heat Exchangers and Sensors
- G. Valves
- H. Injectors
- I. Turbopumps and Compressors
- J. Manifolds
- K. Combustion Chambers
- L. Ignition Systems
- M. Gas Generators

APPENDIX 2
LITERATURE SEARCH ON MATHEMATICAL MODELING FOR
STABILITY OF HYDROGEN AND OXYGEN ROCKET PROPULSION
ENGINES RESPONSE

The following bibliography is furnished in response to your request:

- N63-18207 Mathematical model and tests of rotation detonation wave rocket engine using hydrogen and oxygen propellants.
- N67-27086 Study of random wave phenomena in hypergolic propellant combustion. (analytic model for describing combustion chamber disturbances during start transient and steady state operations for hypergolic liquid rocket engines)
- N68-22095 Computer simulation of high frequency combustion instability and its suppression. Final report.
- X66-22572 Combustion stability limits calculated utilizing a nonlinear model. (liquid propellant rocket engines)
- X67-14913 Generalized steady-state rocket engine performance equations and algorithms of solution. (General equations for constructing mathematical model on steady state liquid propellant rocket engine performance, and algorithms of solution)
- X67-22246 Combustion instability analysis at high chamber pressures. (Modification and extension of analytical liquid rocket engine combustion instability model.)
- X68-15979 Experimental verification of a double-dead-time model describing chugging in liquid bipropellant rocket engines.
- X68-80749 High frequency combustion instability mathematical analysis. Monthly progress report.
- X69-17012 An experimental investigation of injection circulation on the suitability of hydrogen oxygen engines.

APPENDIX 2 (CONTINUED)

LITERATURE SEARCH ON LIQUID HYDROGEN/OXYGEN
ROCKET PROPULSION SYSTEM RESPONSE

The following bibliography is furnished in response to your request:

- A68-21387 (AIAA paper 67-461) M-1 injector development-philosophy and implementation.
- A68-23597 The design and manufacture of a liquid hydrogen/oxygen thrust chamber.
- A68-28827 Development of high-power rocket engines.
- A68-33767 Development of LOX-hydrogen engines for Saturn Apollo launch vehicles.
- A69-16064 Design and development of the SEPR HM₄ 40Kn thrust liquid oxygen/hydrogen rocket motor.
- A69-23561 Secondary-injection thrust vector control systems.
- A69-31749 Oxidizer injector face configuration for high power variable thrust rocket engine using hydrogen/oxygen propellant.
- A69-32759 An analysis of two-phase flow in LH₂ sub 2 pumps for C₂H₂/H₂ sub 2 rocket engines.
- A69-33345 The SEPR rocket engine - HM₄ with liquid oxygen and hydrogen - design and operation.
- N68-11043 Effect of combustor parameters on the stability of gaseous hydrogen-liquid oxygen engine.
- N68-11044 An experimental on articulate damping in a two-dimensional hydrogen/oxygen combustor.
- N68-15879 Design criteria for high-pressure rocket engines.
- N68-15939 Development of SEPR-HM₄ engine - 440Kn thrust liquid oxygen and hydrogen engine.
- N68-21673 Stabilizing effects of several injector face bevel configurations on screens in a 20,000 lb. thrust rocket-engine hydrogen/oxygen system.
- N68-37517 Correlative analysis of liquid oxygen-liquid hydrogen rocket engines.
- Other papers in progress, potential future publications

APPENDIX 2 (CONTINUED)

N69-32340 Effect of injection element radial distribution and chamber geometry on acoustic mode instability in a hydrogen/oxygen engines.

N69-33584 Analytical performance prediction for high energy spacecraft propellants in the presence of heterogeneous combustion products.

N69-34345 Estimation of the maximum possible pressure in an oxygen-hydrogen engine. (turbopump drive)

Cryogenic ignition of hydrogen and oxygen with Raney Nickel. W.B. Lee. Industrial & Eng. Chem. V6 N1 Mr '67. p59-64.

For all - round propellant performance; 93 per cent H₂O₂. J.C. McCormick. bibliog. Space/Aeronautics 39:101+ Mr '63.

High-energy rocket engines. il diagr. Engineer 218:364-6, 415-17, S 4-11 '62. Discussion. 218:510, 763, 525. N 6, '64.

New combinations of liquid H₂, liquid O₂, flourine, ozone ready for rockets. R.F. Freed. il. Chem Eng 63:69-74. N2 '59.

Pratt & Whitney picked to build cryogenic rocket engine for late 70's use. H. Taylor. Aerospace Tech 21:15 Ja 15 '68.

Round-up of cryogenic fluids for missile and space propulsion systems. E.L. McCandless. SAE J. 68:64-5 S '60.

Theory of liquid propellant rocket combustion instability and its experimental verification. L. Crocco et al. AIAA J. 30:159-68 F '60.

This bibliography will be supplemented with a Defense Documentation Center computer search upon receipt.

APPENDIX 2 (CONTINUED)

BIBLIOGRAPHY ON DYNAMIC MATHEMATICAL MODELS OF PROPULSION SYSTEMS

The following bibliography is furnished in response to your request:

- A66-28442 - Probability model for defining explosive yield and spill of liquid propellant.
- A66-36889 - Mathematical model of combustion instability in solid propellant rocket engines, noting system dynamic behavior, appearance of limit cycle and effect of large amplitude oscillations on burning rate.
- A67-20072 - Nonconventional rocket propulsion systems performance and base environment characteristics evaluated, using separate cold flow and combustion models.
- A67-28113 - Model for solid rocket motor instability caused by chamber and propellant combustion characteristics, relating combustion and acoustics instabilities.
- A67-39539 - Combustion in solid propellant rocket engines using mathematical model.
- A67-41319 - Improvement of high performance liquid fuel rocket engine by optimisation of liquid hydrogen/LOX/propulsion mixtures.
- A68-13610 - Rocket combustion chamber ignition studied by mass spectroscopy of chemical species.
- A68-20743 - Rocket combustion instability studied experimentally using theoretical model characterizing combustion by time lag and interaction index.
- A69-18100 - Monosteady combustion models for gases, liquid fuels and solid propellants, reviewing errors in physics and mathematics.
- A69-24908 - Book on rocket propellants covering propulsion fundamentals, liquid, solid and hybrid propellants properties calculations, rocket technology, etc.
- A69-32778 - Chemical reactor, rocket engine thermodynamics - definition and classification, calculation methods, propellant and rocket by chemical reaction, rocket engine propellant selection
- A70-10766 - High energy density rocket propellants, (solid, liquid + liquid) - definition and classification, calculation methods, propellant and rocket by chemical reaction, rocket engine propellant selection
- A70-11700 - High energy density rocket propellants, (solid, liquid + liquid) - definition and classification, calculation methods, propellant and rocket by chemical reaction, rocket engine propellant selection

APPENDIX 2 (CONTINUED)

- A69-34773 - Chemical relaxation, optimum propellant mixture ratio, combustion chamber pressure, gas jet impulse, mass flow and drive capacity of space propulsion systems.
- A70-12007 - Nonlinear combustion instabilities in liquid propellant rockets, considering various combustion models and experimental techniques.
- A70-12011 - Three dimensional linear combustion instability in liquid propellant rocket motors using concentrated combustion model, presenting mathematical analysis as boundary value problem.
- A70-18671 - Boundary value problems and Cauchy problem considered for mathematical model of turbulent motion in liquid or gas.
- A70-20008 - Mathematical model for calculating radiative heat transfer from turbulent diffusion buoyant flame and predicting liquid fuel burning ratio.
- AD-502 957 - Combustion model for composite modified low burning rate double base rocket propellants.
- AD-505 101 - Mathematical model for combustion tailoring of solid rocket propellants.
- AD-842 960 - Analytical model development to study liquid rocket engine combustion instability at high chamber pressures.
- AD 845 936 - Absolute reaction rate theory applied to problem of cumulative damage in solid rocket propellants.
- AD 851 902 - Analytical model for predicting turbocompressor performance with combined circumferential and radial inlet distortion.
- AD 851 905 - Development of turbocompressor rotating stall prediction model.
- N66-26000 - FORTRAN II computer program for aerothermodynamic behavior of cospace heat exchanger component models for nuclear ramjet and rocket engines based on real gas properties.
- N66-32336 - Digital distributed parameter model for computing dynamic response of rocket propellant feed systems to pressure and flow disturbances.
- 767-20360 - Computer programs for steady-state pressure and cost optimization of fluid flux test facility heat removal systems using air heat dump.
- 767-17127 - Test firings and analytical model to examine hydrogen instability in aircircu experiments with LLE gaseous hydrogen combustion.
- 767-17128 - The analytical model for propagation of aircircu induced hydrogen instability.
- 767-17129 - Aircircu and analytical model to examine hydrogen instability during aircircu combustion and propagation of aircircu induced hydrogen instability.

APPENDIX 2 (CONTINUED)

N68-17557 - FORTRAN computer program for predicting aerodynamic and heat transfer characteristics of annular and rectangular gas turbine combustors.

N68-23231 - Analytic model of thermal flow oscillations in heat exchangers for supercritical fluids.

N68-25102 - Double dead-time model for combustion stability analysis in liquid bipropellant rocket engines.

N68-30581 - Mathematical model of cylindrical electric gas dynamic generator.

N68-36861 - Mathematical model for combustion at zero gravity in Spacecraft environments.

N69-10521 - Computer programs for analysis of liquid heat exchangers for convective and radiative systems of ducts and fins.

N69-11891 - Mathematic model describing dynamic behavior of high speed reciprocating compressors.

N69-25539 - Mathematical model for calculating heat exchange capability of tubular spacecraft radiator with meteorite shielding. (AD 683 578)

N69-27561 - Computerized simulation of optimal hydraulic control system with dynamic pressure feedback servovalve for positioning gimbal engine.

N69-31489 - Computer analyzed hydrogen reliquefier cycles for selection of optimal cycle, rates and heat exchangers.

N69-33319 -- Analytical model for use in design of pump inlet accumulators for prevention of liquid rocket longitudinal oscillation.

M69-39420 - Computer models for inducer system of hydraulic turbine drive for liquid hydrogen.

N69-40186 - Linearized mathematical models of feed system coupled combustion instability of liquid propellant rocket engines.

X84-15581 - Mathematical model for liquid hydrogen propellent reentry temperature rise prediction in reactor in-flight test/Riffler/Vehicle - Seratoff's flow model.

X-65-15223 - Digital computer program to calculate behavior of nozzle and
emitting sheath material exposed to solid propellant rocket exhaust
environment

Table 169. *Geographic distribution, abundance, and performance of the ctenophores in the Bay of Biscay and the North Sea*

APPENDIX Z (CONTINUED)

- X66-11722 - Mathematical mass spring models of partially filled thin wall propellant tanks.
- X66-12015 - Mathematical model for hypergolic ignition and ignition propagation across solid propellant surface in dynamic flow-hypergolic propellant studies.
- X66-13777 - Stress analysis mathematical model for tubular thermoelectric generator for isotopic power systems.
- X66-21998 - Development and state-of-art in analytical steady-state liquid propellant rocket combustion models.
- X66-22572 - Nonlinear model for calculating combustion stability in liquid propellant rocket engines.
- X66-23901 - Theoretical propellant combustion model for rapid depressurization effects.
- X67-11406 - Mathematical model of hypergolic ignition delay in space-ambient engines.
- X67-14913 - General equations for constructing mathematical model on steady state liquid propellant rocket engine performance, and algorithms of solution.
- X67-17396 - Analytical model for predicting combustion wave instability characteristics of solid propellants.
- X67-18780 - Mathematical model for steady state combustion of solid propellant rocket engine.
- X67-18791 - Computer model of solid rocket motor ignition transient.
- X68-12281 - Digital computer programs, mathematical models and propulsive system disturbance functions for integrating engine and inlet dynamic controls in turbine engine design.
- X68-12882 - Mathematical model for computerized simulation of multistage, liquid propellant stage by means of linearized engine coefficients.
- X68-17523 - Experimental verification of mathematical models for predicting lateral forces induced by secondary injection into rocket engine nozzle.
- X74-17777 - Mathematical model of stability, energy storage, and conversion of heat for propellant combustion in closed loop combustion chamber.
- o Model - mathematical model describing entropy, stability, energy conversion, and closed loop combustion.

APPENDIX 2 (CONTINUED)

X69-17008 - Mathematical model for solving 3-dimensional combustion instability in liquid propellant rocket engines.

X70-12673 - Combustion stability model of advanced injector for use on high pressure hydrogen oxygen engines.

Approximate but complete model for ignition response of solid propellants.
A. D. Baer, N. W. Ryan, AIAA J. v.6, n.5 May 1968 P. 872-7.

Computer model for a LOX manifold system. J. S. Windsor & E. Vallee, flow chart diagrs. Am. Soc. C. E. Proc. 95[WW 2 no. 65537]:149-62 My '69.

Development of fundamental model of hypergolic ignition in space-ambient engines.
T. F. Seamens, M. Vanpee, V. D. Agosta. AIAA J. v.5, n.9 Sept. 1967, p. 1616-24.

Digital computer methods in dynamic-response analyses of turbogenerator units.
W. D. Rumpage, T. N. Soha. bibliog. flow diagrs. Inst. E. E. Proc. 114:1115-30 ag'67: Discussion 115:1498-500: Reply. 1500-2 O'68.

Electric space heating with active boundary members. W. K. Roots. bibliog.
Inst. EE proc. 114:1018-1019 Jl'67.

Fluid and thermodynamic modeling of nuclear rocket vehicle. D. W. Westerheide,
R. C. Erickson, F. P. Kirkland; SAE Paper 690201 for meeting January
13-17, 1969. 11p.

Mathematical model of a packed-bed heat-exchanger reactor for dehydrogenation of
Methylcyclohexane; comparison of predictions with experimental results.
R. D. Hawthorn and others. bibliog. diagrs. AIChE J 14:69-76 Jan.'68.

Measurement of hydrogen utilization in the blast furnace by steam pulse and oil
injection techniques. C. Richmond and G. Wilson. diagrs. Iron and Steel
Inst. J. 205:630-6 Jl'67.

Mechanism of heat transfer in a spray column heat exchanger. R. Letan & E. Rebaï
bibliog. diag. AIAA J. 7:497-502 Mr. '69.

Optimization and design of fin-tube heat exchangers by experiment and computer
technique. T. F. Joyce. Inst. Heating and Vent Engng. J. v. 30
Apr. 1967. p. 8-16.

Testing of polymeric materials for use in multistage cryogenic distillation
of organic liquids. G. H. Price and J. M. Lemoine. J. Polym. Sci. Part I
5:255-64 Mr. '63.

Theory for ignition and diffusion of fuel droplets. R. L. Anderson. R.
AIAA J. v. 5, n. 1, Mar. '67. Opt. Mech. Phys. 1967.

The technique of the investigation of the diffusion of
the organic substances in the liquid phase.
Dissertation. Institute of Technology, U.S.S.R., 1957.

APPENDIX 3

PROGRAMS FOR POTENTIAL USE

<u>PROGRAM NO.</u>	<u>PROGRAM NAME</u>	<u>DESCRIPTION</u>
F MSC 554070	Heat Exchanger	S.S. performance at specified intervals along heat exchanger tubes.
F MSC 554630	Heat Transfer to a Spherical Container	Transients for sphere with cryogenic gas.
F MSC 545420	Heat Transfer Sphere	Gas inside a spherical container.
F MSC 566030	SIV Pump Cooling	Heat-up and chill-down characteristics for turbopumps.
H MSC H089	Tank Pressurization Program	Gas pressures, volume, weight.
H MSC H094	Propellant Feedline Heat Exchanger	S.S. heating of a gas by a liquid.
H MSC H095	Analysis of Propellant Tank Pressurization	Liquid propellant tank thermodynamics.
H MSC H116	Axisymmetric Two-Phase Perfect Gas Program	Propellant systems having both gaseous and condensed exhaust products.
H MSC H120	Lunar Module Reaction Control System Engine Injector	Simulates fluid dynamics. Requires analog/digital computer.
B MSC EC86	Fifth Order Runge-Kutta Integration Subroutine	1st order differential eqs.; 25 simultaneous eqs; variable step size.
R MSC E120	Newman Real Root Approximation Subroutine	Newton-Raphson
S MSC 6132	Non-Linear Simultaneous Equations Solver	Solves system of non-linear eqs. without using derivatives
F MSC H191	Spacecraft ECS Heat Exchanger Program	Get to get heat exchanger.
F MSC F01	Thermal and Cryo. Fluid Flow Computer Program	Program for calculating properties of liquid and dispersed droplets.
	None	None

APPENDIX 3 (Cont'd)

<u>PROGRAM NO.</u>	<u>PROGRAM NAME</u>	<u>DESCRIPTION</u>
M70-10069	Computer Programs for the Design & Performance Analysis of Compact Multi-Fluid Heat Exchanger	Parallel, counter, multi-fluid cross flow; plates/fin configuration.
M69-10241	Radial Turbine Synthetic (sic) Mapping Program	Provides method of calculating an estimated radial turbine performance map when turbine geometry, inlet conditions, and gas properties are known
MSF-443	Solution of Compressible Flows in Piping Systems	Description not available.
MSF-2129	Heat Exchanger Program	Not Available.
NUC-10328	Actuation Timing of a Linear Actuated Valve	Not Available.
NUC-10189	Transient and/or Steady State Thermal Analysis with Coupled Fluid Flow and Heat Conduction	Not Available.
MSF-1675	Orifice Sizing for Fluid Systems	Not Available.
MSF-36927	Heat Transfer and Thermal Problems	Transient, compressible, subsonic.
F MFC 158	Generalized Explicit Two-Phase Flow Finite Difference Generalized Heat Exchanger	Apollo fuel cells.
MSF-584	Computer Program for the Prediction of Flow Distribution in a Ring Baffle	Not Available.
H-242-1025	Heat Transfer and Heat Exchange with Temperature Variation	Large Number of Applications
H-242-1026	Heat Transfer and Heat Exchange with Temperature Variation	Large Number of Applications

APPENDIX 3 (Cont'd)

<u>PROGRAM NO.</u>	<u>PROGRAM NAME</u>	<u>DESCRIPTION</u>
H NAA APD 153	RCS Steady State Analysis	Flow rate, pressure drops, engine performance.
J MSC J067	Design and Performance Analysis of Compact Heat Exchangers	Description not available.
J MSC J071	Fan, Blower, and Pump Design	Predicts performance curves, size, and wt. required to operate at a given set of design point conditions.
H NAA AP 237	SPS Feed Lines	Description not available.
J MSC J197	Optimization/Evaluation of Fans, Compressors, and Pumps	Description not available.
F MSC F231	Oxygen Cryogenics Program	Description not available.
F MSC F246	Nuclear Shuttle Hydrogen Tank Program	Description not available.

APPENDIX A

UNAVAILABILITY OF PROGRAM DOCUMENTATION REQUESTED FROM THE ADP PROGRAM SHARING LIBRARY

Four of the computer program descriptions requested were not available for one or more of the following reasons:¹

- No formal documentation was prepared.
- Personnel turnover caused incomplete programs or documentation.
- Program is now obsolete and documentation on it has been destroyed.
- Program was not perfected and therefore withdrawn from circulation.

The ADP Program Sharing Library was unable to say which reason applied to the following programs:

- F MSF 554070 Heat Exchanger (cancelled December 6, 1969)
- F MSC F 192 Spacecraft ECS Heat Exchanger Program
(cancelled February 9, 1970)
- F MSF 360 330 Duct Flow NL/D, Q, DA (project probably not completed)
- F MSF 361 440 Transient Start-up (cancelled December 6, 1969)

¹Queries were directed to the cognizant HSC personnel as to what individual determined the status of a given program (i.e., as to whether it was "Obsolete" or not, etc.). HSC's reply to this question was - we do not have this information and cannot obtain it.

SKIZZEN RECHTSVILDENS KOMMISSIONS SÄTT
AV 1863

PRIYGERMAN
FSTRN 2
FH4324
FH4325
FH4326

卷之三

卷之三

4

117

卷之三

NOT REPRODUCIBLE

1. 100% DELX 100% SINKABLE
2. 100% DELX 100% SINKABLE

TEMPORARILY BASED ON STARTING PRESSURE IS SPECIFIED AT LOWEST POINT IN

1. *On the other hand, the first two terms in the expansion of* $\frac{1}{1-x}$ *are* $1+x$, *so that* x^2 *is the third term.*

J=1-J=0 MODELL
J=0-J=1 MODELL
S=1-S=0 MODELL
S=0-S=1 MODELL

NOT REPRODUCIBLE

卷之三

卷之三

REVIEW OF THE LITERATURE ON THE EFFECTS OF STRESS AND PERIODIC INTERATIONS
ON THE PERFORMANCE OF KAYAKERS

卷之三

MEASUREMENTS FOR SONIC FLUX AND THE ASSUMPTION OF UNIFORMITY

23
INDIANAPOLIS 25 JULY 1942

卷之三

NOT REPRODUCIBLE

CR2T0043
CR2T0044
CR2T0047
CR2T0048
CR2T0049
CR2T0050
CR2T0051
CR2T0052
CR2f0052

SEGMENT INPUT DATA FILE ..
SEGMENT INPUT DATA FILE ..
SEGMENT INPUT DATA FILE ..

卷之三

1964-07-22 10:00 AM - PROPRIETARY INFORMATION - GC&PS 144.

MARCH 2002

卷之三

RECEIVED BY LIBRARIAN 16X RHODE ISLAND LIBRARIES & MUSEUMS OCTOBER 14, 1968
SEARCHED INDEXED SERIALIZED FILED 1968
LIBRARY OF THE STATE OF RHODE ISLAND LIBRARIES & MUSEUMS
PROVIDENCE, RHODE ISLAND 02803

DEPT. OF EXTERNAL AFFAIRS, GOVT. OF INDIA, DEPPR. 1
14 NOVEMBER 1947

DEPTAG 6255-31

卷之三

卷之三

卷之三

卷之三

卷之三

卷之三

卷之三

卷之三

THE INFLUENCE OF VARIOUS GENOTYPES ON THE VITAMIN C STATUS

卷之三

NOT REPRODUCIBLE

مکالمہ ملک

104

卷之三

卷之三

GC%PR*144.
SIGNALP111 INDENT 4
12.15.11 12.15.11 12.15.11 12.15.11

卷之三

卷之三

卷之三

卷之三

¹ See, e.g., *U.S. v. Babbitt*, 100 F.3d 1250, 1255 (10th Cir. 1996) ("[T]he [Bald Eagle] Act is a clear example of Congress's attempt to regulate a species that spans state boundaries.").

۱۰۷

وَلِمَنْدَلَةَ - وَلِمَنْدَلَةَ - وَلِمَنْدَلَةَ - وَلِمَنْدَلَةَ - وَلِمَنْدَلَةَ -

12. * 11.11.2011 / 2.2.2012 * 11.11.2011 / 2.2.2012 * 11.11.2011 / 2.2.2012 *
11.11.2011 / 2.2.2012 * 11.11.2011 / 2.2.2012 * 11.11.2011 / 2.2.2012 *
11.11.2011 / 2.2.2012 * 11.11.2011 / 2.2.2012 * 11.11.2011 / 2.2.2012 *

11.11.2011 / 2.2.2012 * 11.11.2011 / 2.2.2012 * 11.11.2011 / 2.2.2012 *
11.11.2011 / 2.2.2012 * 11.11.2011 / 2.2.2012 * 11.11.2011 / 2.2.2012 *

11.11.2011 / 2.2.2012 * 11.11.2011 / 2.2.2012 * 11.11.2011 / 2.2.2012 *

11.11.2011 / 2.2.2012 *

11.11.2011 / 2.2.2012 * 11.11.2011 / 2.2.2012 * 11.11.2011 / 2.2.2012 *

11.11.2011 / 2.2.2012 * 11.11.2011 / 2.2.2012 * 11.11.2011 / 2.2.2012 *

11.11.2011 / 2.2.2012 * 11.11.2011 / 2.2.2012 * 11.11.2011 / 2.2.2012 *

11.11.2011 / 2.2.2012 * 11.11.2011 / 2.2.2012 * 11.11.2011 / 2.2.2012 *

11.11.2011 / 2.2.2012 * 11.11.2011 / 2.2.2012 * 11.11.2011 / 2.2.2012 *

11.11.2011 / 2.2.2012 * 11.11.2011 / 2.2.2012 * 11.11.2011 / 2.2.2012 *

11.11.2011 / 2.2.2012 *

THE MARVELS VALLEY

الطبعة الأولى

```

    r512 = SQRT(C5**2 + h0*C6)/2.0
    r512 = SQRT((C5+C6)**2 + h0*(C6-C5)) - C3*C4
    r512 = SQRT((C5+C6)**2 + h0*(C6-C5)) + C3*C4

```

100% C2 = 100% C2

NOT RELE

1920-1921
1921-1922
1922-1923
1923-1924
1924-1925
1925-1926
1926-1927
1927-1928
1928-1929
1929-1930
1930-1931
1931-1932
1932-1933
1933-1934
1934-1935
1935-1936
1936-1937
1937-1938
1938-1939
1939-1940
1940-1941
1941-1942
1942-1943
1943-1944
1944-1945
1945-1946
1946-1947
1947-1948
1948-1949
1949-1950
1950-1951
1951-1952
1952-1953
1953-1954
1954-1955
1955-1956
1956-1957
1957-1958
1958-1959
1959-1960
1960-1961
1961-1962
1962-1963
1963-1964
1964-1965
1965-1966
1966-1967
1967-1968
1968-1969
1969-1970
1970-1971
1971-1972
1972-1973
1973-1974
1974-1975
1975-1976
1976-1977
1977-1978
1978-1979
1979-1980
1980-1981
1981-1982
1982-1983
1983-1984
1984-1985
1985-1986
1986-1987
1987-1988
1988-1989
1989-1990
1990-1991
1991-1992
1992-1993
1993-1994
1994-1995
1995-1996
1996-1997
1997-1998
1998-1999
1999-2000
2000-2001
2001-2002
2002-2003
2003-2004
2004-2005
2005-2006
2006-2007
2007-2008
2008-2009
2009-2010
2010-2011
2011-2012
2012-2013
2013-2014
2014-2015
2015-2016
2016-2017
2017-2018
2018-2019
2019-2020
2020-2021
2021-2022
2022-2023
2023-2024
2024-2025
2025-2026
2026-2027
2027-2028
2028-2029
2029-2030
2030-2031
2031-2032
2032-2033
2033-2034
2034-2035
2035-2036
2036-2037
2037-2038
2038-2039
2039-2040
2040-2041
2041-2042
2042-2043
2043-2044
2044-2045
2045-2046
2046-2047
2047-2048
2048-2049
2049-2050
2050-2051
2051-2052
2052-2053
2053-2054
2054-2055
2055-2056
2056-2057
2057-2058
2058-2059
2059-2060
2060-2061
2061-2062
2062-2063
2063-2064
2064-2065
2065-2066
2066-2067
2067-2068
2068-2069
2069-2070
2070-2071
2071-2072
2072-2073
2073-2074
2074-2075
2075-2076
2076-2077
2077-2078
2078-2079
2079-2080
2080-2081
2081-2082
2082-2083
2083-2084
2084-2085
2085-2086
2086-2087
2087-2088
2088-2089
2089-2090
2090-2091
2091-2092
2092-2093
2093-2094
2094-2095
2095-2096
2096-2097
2097-2098
2098-2099
2099-20100

NOT REPRODUCIBLE

1. SCENE 140001
2. SCENE 140002
3. SCENE 140003
4. SCENE 140004
5. SCENE 140005
6. SCENE 140006
7. SCENE 140007
8. SCENE 140008
9. SCENE 140009
10. SCENE 140010
11. SCENE 140011
12. SCENE 140012
13. SCENE 140013
14. SCENE 140014
15. SCENE 140015
16. SCENE 140016
17. SCENE 140017
18. SCENE 140018
19. SCENE 140019
20. SCENE 140020
21. SCENE 140021
22. SCENE 140022
23. SCENE 140023
24. SCENE 140024
25. SCENE 140025
26. SCENE 140026
27. SCENE 140027
28. SCENE 140028
29. SCENE 140029
30. SCENE 140030
31. SCENE 140031
32. SCENE 140032
33. SCENE 140033
34. SCENE 140034
35. SCENE 140035
36. SCENE 140036
37. SCENE 140037
38. SCENE 140038
39. SCENE 140039
40. SCENE 140040
41. SCENE 140041
42. SCENE 140042
43. SCENE 140043
44. SCENE 140044
45. SCENE 140045
46. SCENE 140046
47. SCENE 140047
48. SCENE 140048
49. SCENE 140049
50. SCENE 140050
51. SCENE 140051
52. SCENE 140052
53. SCENE 140053
54. SCENE 140054
55. SCENE 140055
56. SCENE 140056
57. SCENE 140057
58. SCENE 140058
59. SCENE 140059
60. SCENE 140060
61. SCENE 140061
62. SCENE 140062
63. SCENE 140063
64. SCENE 140064
65. SCENE 140065
66. SCENE 140066
67. SCENE 140067
68. SCENE 140068
69. SCENE 140069
70. SCENE 140070
71. SCENE 140071
72. SCENE 140072
73. SCENE 140073
74. SCENE 140074
75. SCENE 140075
76. SCENE 140076
77. SCENE 140077
78. SCENE 140078
79. SCENE 140079
80. SCENE 140080
81. SCENE 140081
82. SCENE 140082
83. SCENE 140083
84. SCENE 140084
85. SCENE 140085
86. SCENE 140086
87. SCENE 140087
88. SCENE 140088
89. SCENE 140089
90. SCENE 140090
91. SCENE 140091
92. SCENE 140092
93. SCENE 140093
94. SCENE 140094
95. SCENE 140095
96. SCENE 140096
97. SCENE 140097
98. SCENE 140098
99. SCENE 140099
100. SCENE 140100